

Designing and Testing Different Types of Solar Air Heaters

Mehmet Kalay

Submitted to the
Institute of Graduate Studies and Research
in partial fulfillment of the requirements for the degree of

Master of Science
in
Mechanical Engineering

Eastern Mediterranean University
September 2019
Gazimağusa, North Cyprus

Approval of the Institute of Graduate Studies and Research

Prof. Dr. Ali Hakan Ulusoy
Acting Director

I certify that this thesis satisfies all the requirements as a thesis for the degree of Master of Science in Mechanical Engineering.

Assoc. Prof. Dr. Hasan Hacışevki
Chair, Department of Mechanical
Engineering

We certify that we have read this thesis and that in our opinion it is fully adequate in scope and quality as a thesis for the degree of Master of Science in Mechanical Engineering.

Assoc. Prof. Dr. Hasan Hacışevki
Supervisor

Examining Committee

1. Assoc. Prof. Dr. Hüseyin Çamur

2. Assoc. Prof. Dr. Hasan Hacışevki

3. Asst. Prof. Dr. Devrim Aydın

ABSTRACT

This project aims to design and test different types of solar air heaters. SAHs are used for heat applications and to improve sustainability. The future of the world is dependent on non-conventional energy sources. Moreover, solar energy is necessary for the modern world as fossil fuels are harmful for the environment and will not be available for a long period. For this reason, solar energy is seen as a feasible source for the ever-increasing need for energy and a better way to develop the environment. This project will focus on designing three SAHs with different absorber materials. In this study the cola can, conical and polymer panel type collectors were used due to enhanced heat transfer. The calculations were carried out from the experimental data that was collected the spring and summer periods of 13-16 May and 16-19 July 2019, each day from 9:00 till 16:00. The maximum efficiencies obtained in May were 29 % for cola can, 32 % for conical and 29 % for polymer panel, and in July 30 % for cola can, 35 % for conical and 32 % for polymer panel. Additionally, the maximum heat loss values obtained in May and July were calculated as 172.9 W and 214.1 W for cola can, 132.2 W and 181.3 W for conical type, and 129.3 W and 166.3 W for polymer type, respectively. It can be concluded that the best type of the collector is cola can, because its efficiency is stable as seen from the graphical representation of the experimental data, although the conical type collector has the highest efficiency and the maximum heat loss value of the cola can is relatively high.

Keywords: Solar air heaters, Sustainability, Efficiency, Heat loss, Experimental data

ÖZ

Bu proje, farklı türlerdeki güneş hava ısıtıcılarını tasarlamayı ve test etmeyi amaçlamaktadır. SAH'lar, ısı uygulamaları için ısınmış hava koşulları ve sürdürülebilirliği artırmak gibi birçok farklı amaç için kullanılmaktadır. Gezegenimizin geleceği, konvansiyonel olmayan enerji kaynağının etkin kullanımı seçeneklerine bağlıdır. Bu nedenle, fosil yakıtlar çevre için kötü olduğundan ve uzun süre sürdürülebilir olamayacağından modern dünya için çok önemlidir. Bu yüzden, güneş enerjisi sürekli artan enerjiye olan ihtiyaç için olası bir kaynak ve çevreyi geliştirmek için daha iyi bir yol olarak görülmektedir. Bu proje de kola, konik ve polimer panel tipi kollektörler, havanın geçtiği geniş bir alana sahip olması nedeniyle kullanılmıştır. Deney verileri, ilkbahar ve yaz ayları olan, Mayıs ve Temmuz 2019'da alınmıştır. Mayıs ve Temmuz verilerinde elde edilen en yüksek verim, kola kabı % 29, konik % 32 ve polimer panel için % 29 ve cola kabı % 30, konik % 35 ve polimer panel için % 32 dir. Ek olarak, Mayıs ve Temmuz aylarında elde edilen maksimum ısı kaybı değerleri, kola kabı için 172.9 W ve 214.1 W, konik tip için 132.2 W ve 181.3 W ve polimer tipi için sırasıyla 129.3 W ve 166.3 W olarak hesaplanmıştır. Konik tip toplayıcı en yüksek verime ve maksimum ısı kaybı değerine sahip olmasına rağmen, toplayıcının en iyi tipinin kola olabileceği sonucuna varılabilir, çünkü etkinliğin deneysel verileri grafiksel sunumundan görüldüğü gibi kararlıdır.

Anahtar Kelimeler: Güneş enerjili hava ısıtıcıları, Sürdürülebilirlik, Verimlilik, Isı kaybı, Deneysel veriler

ACKNOWLEDGMENT

I would like express my special thanks to Assoc. Prof. Dr. Hasan HACIŞEVKİ for his guidance and support throughout the entire project as well as giving me much needed advice when it came to certain things in the making of the project. He provided me with constant encouragement and support in various ways. His ideas, experiences, and passions have truly inspired and enriched my growth as a student. I am indebted to him forever.

I would also like to thank my entire family especially my parents for their constant support.

TABLE OF CONTENTS

ABSTRACT.....	iii
ÖZ.....	iv
ACKNOWLEDGMENT.....	v
LIST OF TABLES.....	xiv
LIST OF FIGURES.....	ixv
LIST OF SYMBOLS AND ABBREVIATIONS.....	xivi
1 INTRODUCTION.....	1
1.1 Project definition.....	1
1.2 Objectives of the Study.....	2
1.3 Detailed Project Limitations.....	3
1.4 Organization of the Thesis.....	3
2 LITERATURE REVIEW.....	5
2.1 Background Information.....	5
2.1.1 Overview of Solar Air Heaters.....	5
2.1.2 Research and Developments.....	5
2.1.3 Principles of Solar Air Heater.....	9
2.1.4 Application of Solar Air Heating Systems.....	10
2.1.5 Industrial Buildings.....	10
2.1.6 Process Air.....	11
2.2 Utilization of Solar Air Heater.....	12
2.2.1 Heating and Cooling of Buildings.....	12
2.2.2 Drying and Curing of Agricultural Products.....	12
2.2.3 Applications in Industry.....	13

2.3 Comparison of Solar Air Heaters	13
3 DESIGN AND ANALYSIS.....	15
3.1 Design and Manufacturing	15
3.1.1 Design Selection	15
3.1.2 Design Components and Measurement Equipment.....	15
3.1.3 Digital Anemometer	15
3.1.4 Thermometer	16
3.1.5 Pyranometer.....	17
3.2 Structural Arrangement	18
3.3 Thermal Analysis	20
3.4 Cost Analysis.....	24
4 EXPERIMENTAL STUDY AND TESTING	25
4.1 Manufacturing and Assembly	25
4.2 Detailed Manufacturing Process	26
4.3 Experimental Methodology.....	27
4.3.1 Experiment Procedure	27
5 RESULTS AND DISCUSSIONS	28
5.1 The results of Temperature Difference Between Outlet and Inlet Air Temperature Against Time at Different Mass Flow Rates For Each Collector	28
5.2 Thermal Efficiency of The Collectors.....	34
5.3 Heat Loss of Collector Types.....	39
6 CONCLUSION AND FUTURE WORKS	44
6.1 Conclusion.....	44
6.2 The Future Works.....	45
REFERENCES.....	47

APPENDICES	52
Appendix A: Assembly Drawings.....	54
Appendix B: Tables.....	80

LIST OF TABLES

Table 1: Absorber surface shapes [28].....	13
Table 2: Thermal Properties of Materials [35].....	23
Table 3: Cost analysis table.....	24
Table 4: Obtained data at 0.02 kg/s air mass flow rate for cola can type (13.05.2019)	80
Table 5: Obtained data at 0.02 kg/s air mass flow rate for cola can type (16.07.2019)	80
Table 6: Obtained data at 0.02 kg/s air mass flow rate for conical type (13.05.2019)	81
Table 7: Obtained data at 0.02 kg/s air mass flow rate for conical type (16.07.2019)	81
Table 8: Obtained data at 0.02 kg/s air mass flow rate for polymer panel type (13.05.2019).....	82
Table 9: Obtained data at 0.02 kg/s air mass flow rate for polymer panel type (16.07.2019).....	82
Table 10: Obtained data at 0.04 kg/s air mass flow rate for cola can type (14.05.2019).....	83
Table 11: Obtained data at 0.04 kg/s air mass flow rate for cola can type (17.07.2019).....	83
Table 12: Obtained data at 0.04 kg/s air mass flow rate for conical type (14.05.2019)	84
Table 13: Obtained data at 0.04 kg/s air mass flow rate for conical type (17.07.2019)	84

Table 14: Obtained data at 0.04 kg/s air mass flow rate for polymer panel type (14.05.2019).....	85
Table 15: Obtained data at 0.04 kg/s air mass flow rate for polymer panel type (17.07.2019).....	85
Table 16: Obtained data at 0.06 kg/s air mass flow rate for cola can type (15.05.2019).....	86
Table 17: Obtained data at 0.06 kg/s air mass flow rate for cola can type (18.07.2019).....	86
Table 18: Obtained data at 0.06 kg/s air mass flow rate for conical type (15.05.2019)	87
Table 19: Obtained data at 0.06 kg/s air mass flow rate for conical type (18.07.2019)	87
Table 20: Obtained data at 0.06 kg/s air mass flow rate for polymer panel type (15.05.2019).....	88
Table 21: Obtained data at 0.06 kg/s air mass flow rate for polymer panel type (18.07.2019).....	88
Table 22: Obtained data at 0.08 kg/s air mass flow rate for cola can type (16.05.2019).....	89
Table 23: Obtained data at 0.08 kg/s air mass flow rate for cola can type (19.07.2019).....	89
Table 24: Obtained data at 0.08 kg/s air mass flow rate for conical type (16.05.2019)	90
Table 25: Obtained data at 0.08 kg/s air mass flow rate for conical type (19.07.2019)	90

Table 26: Obtained data at 0.08 kg/s air mass flow rate for polymer panel type (16.05.2019).....	91
Table 27: Obtained data at 0.08 kg/s air mass flow rate for polymer panel type (19.07.2019).....	91
Table 28: Obtained data at 0.02 kg/s air mass flow rate heat loss for cola can type (13.05.2019).....	92
Table 29: Obtained data at 0.02 kg/s air mass flow rate heat loss for cola can type (16.07.2019).....	92
Table 30: Obtained data at 0.02 kg/s air mass flow rate heat loss for conical type (13.05.2019).....	93
Table 31: Obtained data at 0.02 kg/s air mass flow rate heat loss for conical type (16.07.2019).....	93
Table 32: Obtained data at 0.02 kg/s air mass flow rate heat loss for polymer panel type (13.05.2019).....	94
Table 33: Obtained data at 0.02 kg/s air mass flow rate heat loss for polymer panel type (16.07.2019).....	94
Table 34: Obtained data at 0.04 kg/s air mass flow rate heat loss for cola can type (14.05.2019).....	95
Table 35: Obtained data at 0.04 kg/s air mass flow rate heat loss for cola can type (17.07.2019).....	95
Table 36: Obtained data at 0.04 kg/s air mass flow rate heat loss for conical type (14.05.2019).....	96
Table 37: Obtained data at 0.04 kg/s air mass flow rate heat loss for conical type (17.07.2019).....	96

Table 38: Obtained data at 0.04 kg/s air mass flow rate heat loss for polymer panel type (14.05.2019)	97
Table 39: Obtained data at 0.04 kg/s air mass flow rate heat loss for polymer panel type (17.07.2019)	97
Table 40: Obtained data at 0.06 kg/s air mass flow rate heat loss for cola can type (15.05.2019)	98
Table 41: Obtained data at 0.06 kg/s air mass flow rate heat loss for cola can type (18.07.2019)	98
Table 42: Obtained data at 0.06 kg/s air mass flow rate heat loss for conical type (15.05.2019)	99
Table 43: Obtained data at 0.06 kg/s air mass flow rate heat loss for conical type (18.07.2019)	99
Table 44: Obtained data at 0.06 kg/s air mass flow rate heat loss for polymer panel type (15.05.2019)	100
Table 45: Obtained data at 0.06 kg/s air mass flow rate heat loss for polymer panel type (18.07.2019)	100
Table 46: Obtained data at 0.08 kg/s air mass flow rate heat loss for cola can type (16.05.2019)	101
Table 47: Obtained data at 0.08 kg/s air mass flow rate heat loss for cola can type (19.07.2019)	101
Table 48: Obtained data at 0.08 kg/s air mass flow rate heat loss for conical type (16.05.2019)	102
Table 49: Obtained data at 0.08 kg/s air mass flow rate heat loss for conical type (19.07.2019)	102

Table 50: Obtained data at 0.08 kg/s air mass flow rate heat loss for polymer panel type (16.05.2019)	103
Table 51: Obtained data at 0.08 kg/s air mass flow rate heat loss for polymer panel type (19.07.2019)	103
Table 52: Calculation of U-overall of collector types.....	104

LIST OF FIGURES

Figure 1: Working principle of solar air heater [24]	9
Figure 2: Industrial Building [26]	11
Figure 3: Digital Anemometer [29].....	16
Figure 4: Thermometer [31].....	16
Figure 5: Secondary class pyranometer [33].....	17
Figure 6: Cola Can Type Solar Air Heater.....	18
Figure 7: Conical Type Solar Air Heater	19
Figure 8: Polymer Panel Type Solar Air Heater	20
Figure 9: Cola can temperature difference vs time (13-16.05.2019).....	30
Figure 10: Cola can temperature difference vs time (16-19.07.2019).....	30
Figure 11: Conical type temperature differences vs time (13-16.05.2019)	32
Figure 12: Conical type temperature differences vs time (16-19.07.2019)	32
Figure 13: Polymer type temperature differences vs time (13-16.05.2019)	33
Figure 14: Polymer type temperature differences vs time (16-19.07.2019)	34
Figure 15: Efficiency performance at different mass flow rates against time for the cola can type SAH collector in (13-16.05.2019).....	36
Figure 16: Efficiency performance at different mass flow rates against time for the cola can type SAH collector in (16-19.07.2019).....	36
Figure 17: Efficiency performance at different mass flow rates against time for the conical type SAH collector in (13-16.05.2019)	37
Figure 18: Efficiency performance at different mass flow rates against time for the conical type SAH collector in (16-19.07.2019)	37

Figure 19: Efficiency performance at different mass flow rates against time for the Polymer panel type SAH collector in (13-16.05.2019).....	38
Figure 20: Efficiency performance at different mass flow rates against time for the Polymer panel type SAH collector in (16-19.07.2019).....	38
Figure 21: Heat losses values against time for each collector type at (0.02 kg/s)	40
Figure 22: Heat losses values against time for each collector type at (0.02 kg/s)	40
Figure 23: Heat losses values against time for each collector type at (0.04 kg/s)	41
Figure 24: Heat losses values against time for each collector type at (0.04 kg/s)	41
Figure 25: Heat losses values against time for each collector type at (0.06 kg/s)	42
Figure 26: Heat losses values against time for each collector type at (0.06 kg/s)	42
Figure 27: Heat losses values against time for each collector type at (0.08 kg/s)	43
Figure 28: Heat losses values against time for each collector type at (0.08 kg/s)	43
Figure 29: Aluminium Cola Can Type Collector.....	53
Figure 30: Conical Type Collector.....	53
Figure 31: Polymer Panel Type Collector.....	54
Figure 32: Aluminium Cola Can.....	54
Figure 33: Aluminium Cola Can Break View	55
Figure 34: Aluminium Conic	55
Figure 35: Heat-resistant Styrofoam	56
Figure 36: Wooden Cabinet Box (Can Cola Input)	56
Figure 37: Wooden Cabinet Box (Can Cola Output).....	56
Figure 38: Conical Type Cabinet Box (Input)	57
Figure 39: Conical Type Cabinet Box (Output).....	57
Figure 40: Fan Motor	58
Figure 41: Connection element between cabinet and motor (Aluminium).....	58

Figure 42: Plastic pipe.....	59
Figure 43: Glass wool	59
Figure 44: Glass	60
Figure 45: Osb-Board.....	60
Figure 46: Absorber Aluminium Plate.....	61

LIST OF SYMBOLS AND ABBREVIATIONS

A_c	Area of Collector [m^2]
ASME	American Society of Mechanical Engineers
ASTM	American Society for Testing Materials
CEN	European Committee for Standardization
C_p	Specific Heat of the Fluid [$kJ / kg.K$]
EN	European Standard
I	Solar Radiation [W / m^2]
ISO	International Organization for Standardization
k	Thermal Conductivity [$W / m. ^\circ C$]
\dot{m}	Mass Flow Rate [kg / s]
η	Thermal Efficiency of Solar Collector
SAH	Solar Air Heaters
T_{in}	Inlet Temperature [$^\circ C$]
T_{out}	Outlet Temperature [$^\circ C$]
$U_{overall}$	Overall Heat Transfer Coefficient [$W/m^2.K$]
V	Velocity of the Outlet Air [m / s]
ΔT	Temperature Difference [$^\circ C$]
ρ	Density of Air [kg / m^3]
Q_{loss}	Total Heat Loss [W]

Chapter 1

INTRODUCTION

1.1 Project Definition

Fossil fuels cause huge pollution that directly influences waterways, the air we breathe thus, the vegetables, fruits and meat we consume. Fossil fuels like gas and oil are not renewable sources of energy. Once they are processed and used, they can't be replenished. Eventually, we will end up consuming all available fossil fuels and inevitably have to come up with a new way to power our system.

Solar energy has all the perks to favour its share in the market simply because of its infinite amount and zero contributions to global warming compared to rival energy sources. Eco-friendly energy sources like solar energy are relatively less expensive, easier to produce and always renewable. As for humans, solar energy is vital because the sun is a sustainable source of energy which can be used for many purposes such as agricultural purposes and most of our day to day activities. Plantation and livestock are still the most important industries that rely on solar energy.

Solar energy is been absorbed by solar air heaters to heat the passing air so it can either be used for space heating or storing. A black colour is chosen for the collectors due to its heat absorption capability to absorb more energy from the sun and due to its conductive nature, in some cases metal act as heat exchangers. Increasing the flow rate of air using a fan can be observed in many different designs and it can be called

forced convection. A spare collector can also be built to transfer fresh air through the bottom whenever hot air rises. Fans can often increase system performance however they need additional parts and can become more complicated. After initial costs, solar air heaters can consummate traditional indoor heating systems by providing a clean source of heat with no additional cost. On a cloudy day, clouds would affect the energy output of the system, but the metal will store enough energy on a hot day and will compensate for the cloudy day. Optimally, the system should be facing the usual direction of the sun (south for the northern hemisphere, north for the southern hemisphere) and should not be shaded or have any form of covering.

1.2 Objectives of the Study

The main objective of this project is to design and test three solar air heaters in the City of Famagusta, North Cyprus. Other objectives of the study are listed below:

- To optimize the available parameters in order to obtain the best possible product.
- To investigate the cost of manufacturing and choose a suitable method of production.
- To perform experiments and make analysis of the system. Testing will be done and data will be recorded.
- Testing is to be carried out during the spring and summer seasons which is a critical criterion regarding the objectives.
- To obtain a desired output and build and manufacture Solar air heaters using the information in this project.
- Testing is to be carried out during the spring season which is a critical criterion regarding the objectives

1.3 Detailed Project Limitations

This study will focus on three major constraints:

- The first constraint is time; the proper schedule must be drawn to finish before the due date.
- Money is another constraint while doing the project since unpredictable amounts of indirect spending may be encountered. During the manufacturing phase, materials are going to be purchased that I hadn't estimated beforehand.
- Finally, the weather may become very unpredictable during the time of manufacturing, which may play a part in giving inconsistent results.

1.4 Organization of the Thesis

The report is solely about solar air heaters. The introduction includes the definition and brief information on solar energy, the importance of solar energy on human life and a brief description of the working mechanism of Solar air Heaters.

In chapter 2 literature reviews emphasizes on the overview of solar air heater, research and developments, working principles, system application and types of solar air heater applications.

Chapter 3 gives information on design and manufacturing. Brief information is included in design component and measurement equipment, thermal analysis, economic feasibility and economic analysis.

Chapter 4 entails selection of manufacturing method and material, manufacturing and assembly techniques.

The next chapter discusses about the verification and the validation of planned objectives and engineering standards.

Chapter 5 talk about the results obtained and discusses the outcome of the results.

The final chapter gives information on the future works who hope to do on the project and concludes project. The appendix section gives supporting documents that were used throughout the project.

Chapter 2

LITERATURE REVIEW

2.1 Background Information

2.1.1 Overview of Solar Air Heaters

Solar air heaters are systems that collect solar energy in the form of sun rays and transfer the heat to passing air, which can either be accumulated for future use or used for space heating. When hot air is produced more, the primary heating system will work less, therefore the less fuel you need to buy. For solar air heater, all you need to do is to work on the initial investment which is installing the solar air heater. Sunlight becomes your fuel while in the outdated heating system you have to pay for fuel, stove, heat pump etc. Your initial (and only) investment is the air heater. That's it; you have an unlimited and free supply of fuel from the sun.

2.1.2 Research and Developments

There have been many different forms of solar heaters produced over the years, the most common of them all is known to be the flat plate type, because of its easy construction and operation nature, and also its cheap maintenance budget. Considering that the working fluid of air heaters is air, the speculation of the problems associated with freezing or boiling of the fluid do not seem to exist. Some advantages include having its density, thermal capacity and heat conductivity very low, hence demanding bigger size ducts to transport the energy required. Air panels have setbacks, however the fact that they are reliable and cost efficient makes them so worthwhile. A standard solar air heater may generally have absorber plates that

have a parallel plate beneath it, therefore giving it a high aspect ratio where heated air flows. There are two ways to increase useful energy collection from air heaters. Firstly, increasing the collector area by making the absorber plate longer while maintaining the depth channel and mass flow rate. If there are design limitations on fan power and length of collector, increasing the air rates to make a deeper channel maximises useful energy collection from air heaters.

Solar air heating researches and developments started in the 1940s, with research done by Miller [1], Lof [2] and Telkes[3]. Their works had information on the making and testing of solar air heating systems by Lof in 1944 and Telkes in 1947, in houses located in Colorado and Massachusetts, respectively. The overlapped glass solar air heater invented by Lof has been tested by his colleagues [4,5]. Selcuk [6] performed a quasi-steady-state analysis of the overlapped glass plate air heater and tested the model experimentally. In the 1950s, Bliss [7] designed, manufactured, and tested a solar air heating system in an Arizona house. Research on simple flat plate collectors were conducted by Whillier [8], Close [9], and Gupta and Garg [10]. Charters [11] theoretically investigated the performance of a single glazed collector designs having the flow above and beneath the absorber plate. Cope-Appel and Haberstroh [12] theoretically studied the paths of the flow for single flat plate having two glass covers.

Solar air heaters have been made in many different forms such as glazing types, absorber surfaces have included overlapped, spaced, clear and black glass plates, single smooth metal sheets, flow-through stacked screens or mesh, corrugated metal plates, finned metal sheets, etc. In some collector types, air passes below the plate or underlying air gaps reducing heat loss downwards. Sheven et al [13] identified many

air heating collector designs. He divided them under six categories based on the surface absorber. Different design measurements can have effects on the performance improvement techniques.

Theoretical and experimental studies on the flat plate of solar air collectors started by Buelow [14]. The purpose of a V-groove type in the absorber plate is maximising the solar absorptance and the turbulence in the air was given by Hollands [15].

Close [9] tested the effect of triangular cross-sectional grooves with a chosen surface for the many flow paths. Charters and MacDonald [16] also studied the V-grooved absorbing surface for the various flow arrangements. Gupta and Garg [10] examined the absorber composed of two sheets of round corrugated material, transversely placed above one another and welded along the length. Cole-Appel and Haberstroh [12] used a simple linear model to contrast the thermal performance of five flat plate solar air heater designs, two of them were of the straight finned type. Beville and Brandt [17] examined the effects of specularly reflecting fins on a single glazed collector with the airflow and fins located above the absorber plate.

Solar air heaters for different applications are separate according to its price. The cost of air heating by a solar collector is mostly high due to the collector material and air pumping cost. Charters [18] researched the optimization of the aspect ratio of the rectangular flow passage from the viewpoint of decreasing the price for a fixed pumping power. Hollands and Scheven [19] studied the outcome of the dimensions of the rectangular and triangular airflow movement on the coefficient of forced convective heat transfer from the absorber to the air flowing in plate type air heating collectors.

Selcuk [20] recommended using shattered glass pieces for matrix air heaters. Broken pieces are almost without cost, glass is transparent to solar radiation, therefore can be used in three ways for absorbing the solar radiation. Firstly, the top surface is darkened with black paint so that radiation is absorbed in the top. Secondly, radiation is let to be absorbed gradually throughout the volume of the matrix. Finally, the bottom of the matrix is blackened so that the unabsorbed radiation is gathered at the bottom, which is insulated from the surrounding.

Charters [11] also studied heat transfer events in symmetrically heated ducts representing the flat plate solar collector. Karmare and Tikekar [21] experimentally investigated heat transfer to the airflow in the rectangular duct of an aspect ratio 10:1.

The performance of solar air heaters relation with various different types of geometry of roughness elements on the absorber plate was examined by Mittal et al [22]. The effective efficiency has been calculated by using the connection between heat transfer and friction factor developed by many investigators within the investigated range of operating and system design parameters. Sahu and Bhagoria [23] examined heat transfer coefficient by using 90° broken perpendicular ribs on the absorber plate of a solar air heater; the roughened wall was heated while the remaining three walls were well insulated. The roughened wall has roughness with pitch (P), ranging from 10-30 mm, the height of the rib of 1.5 mm and duct aspect ratio of 8. The rate of airflow correlates to Reynolds number between 3000-12,000. The heat transfer calculations have been compared with those for smooth ducts under similar flow and thermal boundary condition to determine the thermal efficiency of the solar air heater.

2.1.3 Principles of Solar Air Heater

The main working principle of SAH is that the sunray engrosses from the sun and charge to heat into the collectors which are covered by glass. The design of the solar air heater has made it in such a way that solar radiation with very high efficiency cannot be absorbed without integrated system so therefore for the heat to go into the building there must be a unique design to make the energy transfer possible and deliver the air into the building.

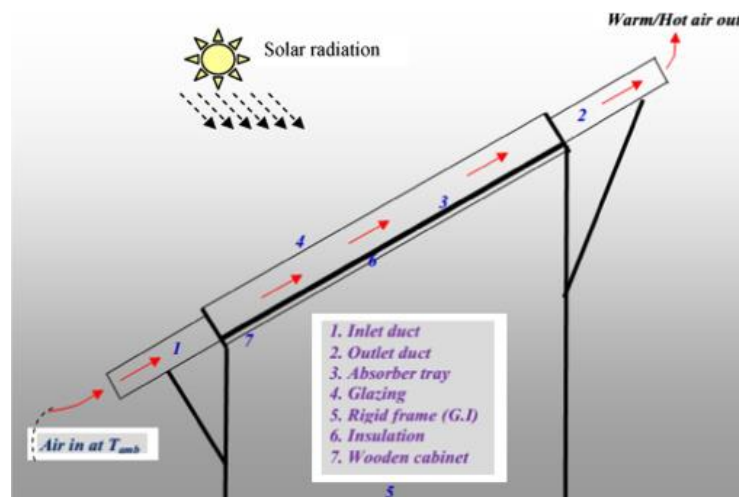


Figure 1: Working principle of solar air heater [24]

The principle of solar air heating system can be explained which are:

- **Convection:** Heat is transferred from the heated solid material to the air as it goes over the surface. One of the examples is fan which is used to force air across the heated material and they can be solar-powered.
- **Radiation:** Taken solar radiation by collector results in the material heating up. The best solar absorption is Black non-reflective surfaces. These basic principles can be used by solar air heater manufacturer but some other components can be added to the collectors. The fan helps in transferring air

across the heated surface and can be used as part of the ducting system to channel the heated air into the normal space [24].

2.1.4 Application of Solar Air Heating Systems

In agricultural and food operation much energy is consumed of which show their sizable portion of their input cost. Solar energy is introduced to help in agriculture because of the high increase in energy price which has been making the income in agriculture to go so low. The solar air heater can be used in both animal and plant sector and crop drying. To maintain the animal farm we don't only need the indoor air but we need the outside air temperature as well. This system has been used for hand [25], red of agricultural and animal buildings. The inside air can preheat up to 27-degree centigrade. Solar air heating system can take up to 1.25 m per square of barn. We can design the solar air heating system for poultry ventilation in such a way it can handle the minimum ventilation requirements for winter and summer. In agricultural cropping, the indoor temperature starts from around 90 °F (32 °C) for the summertime and then reduce to about 70 °F (22 °C) as the crop grow bigger. The main typical meaning of this is that the agricultural cropping takes up to about 5 to 6 months. The SAH has been awarded by decreasing the outdated fuel up to 30 % this reduction increases the profit cost and shows why SAH used mainly in agriculture.

2.1.5 Industrial Buildings

Solar air heaters play a very important role in industries, for industrial building the air heating applies to the building need a huge amount of volume of the outside air to put in place of the air exhausted from welding, painting areas etc. In avoiding convectional use of a heater to create solar air heater can be put in place of a conventional heater which means we can join preheated air with warm building ceiling air and bring this air out to the building. It's possible to design a solar air

heater that can be used as a standard air makeup heater because the ceiling and other parts of the area are very wide open. In most companies that the air cannot go round to achieve a constant flow of temperature, we have the interior components of the system and a circulation damping system, fan and a fabric distribution. In many cases, the flow ratio inside the solar air heater is not the same it has a change in the collector of the outside because of the inlet and outlet temperature. They can as well be designed in a form so as the temperature will go round to achieve the constant flow of temperature [26].

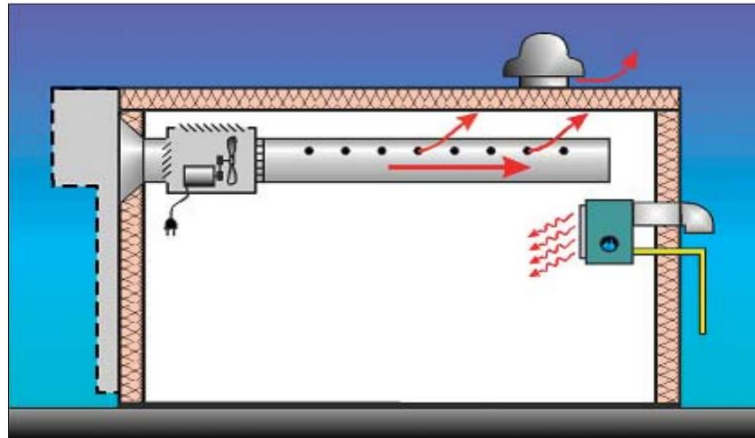


Figure 2: Industrial Building [26]

2.1.6 Process Air

Solar process air heating systems are almost identical to ventilation air preheating system. The perforated plate absorber is located in any suitable place that can be easily exposed to the sun. Sloped roofs, as well as walls, are acceptable mounting structures. A continual flow of air is taken throughout the collectors and is ducted into the air intake of the process. If need be, additional heat can be added from back up sources to reach the desired air temperature and some or all of the process air can bypass the collectors if the air is above the desired temperature [26].

States that every understudy requires at least 15 m of natural air, and it is exorbitant to warmth this vast volume of ventilation air utilizing traditional techniques. Schools aimed the daytime when sun based vitality is accessible, making sun-powered warming of outside air one of the best applications. Showcasing the best sun based innovations is of critical instructive esteem. Many schools loads up perceive that introducing heavenly bodies nearby serves as an instructive device to train understudies about the renewable vitality innovations that will get to be standard in their lifetime.

2.2 Utilization of Solar Air Heater

It is generally practical to use solar air heaters to supply energy for any application that uses solar-heated liquids. The following are the areas applicable for solar air heating:

2.2.1 Heating and Cooling of Buildings

Many different air heaters have been used in space heating and cooling. Air heaters can be actively used for heating and cooling buildings. They can also useful with desiccant beds for solar air conditioning. The heat produced from air heaters can be utilized to heat generators of an absorption air conditioner for cooling purposes.

2.2.2 Drying and Curing of Agricultural Products

The application of solar air heaters in this area is quite encouraging. Consider a third world country like India where cultivation is the foundation of the economy [27]. The significant of drying is very necessary when it comes to the economic growth of the country. Crops can now be dried using solar air heaters indirectly .The leading edge of this is the sanitary measures used to dry the crops. The likelihood of contaminating the food products with dust or bacteria is very minimal. When drying the crops indirectly, hot air from solar air collector is spread throughout the crop to

decrease the dampness. The air can flow using a fan or by natural convection, the air heaters are called active or passive dryers. In the passive dryer, the warm air rises through the air heater and moves into the drying chamber due to the buoyancy effect.

2.2.3 Applications in Industry

The uses of air heaters are becoming more apparent in industries. In the wood industry, hot air is being used to season timber. In that of the plastic sector, solar air heaters are being used to cure the plastics. Air heaters are also being used in the regeneration of dehumidifying agents. Solar air heaters are attached to an industrial application on the basis of industrial cogeneration.

2.3 Comparison of Solar Air Heaters

Depending on the absorber plate used, SAHs can be categorised into Porous and non-porous. Porous type absorber plates have materials like matrix, metal sponge wire mesh etc., whilst non porous types comprise of standard SAHs like V-corrugated sheets, flat plates etc.

Table 1: Absorber surface shapes [28]

Description	Advantage	Disadvantage
Fins and extended surfaces	<ul style="list-style-type: none"> • Efficiency increases as number of fins increases. • Efficiency increases as Length of fin increases. 	<ul style="list-style-type: none"> • Entropy decreases as number of fins increase
Baffles	<ul style="list-style-type: none"> • Increase heat transfer area • Controls flow direction • Have higher flow blockage than fins 	<ul style="list-style-type: none"> • Higher flow blockage than fins

Combination of fins and baffles	<ul style="list-style-type: none"> • Thermal efficiencies higher when compared to both fins and baffles 	<ul style="list-style-type: none"> • Increase in hydraulic dissipation due to higher friction factor
Roughened Surfaces	<ul style="list-style-type: none"> • Increases heat transfer • Thermal and effective efficiency also increases • Less heat loss 	<ul style="list-style-type: none"> • Increases the friction factor • Increases the blower power
Corrugated sheets	<ul style="list-style-type: none"> • Increase in useful heat gain 	<ul style="list-style-type: none"> • Increase pumping power
Wire mesh	<ul style="list-style-type: none"> • Thermal and effective efficiency also increases 	<ul style="list-style-type: none"> • Lesser solar radiation absorbance
Honey comb	<ul style="list-style-type: none"> • Helps to reduce convective heat loss 	<ul style="list-style-type: none"> • Heavy and vulnerable • Drop in efficiency due to thickness of the matrix.

Chapter 3

DESIGN AND ANALYSIS

3.1 Design and Manufacturing

3.1.1 Design Selection

In this project, 3 different collector types are being used which are cola can, conical and polymer panel type, but the dimensions are similar which 1930 mm in length are 960 mm in breadth and 120 mm in height.

Constructing solar air collector is a very important project for engineering student. The importance of solar air heating is mainly discussed in the background information. Its history and development and environmental use are also discussed.

3.1.2 Design Components and Measurement Equipment

For the designing of the Solar Air Heater; proper consideration should be put into some vital components that constitute the makeup for the simple manual and automatic operated the components and the role which they fulfil in designing of solar air heater are detailed below.

3.1.3 Digital Anemometer

Anemometer or often known as a wind Speed meter measures the wind velocity, which simply means the speed of which the wind travels. We have different types of Anemometer of which have different measurement features. The most common anemometer today is used to measure the speed of wind and pressure.



Figure 3: Digital Anemometer [29]

3.1.4 Thermometer

A thermometer is used to measure the temperature of different materials or substances. It can be used for solids, liquids or even gases [30]. We have a thermometer for different temperature ranges, which consist of different thermocouples which made from different materials; they are joined through an electric circuit. A voltage is produced with a ratio between temperature differences of the points.



Figure 4: Thermometer [31]

3.1.5 Pyranometer

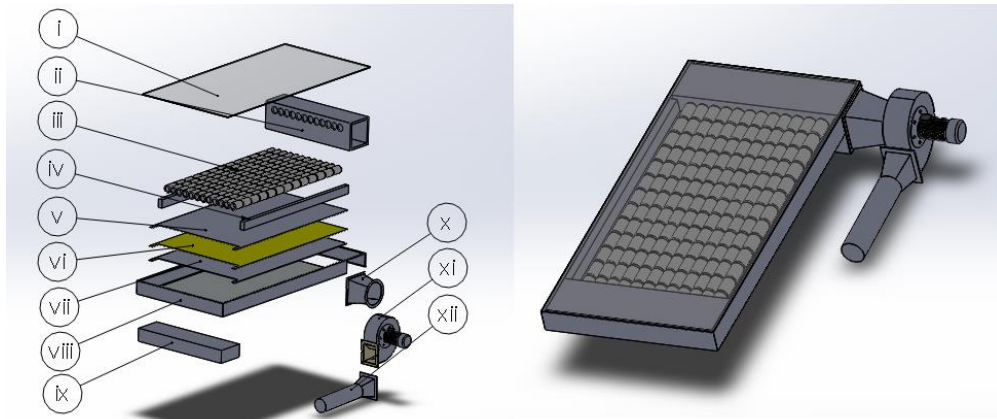
Pyranometer is utilized to quantify the irradiance from all heading. Dmytro Podolsky, business director of pyrometer maker Kipp and Zonen, [32] said that irradiance information is essential at all phases of sun-powered vitality extend. Pyrometer is operated based on the measurement of temperature difference between surfaces.



Figure 5: Secondary class pyranometer [33]

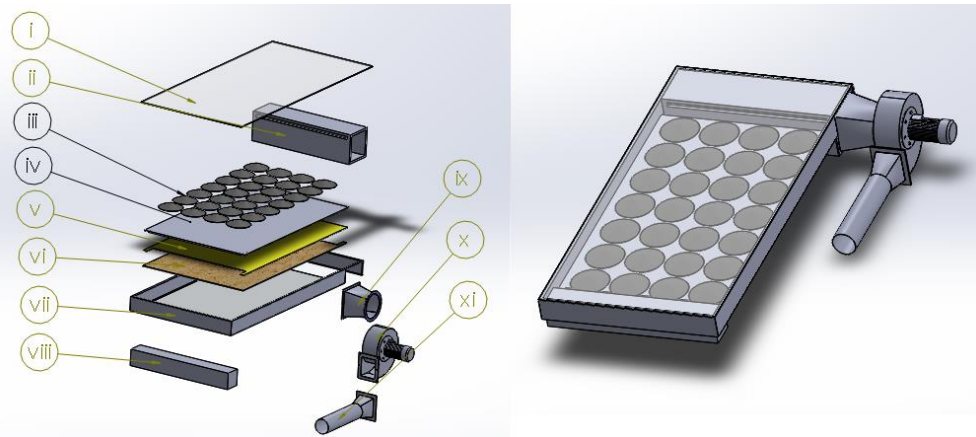
3.2 Structural Arrangement

A solar heater collector consists four main parts which are frame, absorber materials, glazing materials and insulation materials. All collector designs are shown in Figures 6 – 8.



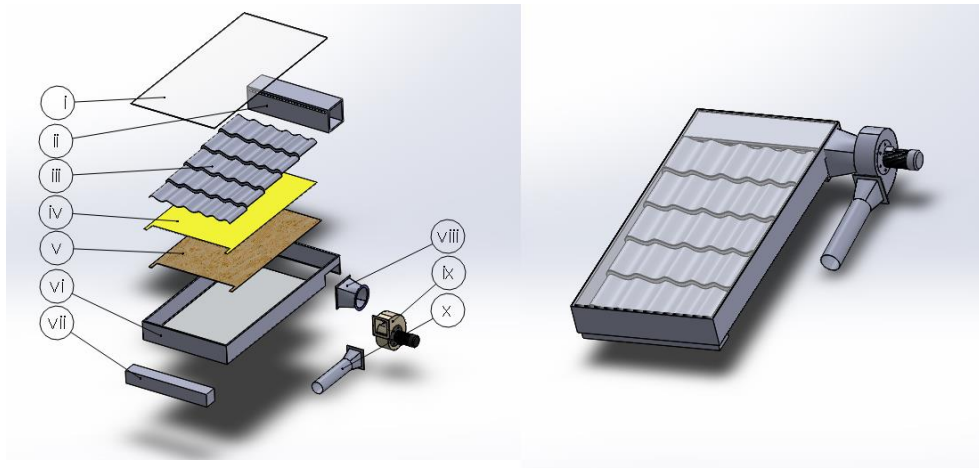
- i. Glass (width: 935 mm, h: 1935, t: 5 mm)
- ii. Collector box (output)
- iii. Cola can
- iv. Heat-Resistant Styrofoam
- v. Absorber plate
- vi. Polystyrene
- vii. Osb board
- viii. Collector panel
- ix. Collector box (input)
- x. Connection lug (al)
- xi. Power
- xii. Connection lug (al)

Figure 6: Cola can type solar air heater



- i. Glass (width: 935 mm, h: 1935, t: 5 mm)
- ii. Fan box (output)
- iii. Conic plate
- iv. Absorber plate
- v. Polystyrene
- vi. Osb board
- vii. Collector panel
- viii. Collector box (input)
- ix. Connection lug (al)
- x. Power
- xi. Connection lug (al)

Figure 7: Conical type solar air heater



- i. Glass (width: 935 mm, h: 1935, t: 5 mm)
- ii. Fan box (output)
- iii. Polymer panel plate
- iv. Polystyrene
- v. Osb board
- vi. Collector panel
- vii. Collector box (input)
- viii. Connection lug (al)
- ix. Power
- x. Connection lug (al)

Figure 8: Polymer panel type solar air heater

3.3 Thermal Analysis

The energy analysis is related to thermodynamics and heat transfer laws and the thermal efficiency has been calculated based on the recorded data. The energy analysis presents us limits of efficiencies with different types of collector applications. By using the following formulas, I examined mass flow rate and thermal efficiencies of different types of solar air heating collectors. The efficiency of a solar collector is the ratio of the amount of useful heat collected to the total amount of solar radiation striking the collector surface during any period [34].

The efficiency of solar collector can be expressed as:

$$\eta = \frac{Q_u}{I \times A_c} \quad (1)$$

where:

A_c is the collector area, [m²]

I is solar intensity, [W / m²]

Q_u is useful heat collected, [W]

Useful heat collected for an air-type solar collector can be expressed as:

$$Q_u = \dot{m} \times C_p \times (T_{out} - T_{in}) \quad (2)$$

where:

\dot{m} is the mass flow rate, [kg / s]

C_p is the specific heat of fluid, [J / kg.°C]

T_{in} is the air temperature of the fluid at the environment, [°C]

T_{out} is the air temperature of the fluid at the exit, [°C]

Mass flow rate can be expressed as:

$$\dot{m} = \rho \times \dot{V} \quad (3)$$

where:

ρ is the density of the fluid, [kg / m³]

\dot{V} is the volume flow rate, [m³ / s]

Volume flow rate can be expressed as:

$$\dot{V} = v \times A \quad (4)$$

v is the flow velocity of the mass elements, [m / s]

A is the cross-sectional vector area/surface, [m²]

Heat loss can be determined as :

$$Q_{loss} = U_{overall} \times A_{surface} \times \Delta T \quad (5)$$

Where ;

Q_{loss} is the heat loss, [W]

$A_{surface}$ is the surface area for each collector, [m²]

$U_{overall}$ is the overall heat transfer coefficient, [W/ m².K]

ΔT is the difference between the internal and external collector surface, [°C]

$U_{overall}$ can be determined as :

$$U_{overall} = U_{Top} + U_{edge} + U_{bottom} \quad (6)$$

Where:

$U_{overall}$ is the overall heat-loss coefficient, [W/ m².K]

U_{Top} is the heat-loss coefficient for top surface of the collector, [W/ m².K]

U_{bottom} is the heat-loss coefficient for bottom surface of the collector, [W/ m².K]

U_{edge} is the heat-loss coefficient for edge surface of the collector, [W/ m².K]

U_{Top} , U_{edge} and U_{bottom} can be determined as :

$$U_{Top}, U_{edge}, U_{bottom} = \frac{1}{R_{os} + \sum \frac{l_{materials}}{k_{materials}} + R_{is}} \quad (7)$$

Where ;

$k_{material}$ is the thermal conductivity of using material, [W/ m °C]

$l_{material}$ is the thickness of using material, [m]

R_{os} is the outside surface resistance, [m²°C/W]

R_{is} is the inside surface resistance, [m²°C/W]

Using materials are stated in following Table 2;

Table 2: Thermal Properties of Materials [35]

Insulation Materials	Thermal Conductivity(<i>k</i>)	Thickness(<i>l</i>)
Soft wooden fan box	0.14W/ m°C	18 mm
Aluminium conic	213W/ m°C	0.4 mm
Soft Wooden collector box	0.14 W/ m°C	15 mm
Aluminium cola can	213W/ m°C	0.1 mm
Glass at the mid-point	1.09 W/ m°C	4 mm
OSB	0.16 W/ m°C	10 mm
Glass wool	0.08 W/ m°C	10 mm
Outside glass	1.09 W/ m°C	4 mm
Aluminium Collector panel	213W/ m°C	1 mm
Aluminium Polymer Panel	213 W/ m°C	1 mm

3.4 Cost Analysis

Here is a break-down for the cost estimation for the solar air heater. Table 3 includes all of the instruments that are used to build the collectors. The most expensive part is related to motor. For capturing more solar energy and producing more hot air subsequently, the same motor could be use in larger planet.

Table 3: Cost analysis table

	AMOUNT	PRICE \$	TOTAL \$
MOTOR	3	80	240
GLASS (935*1935mm)	3	20	60
ALUMINIUM ABSORBER PLATES	9	8	72
SEMI CIRCULAR PARTS (CONIC)	16	2	32
COLLECTOR PANEL	3	30	90
COLLECTOR BOX	3	9	27
COLLECTOR FAN BOX	3	8	24
OSB	3	6	18
SCREW	3 (BOX)	5	15
SILICONE	15	4	60
GLASS WOOL (900*1560*5mm)	3	5	15
BLACK PAINT	15	1.5	22.5
TOTAL			676.5

Chapter 4

EXPERIMENTAL STUDY AND TESTING

4.1 Manufacturing and Assembly

The manufacturing process was carried out successfully within a span of four (4) days. The testing of the finished product was done on the last day of completion. Three different designs of SAHs with each having different dimensions were to be manufactured. However, most parts of the SAHs were similar such as the collector boxes, fan boxes, glasses, polystyrenes motors, absorber plates and osb. Osb's were bought from a carpenter and then fastened to the inner surface of the collector with screwing. Then, glass wool material was glued on the osb's with silicon to prevent heat loss. 3 collector boxes and 3 fan boxes were produced in the mechanical engineering workshop. Woods were been cut in square shapes according to dimensions and boxes were made with these woods. Fan boxes of the collectors were placed on the top side of collectors having a gap from fan side to allow the airflow from the collector to fan. All collector boxes were assembled with screws and silicon. Finally, different absorber plates such as cola can type, conical type and polymer type were made. In cola can, 156 piece square tubes were used and assembled vertically to base of collector. In conical absorber plate, 2 pieces of aluminum sheet metal were constructed into 28 pieces of conical parts with cutting and bending processes. For the polymer panel, the water passage channels on the roofs of the buildings were used. All the parts were assembled one by one on the absorber plate with screwing again.

4.2 Detailed Manufacturing Process

The solar absorbent collectors were manufactured using cola can, conical and polymer panels that were painted matte black. They were done so to resist high temperatures. The upper parts (cover) of cans were designed in a specific way to help increase the heat exchange performance between the air passing and the collector cans. At first, the cans were emptied to make the solar panels. To get the bad smell out of the cans, they were washed thoroughly. All cans were glued together using adhesive silicone. Top and bottom of all pop cans were compatible and fit perfectly. Some glue/silicone was put on the edge of one can and pressed it against another one. In that way, the glue/silicone did not run from the edge. Air intake and exhaust boxes for cola cans solar panels were made using wood or aluminium, 1 mm/(0.04in) thick. Gaps around the edges were filled with adhesive tape or heat-resistant silicone. 55 mm/(2.16in) diameter cut-outs were drilled on one side of the intake/exhaust box. The adhesive dried very slowly, therefore, it was left to dry for over 24 hours. The backside of cola can solar panels box was made out of plywood. Insulation of solar panel was achieved by applying rock wool. Pay special attention to insulation around the openings for the solar collector air inlet/outlet. Special hooks were attached to all four corners of the solar collector so that it can be easily mounted on the inclined of iron using 10mm/0.4in screws. An empty box was placed on the wall to precisely mark the spot for drilling the air inlet/exhaust. The casing of cola can solar panel is covered with Plexiglas attached to the frame and thoroughly corked with silicone.

4.3 Experimental Methodology

The steps of experimental methodology that used in this research study are as follows;

- Turn on fan motor.
- Measure glass temperature at different times throughout the day.
- Measure Absorber temperature at different times throughout the day.
- Measure air temperature at different times throughout the day.
- Measure Outlet air temperature at different times throughout the day.
- Measure solar intensity radiation at different times throughout the day.
- Tabulate data on spreadsheet.
- Use recorded data to calculate the useful heat collected.
- Calculate efficiency and heat loss from data obtained.

4.3.1 Experiment Procedure

The collectors were tested and the data was taken at the roof of the Mechanical Engineering Department in Eastern Mediterranean University in Famagusta during the spring semester in between 13.05.2019 and 16.05.2019. All collectors were placed at the same tilt angle which was 36 degree. This angle was selected because the latitude angle of North Cyprus is around 35 degree. During testing stages, the inlet temperature, glass temperatures, outlet temperatures. Solar irradiance was measured with a pyranometer and the velocity of the air which exist the fan pipe with a digital anemometer for settings of the mass flow rate of the air was measured. Then, the thermal efficiency of the cola can, conical and polymer panel type of collectors was calculated one by one with different mass flow rates. Finally, these efficiencies were compared with each other.

Chapter 5

RESULTS AND DISCUSSIONS

5.1 The results of Temperature Difference Between Outlet and Inlet Air Temperature Against Time at Different Mass Flow Rates For Each Collector

After completing the final stages of the project, results were obtained and presented in the figures below. These figures contain the temperature difference between the outlet and inlet air temperature against time at different mass flow rates for each collector type. The temperature difference between outlet and inlet air temperature against time at each mass flow rate are illustrated separately for each collector type and the efficiency performance at different and same mass flow rates against time for each collector types are also shown. After observing all these figures, I have presented the data which indicates the collector type efficiency at certain mass flow rates.

Figure 9 shows the temperature difference throughout the day at different mass flow rates for cola can type collector. From the figure below we can see that when the flow rate was 0.02 kg/s, the graph indicates a steady increase in temperature difference (between 9:00 and 12:30), but at 13:00 there is a sudden decline in the temperature difference. This may be due to weather conditions, there might have been clouds in the sky at that time. The maximum temperature difference at flow rate 0.02 kg/s was 25.2 °C (at 13:30). After 14:00, there is a decrease in temperature due

to the sun going down. When the mass flow rate was 0.04 kg/s, the maximum temperature difference was observed to be 14.5 °C (at 11:30). The graph has a parabolic shape indicating the changes in the sun as the day goes on. At mass flow rate of 0.06 kg/s, the graph has a continuous U shape with increasing temperature difference with maximum at 9.3 °C (at 13:30). There was a rapid reduction in temperature difference at 14:30 due to weather conditions. Finally, when the mass flow rate was 0.08 kg/s, the maximum temperature difference was 6.3 °C. These data were recorded during spring time between 13th-16th of may 2019 (from 9:00 to 16:00).

Figure 10 illustrates the temperature difference throughout the day at different mass flow rates for cola can type collector but in the summer time between 16th-19th of july 2019 (9:00 to 16:00). From the figure below we can see that the maximum temperature difference when the flowrates were 0.02 kg/s, 0.04 kg/s, 0.06 kg/s and 0.08 kg/s are 31.2 °C, 17.5 °C, 11.6 °C and 8.9 °C. The figure compares the temperature differences at different mass flow rates. From the figure we can conclude that the the mass flow rate has an inversely proportional relationship with he temperature difference. The graphs on the figure shows some sudden decrement at times when it was suppose to increase steadily. This could be due to weather conditions or even measurement errors. The graphs increase steadily as the day goes on and reaches their maximum temperature differences, then decrease as the sun goes down.

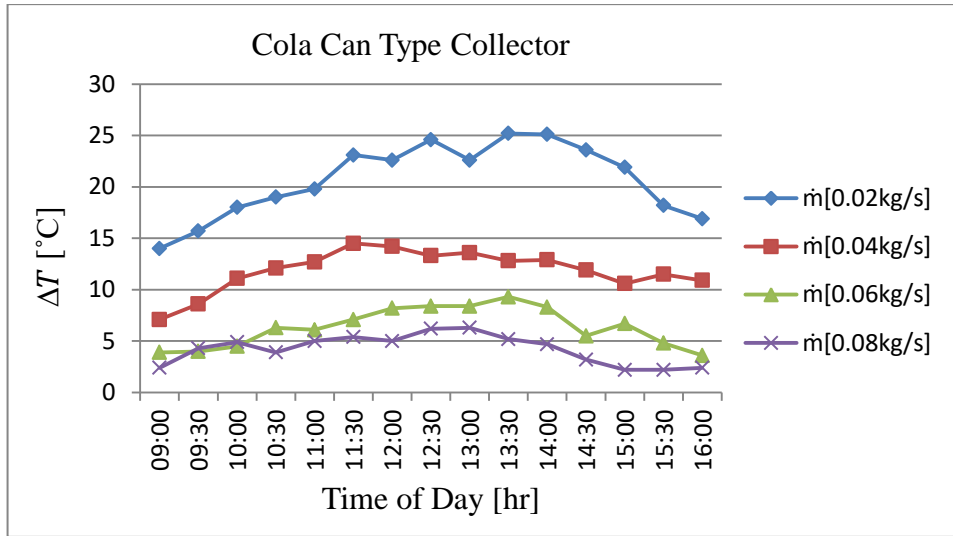


Figure 9: Cola can temperature difference vs time (13-16.05.2019)

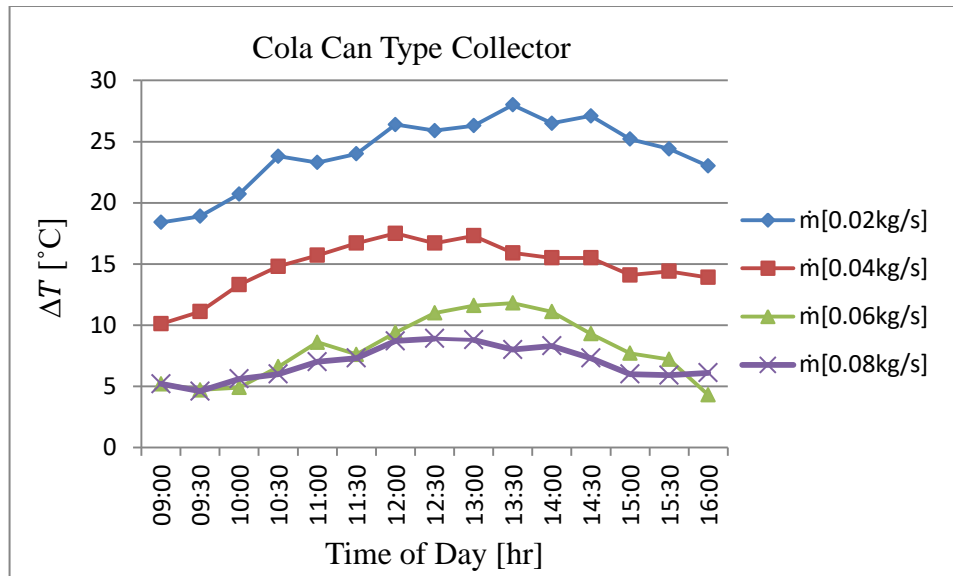


Figure 10: Cola can temperature difference vs time (16-19.07.2019)

Figure 11 compares graphs of temperature difference versus time of day at different mass flow rates for conical type collector. The figure below provides information of the maximum temperature differences when the flow rates are 0.02 kg/s, 0.04 kg/s, 0.06 kg/s and 0.08 kg/s are 21 °C, 14.4 °C, 9.1 °C and 6.5 °C respectively. These data were recorded during spring time between 13th-16th of may 2019. The figure shows a variations in temperature difference through out the day, there are rises and falls in temperature difference in all of the different mass flow rates. At mass flow

rates of 0.06 kg/s and 0.08 kg/s, the two graphs intersect at different points. Even though the two graphs have different mass flow rates, some of their temperature difference values are very close. All four graphs have parabolic-like shape to them.

Figure 12 also shows the graph of temperature difference versus time of day at different mass flow rates for conical type collector but in the summer time between 16th-19th of July 2019. From the figure below, it can be seen that the maximum temperature difference when the flow rates were 0.02 kg/s, 0.04 kg/s, 0.06 kg/s and 0.08 kg/s are 26.6 °C, 18.1 °C, 11.5 °C and 8.3 °C. At mass flow rate of 0.02 kg/s, the graph increases steadily from 9:00 to 11:30. Then, there is a slight decrease in temperature difference between 12:00 to 12:30 (due to weather conditions). After this, there is a sudden rise in temperature difference at 13:00 reaching its maximum temperature difference. The graph gradually declines as the day goes on. Fluctuations in temperature difference can also be seen with flow rates at 0.04 kg/s, 0.06 kg/s and 0.08 kg/s. These sudden rise and decrease in temperature differences can be attributed to weather changes. At mass flow rate of 0.06 kg/s and 0.08 kg/s, there are points where the two graphs intersect at various times.

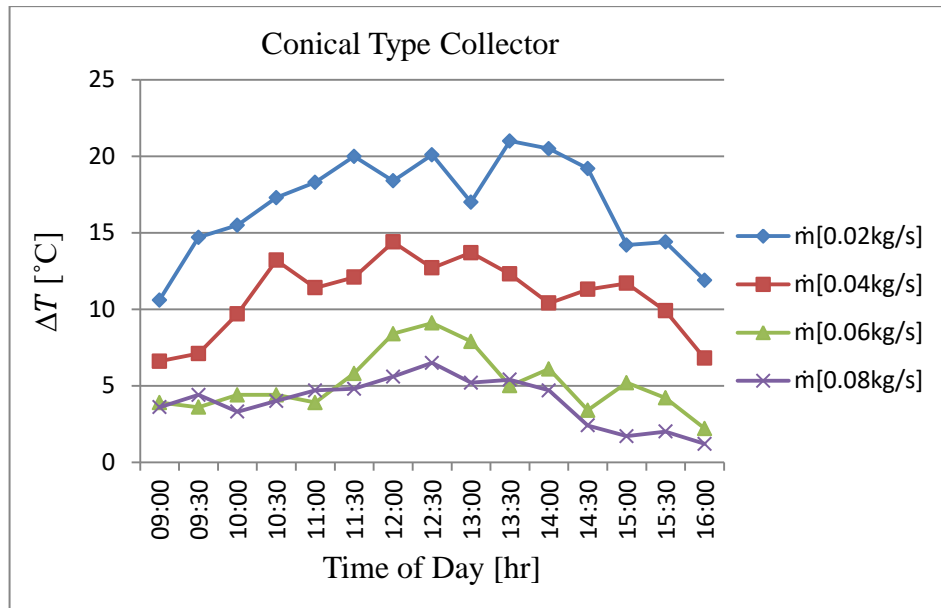


Figure 11: Conical type temperature differences vs time (13-16.05.2019)

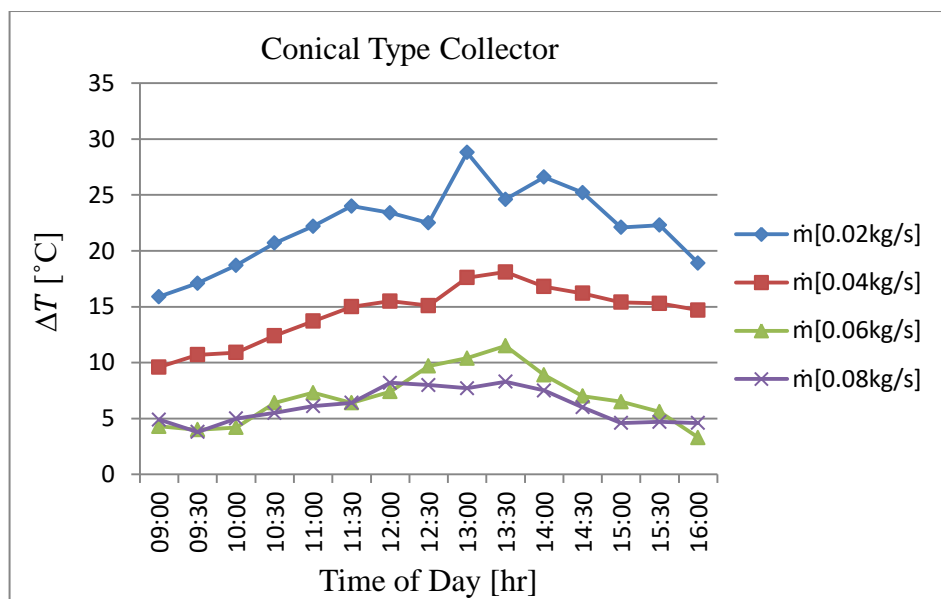


Figure 12: Conical type temperature differences vs time (16-19.07.2019)

Figure 13 shows a graph of temperature difference versus time of day at different mass flow rates for polymer panel type collector. From the figure below, it can be seen that the maximum temperature difference when the flowrates are 0.02 kg/s, 0.04 kg/s, 0.06 kg/s and 0.08 kg/s are 19.6 °C, 13.2 °C, 8.6 °C and 5.8 °C respectively. These data were recorded during spring time between 13th-16th of may 2019. At mass

flowrate of 0.02 kg/s, there is increase in temperature difference between 9:00 to 12:30 with slight fluctuations in between these times. But at 13:00, there is a big fall in the temperature difference that touches the graph when the flow rate was 0.04 kg/s. The graph then increases for a while continues to decline again until the day ends. The other three graphs also show rises and falls of temperature difference at various times.

Figure 14 also shows the graph of temperature difference versus time of day at different mass flow rates for polymer panel type collector but in the summer time between 16th-19th of July 2019. From the figure below, it can be seen that the maximum temperature difference when the flowrates were 0.02 kg/s, 0.04 kg/s, 0.06 kg/s and 0.08 kg/s are 25.2 °C, 17.8 °C, 10.4 °C and 7.7 °C. The graphs increase steadily, reaches maximum temperature difference and declines steadily as well. There are fluctuations in the temperature difference values at different times. At mass flow rates of 0.06 kg/s and 0.08 kg/s, the the temperature difference values at most points are very similar with some points intersecting.

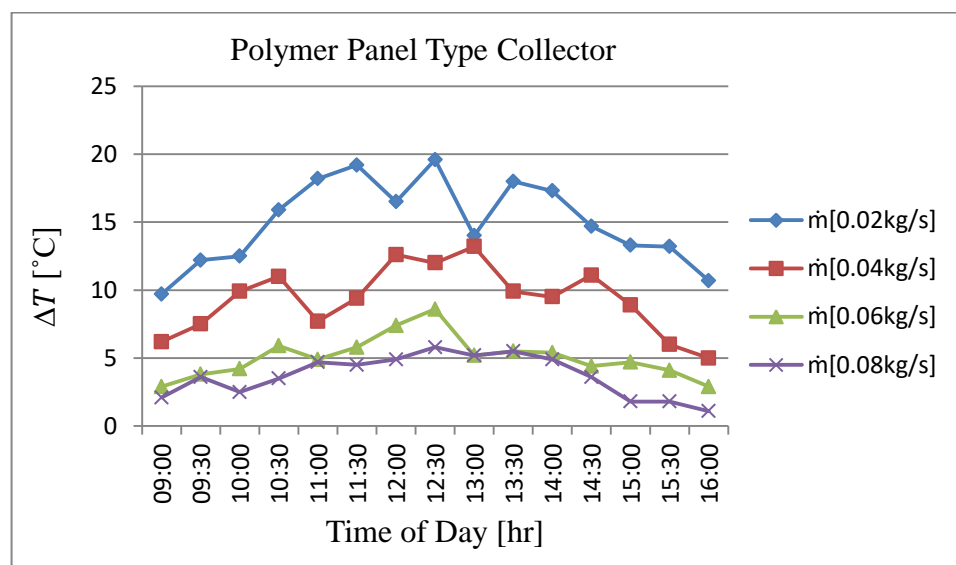


Figure 13: Polymer type temperature differences vs time (13-16.05.2019)

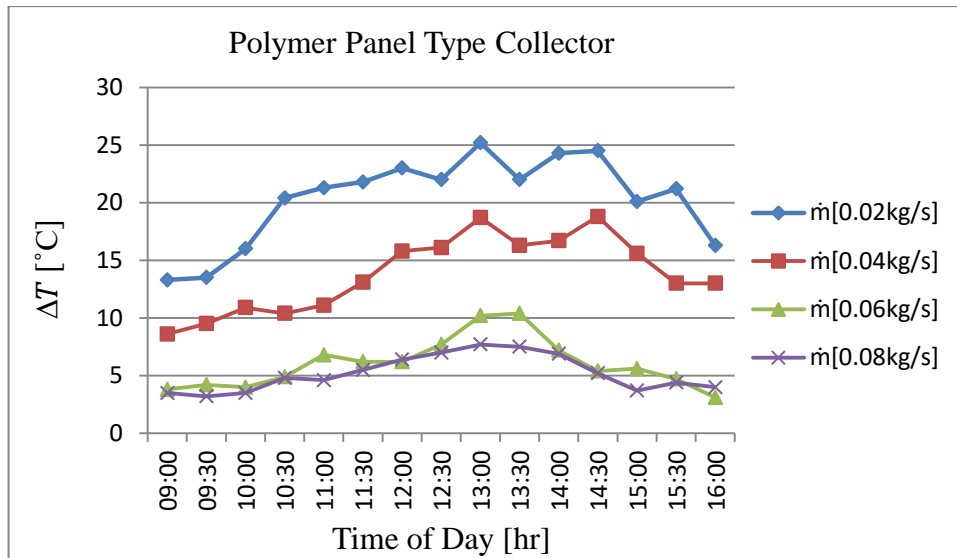


Figure 14: Polymer type temperature differences vs time (16-19.07.2019)

5.2 Thermal Efficiency of The Collectors

This section discusses the experimental thermal efficiency analysis for each collector with different mass flow rates. The studied parameters were the solar intensity factor, the absorbing plate temperature, the ambient temperature and the temperature difference between outlet and inlet air. The thermal efficiencies allow us to understand the design effects and the effect of different mass flow rates on the collectors. During the spring time in the month of May 2019, the optimum efficiency was obtained as 30 % at 0.06 kg/s mass flow rate (at 13:30) for the cola can collector type. The maximum efficiency for the conical type collector was calculated as 32 % at 0.04 kg/s mass flow rate (at 13:00). Finally, the maximum efficiency for polymer panel type collector was calculated as 29 % at 0.04 kg/s mass flow rate (at 16:00). In the summer time for the month of July 2019, the maximum efficiency for the cola can type collector was evaluated as 30 % at 0.04 kg/s mass flow rate (at 12:30). For the conical type collector, the maximum efficiency was 35 % at 0.04kg/s mass flow rate (at 13:30). Lastly, the maximum efficiency for polymer panel type collector was calculated as 32 % at 0.04 kg/s mass flow rate (at 13:00). From the above

information, it can be concluded that the efficiencies of the collectors increased during the summer time compared to the spring time. This is due to the fact that the weather is hotter in July than in May.

The results cannot be compared with mass flow rate changes because the flow rates were not changed during experiment throughout the day. However, comparison can be done for collector type efficiency values at the same mass flow rate. To compare these result, the average for all efficiency values in one experiment for the entire day was obtained and the results proved that cola can type collector had the highest efficiency for different mass flow rates. The conical type collector had higher efficiency than polymer panel type collector at different mass flow rates. Figures 15, 17 and 19 show the data obtained during the month of May 2019 for different mass flow rates for the cola can, conical and polymer panel type collectors respectively. Figures 16, 18 and 20 displays the data gathered during the month of July 2019 for varying mass flow rate values for cola can, conical and polymer panel type collectors.

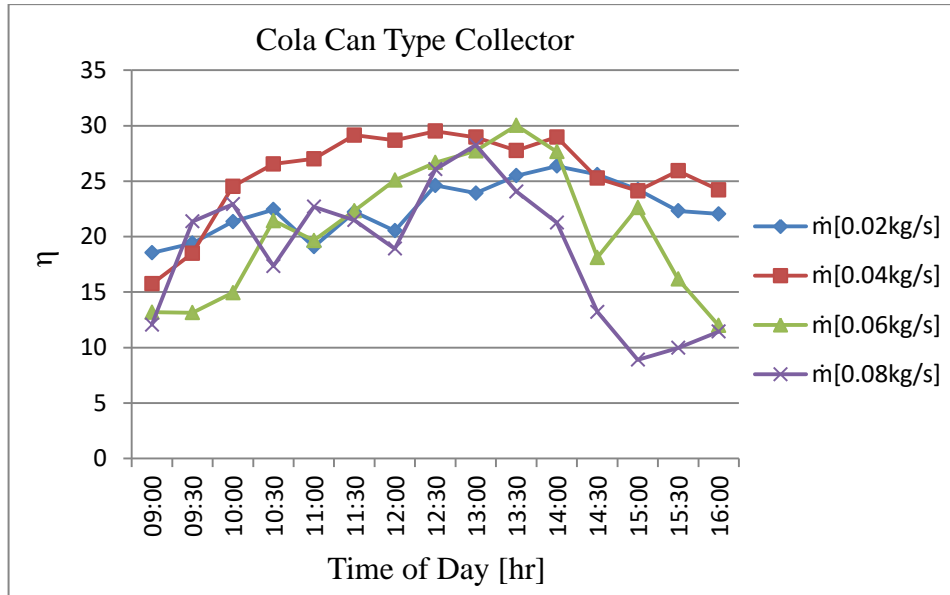


Figure 15: Efficiency performance at different mass flow rates against time for the cola can type SAH collector in (13-16.05.2019)

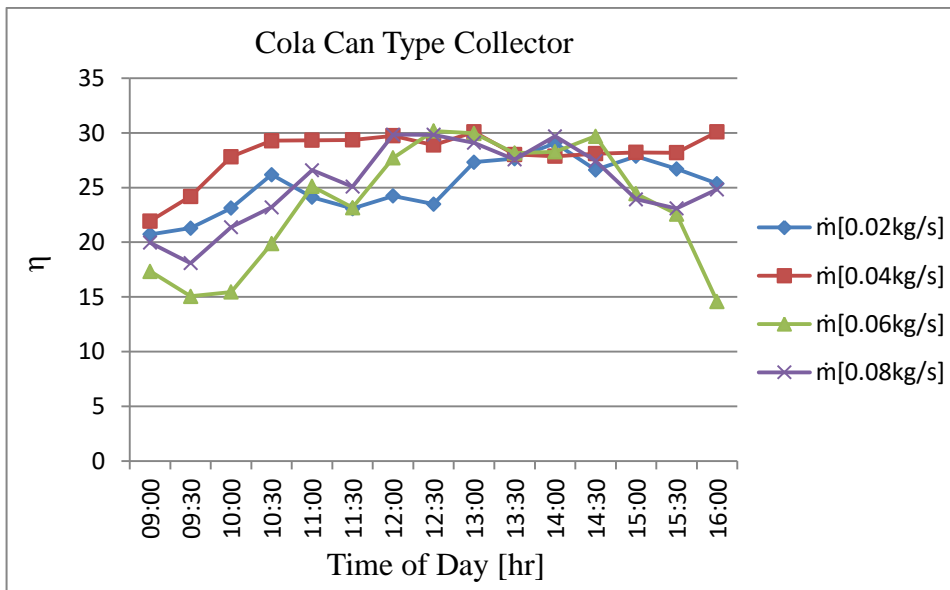


Figure 16: Efficiency performance at different mass flow rates against time for the cola can type SAH collector in (16-19.07.2019)

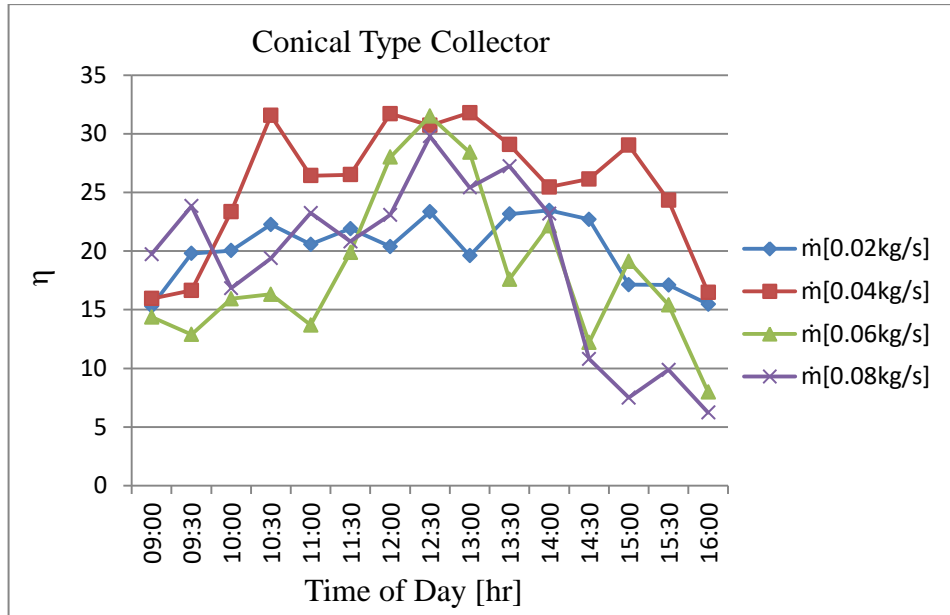


Figure 17: Efficiency performance at different mass flow rates against time for the conical type SAH collector in (13-16.05.2019)

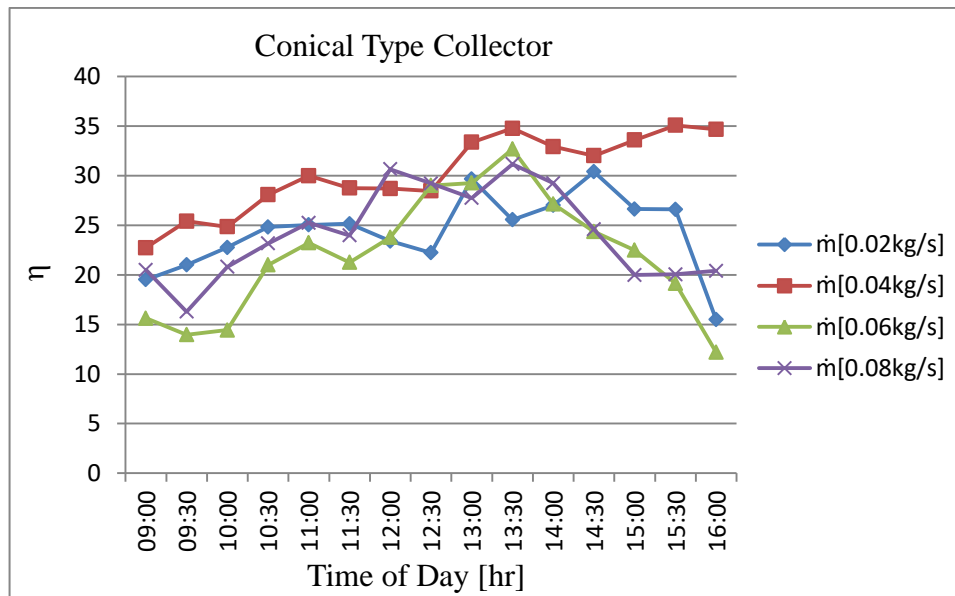


Figure 18: Efficiency performance at different mass flow rates against time for the conical type SAH collector in (16-19.07.2019)

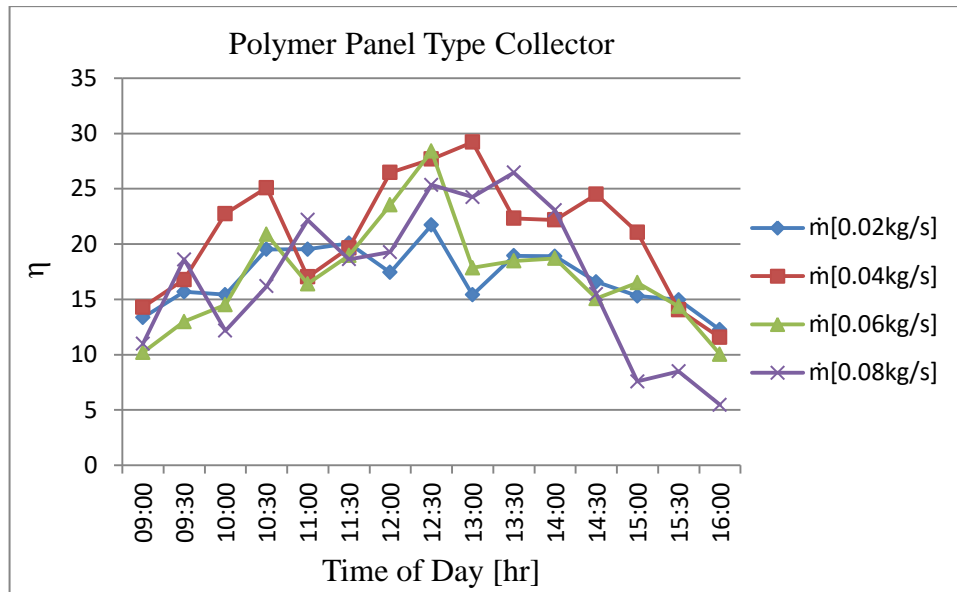


Figure 19: Efficiency performance at different mass flow rates against time for the Polymer panel type SAH collector in (13-16.05.2019)

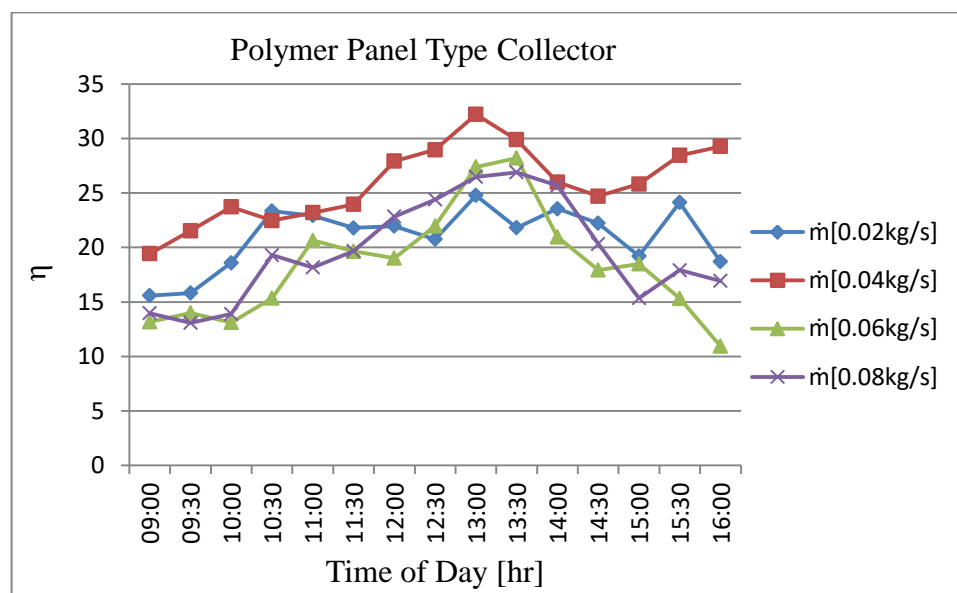


Figure 20: Efficiency performance at different mass flow rates against time for the Polymer panel type SAH collector in (16-19.07.2019)

5.3 Heat Loss of Collector Types

To get the best possible efficiency results, well-insulated materials are required such as foam, glass wool, aluminum plates, osb plate, aluminum foil, glass. Different designs may require different insulation materials, in spite of the fact, you can use the same materials to determine the absorber shape effect on each collector type. Despite all these insulation, there is still going to be heat loss. The thickness of the material, the values for thermal conductivity and heat loss equations are a must for heat loss analysis. See chapter 3 for calculations. The coefficient of the heat loss value for the top surface of the collectors were calculated as $0.56 \text{ W/m}^2\text{K}$, for edges of the collectors were calculated as $1.63 \text{ W/m}^2\text{K}$ and for bottom surface were calculated as $1.58 \text{ W/m}^2\text{K}$. The U-overall heat transfer coefficient was found as $3.77 \text{ W/m}^2\text{K}$ and it was roughly the same for each collector type. For that reason, the temperature difference is an effective parameter for calculating the heat loss, due to conduction through the surface, since this calculation requires the measurement of the surface temperatures at the top, bottom, and at the edges of the collectors, by using digital K type thermometer. This means that the heat loss directly proportional to the temperature difference. The surface areas were calculated for each collector type. The highest heat loss values for the month of May 2019 were calculated as 172.9 W for the cola can type, 132.2 W for the conical type and 129.3 W for the polymer panel type at 13:00 on 13.05.2019 (at 0.02 kg/s). For the month of July 2019, the highest heat loss values were obtained as 214.1 W for the cola can type, 181.3 W for the conical type and 166.3 W for the polymer panel type at 13:00 on 16.07.2019 (at 0.02 kg/s). From the results above, it is evident that the heat loss values were greater in July compared to the ones in May. After finishing the calculations, some figures were plotted for the month of May 2019. Figures 21, 23, 25 and 27 show the heat

losses during the time of the day. During the month of July 2019, the heat loss values were also displayed in figures 22, 24, 26 and 28.

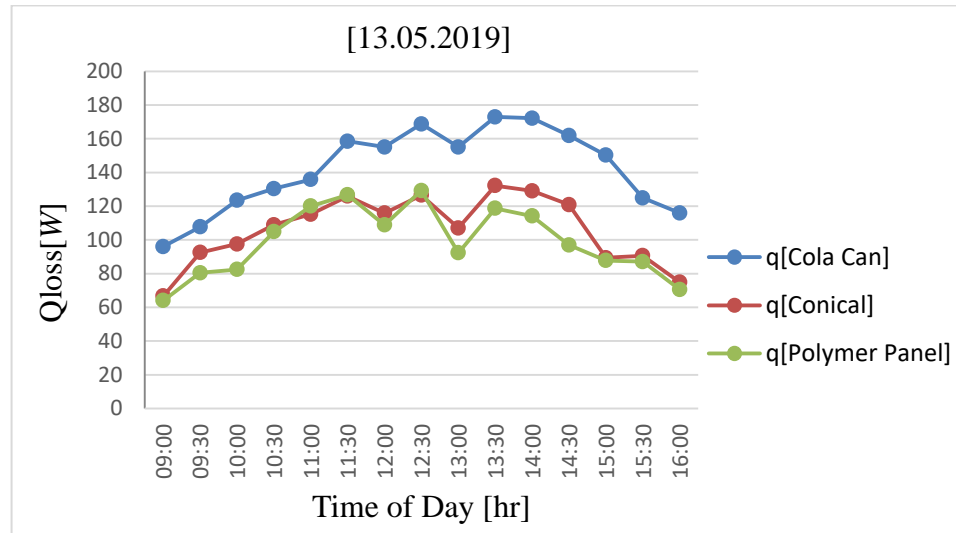


Figure 21: Heat losses values against time for each collector type at (0.02 kg/s)

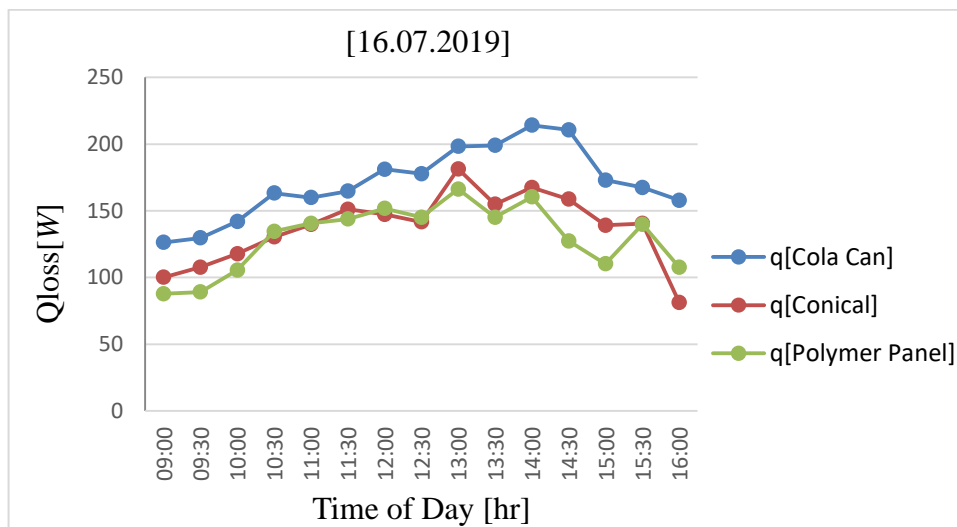


Figure 22: Heat losses values against time for each collector type at (0.02 kg/s)

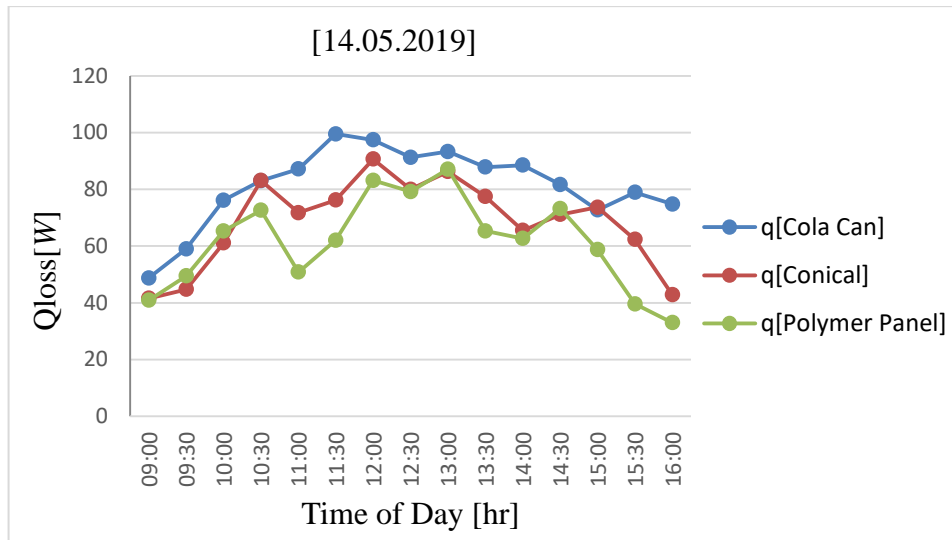


Figure 23: Heat losses values against time for each collector type at (0.04 kg/s)

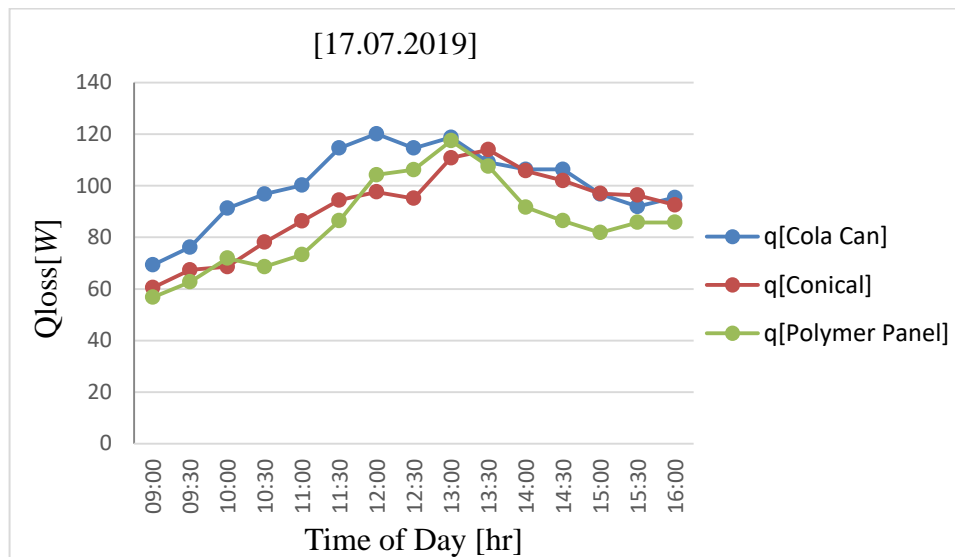


Figure 24: Heat losses values against time for each collector type at (0.04 kg/s)

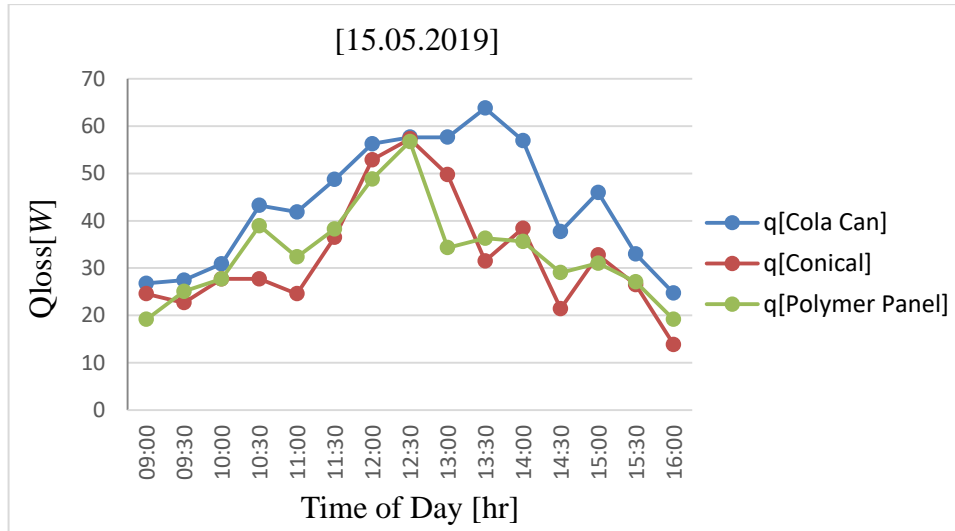


Figure 25: Heat losses values against time for each collector type at (0.06 kg/s)

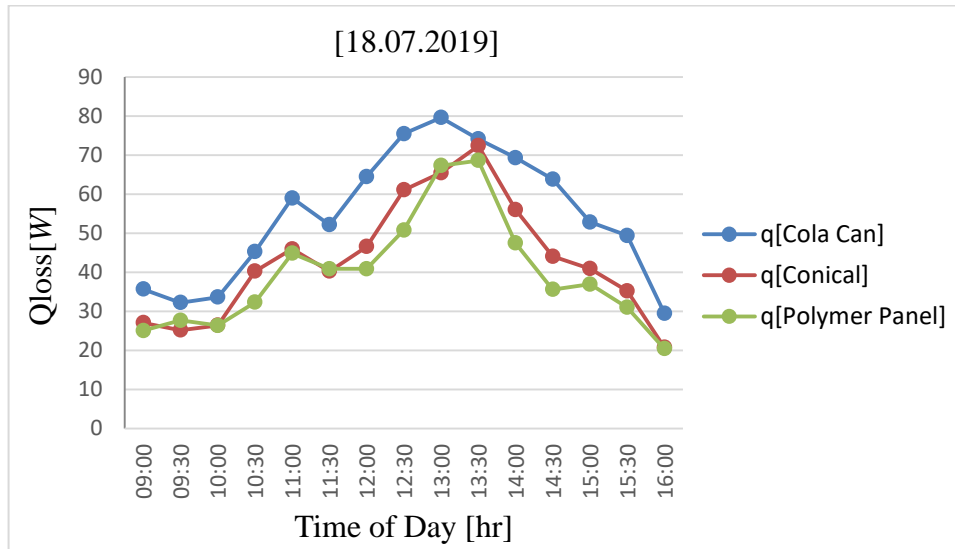


Figure 26: Heat losses values against time for each collector type at (0.06 kg/s)

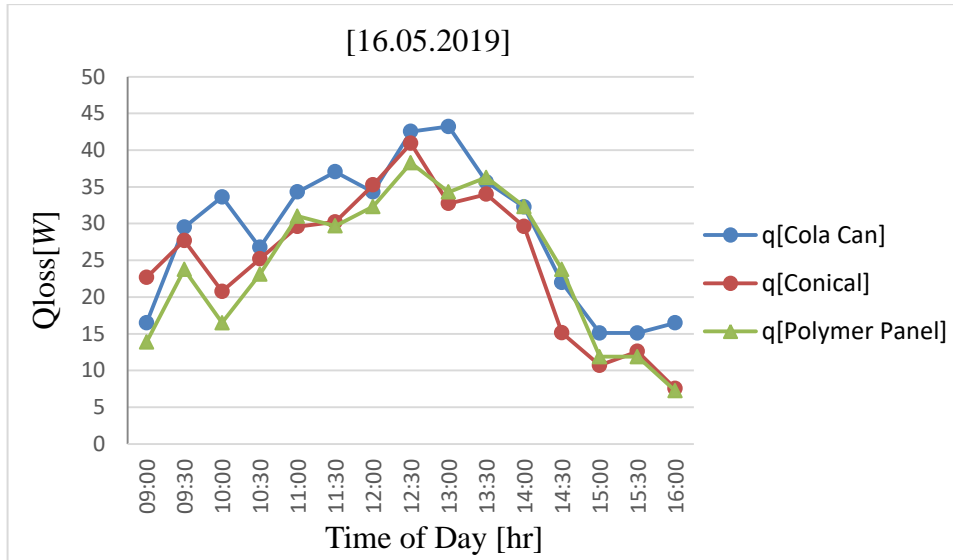


Figure 27: Heat losses values against time for each collector type at (0.08 kg/s)

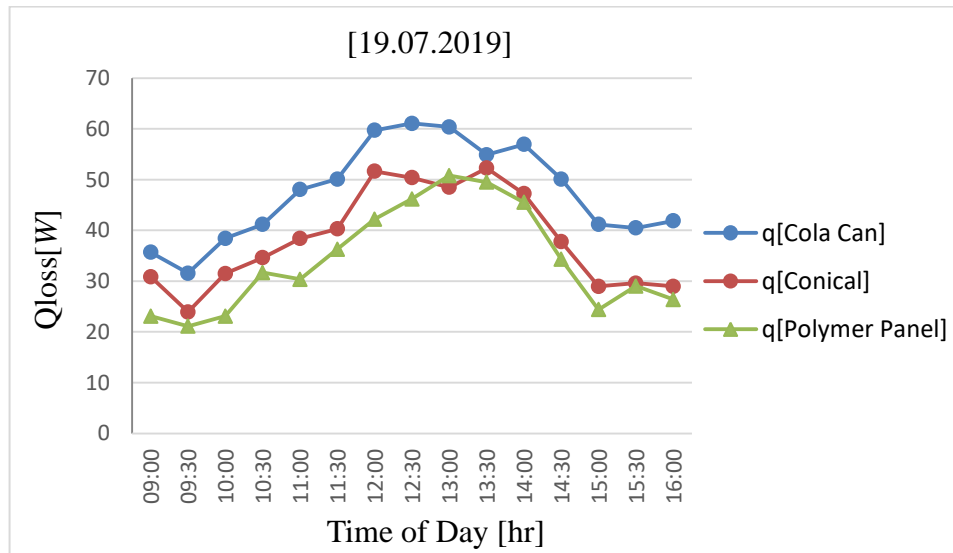


Figure 28: Heat losses values against time for each collector type at (0.08 kg/s)

Chapter 6

CONCLUSION AND FUTURE WORKS

6.1 Conclusion

In this study, different kinds of solar air heater collectors were designed and manufactured with regards to their different absorber plate shapes which were cola can, conical and polymer panel type. The principal objective of this project was to make a comparison of the thermal performance of these types of solar air collectors in spring and summer conditions on the roof of the Mechanical Engineering Department of Eastern Mediterranean University in the city of Famagusta in May and July of 2019.

Based on the results, the performance of the SAHs were noteworthy. In the light of the data obtained, the maximum temperature differences in cola box, conical and polymer type panels were 26.4 °C, 23.5 °C and 19.2 °C for May, and 29.1 °C, 30.4 °C and 24.8 °C for July, respectively. There were some differences in the efficiencies because of changing environmental circumstances and their different design parameters. The maximum efficiencies obtained for cola can, conical and polymer panels were 29%, 32% and 29% in May and 30%, 35% and 32% in July, respectively. Nevertheless, the heat loss analysis verify that the amount of heat loss is directly proportional with temperature difference and maximum heat loss value was evaluated as 172.9 W for cola can type collector in the month of May 2019 and

214W in the month of July 2019, while it reads respectively as 132.2 W and 181.3 W for conical type, and, 129.3 W and 166.3 W for polymer type.

The information gathered from this project showed that the cola can type collector had the best efficiencies at different mass flow rates. The conical type collector had better efficiencies and polymer panel type collector had the worst out of the three collectors at different mass flow rates. Although the maximum efficiency value was obtained for the conical type collector, this value was measured for only one day in the relevant period. Therefore, one can conclude that the most efficient collector is the cola can type since its efficiency is stable over the period. In summary, solar air collectors can be useful in many different applications for energy saving and they can be economically feasible in the long run. As a result, if the types of equipment are available to install these systems, the best collector type based on its efficiency or its cost is the cola can type collector.

6.2 The Future Works

Numerous different changes, assessments, and experiments have been left for future works because of time factor (i.e. the investigation with real data are time-consuming, taking days to finish a single run). Future works entail more profound evaluation of specific mechanisms, new plans to try different methods, or simply inquisitiveness.

There were some ideas that I would have loved to try during the analysis and the manufacturing of the collectors in Chapter 3 and chapter 4. The project has been predominantly fixated on the performance of SAH and most of the procedures for the design were obtained from literature reviews of adapted studies, leaving the study of

SAH outside the scope of the project. The following ideas could be tested:

It would be interesting to construct robotic movements and sensor at the bottom of the collector for taking sunlight perfectly. If we use this idea, the collector can turn easily thereby obtaining a better efficiency.

A thermal paint that can absorb and store the heat from sunlight.

It may be very practical to use copper pipes in certain parts of the collectors. Copper has fast and soft material handling and processing. Copper pipes are easily permeable by heat, conduct heat very well and are resistant to corrosion.

In the cola can type collector, we can try and use rock wool and glass wool to get better insulation. They have high thermal resistance, very stable and are capable of repelling water. Rock wool and glass wool insulation can be recycled at the end of the life of the building element where it is being used. Hopefully, the better groundwork for more future works, improvement for advance use and even a good room for adjustment and redesigning for more effectiveness and efficiency can be done.

REFERENCES

- [1] Miller, K. W. (1954). *U.S. Patent No. 2,680,437*. Washington, DC: U.S. Patent and Trademark Office.
- [2] Löf, G. O. G. (1946). *Solar energy utilization for house heating* (No. PB-25375). Department of Commerce, Washington, DC (USA).
- [3] Telkes, M., & Raymond, E. (1949). Storing Heat in Chemicals. *A Report on the Dover House, Heating and Ventilating*, 80.
- [4] Loef, G. O. G. (1950). Performance of solar energy collectors of overlapped glass type in space heating with solar energy.
- [5] Lof, G. O., & Nevens, T. D. (1953). Heating of air by solar energy.
- [6] Selcuk, K. (1971). Thermal and economic analysis of the overlapped-glass plate solar-air heater. *Solar Energy*, 13(2), 165-191.
- [7] Bliss Jr, R. W. (1955). Design and performance of nation's only fully solar-heated house. *Air Cond., Heat., Vent.;*(), 52(10).
- [8] Whillier, A. (1964). Performance of black-painted solar air heaters of conventional design. *Solar Energy*, 8(1), 31-37.

- [9] Close, D. J. (1963). Solar air heaters for low and moderate temperature applications. *Solar energy*, 7(3), 117-124.
- [10] Gupta, C. L., & Garg, H. P. (1967). Performance studies on solar air heaters. *Solar energy*, 11(1), 25-31.
- [11] Charters, W. W. S. (1971). Some aspects of flow duct design for solar-air heater applications. *Solar Energy*, 13(2), 283-288.
- [12] Cole-Appel, B. E., & Haberstroh, R. D. (1976). Performance of air-cooled flat plate collectors. In *Sharing the Sun: Solar Technology in the Seventies, Volume 2* (Vol. 2, pp. 94-106).
- [13] Sheven, E. C., Balakrishnan, A. R., & Origill, J. F. (1977). Development of a Solar air Heater. *Waterloo Research Institute, Report No. 77-04, Final Report Phase 1*.
- [14] Buelow, F. H., & Boyd, J. S. (1957). Heating air by solar energy. *Agric. Eng.*, 38(1).
- [15] Hollands, K. G. T. (1963). Directional selectivity, emittance, and absorptance properties of vee corrugated specular surfaces. *Solar Energy*, 7(3), 108-116.
- [16] Charters, W. W. S., & MacDonald, R. W. G. (1973). Heat transfer effects in solar air heaters. In *Proc. ISES Conference, Paris* (pp. 137-41).

- [17] Bevill, V. D., & Brandt, H. (1968). A solar energy collector for heating air. *Solar Energy*, 12(1), 19-29.
- [18] Charters, W. W. S. (1971). Some aspects of flow duct design for solar-air heater applications. *Solar Energy*, 13(2), 283-288.
- [19] Hollands, K. G. T., & Shewen, E. C. (1981). Optimization of flow passage geometry for air-heating, plate-type solar collectors. *Journal of Solar Energy Engineering*, 103(4), 323-330.
- [20] Selcuk, M. K. (1977). *Solar Thermal Engineering* (edited by AAM Sayigh).
- [21] Karmare, S. V., & Tikekar, A. N. (2007). Heat transfer and friction factor correlation for artificially roughened duct with metal grit ribs. *International Journal of Heat and Mass Transfer*, 50(21-22), 4342-4351.
- [22] Mittal, M. K., Saini, R. P., & Singal, S. K. (2007). Effective efficiency of solar air heaters having different types of roughness elements on the absorber plate. *Energy*, 32(5), 739-745.
- [23] Sahu, M. M., & Bhagoria, J. L. (2005). Augmentation of heat transfer coefficient by using 90 broken transverse ribs on absorber plate of solar air heater. *Renewable Energy*, 30(13), 2057-2073.
- [24] Saxena, A., & El-Sebaei, A. A. (2015). A thermodynamic review of solar air heaters. *Renewable and Sustainable Energy Reviews*, 43, 863-890.

- [25] Henning, H. M. (2007). Solar assisted air conditioning of buildings—an overview. *Applied thermal engineering*, 27(10), 1734-1749.
- [26] P. Analysis and RETScreen, (2004). “RETScreen ® International CLEAN ENERGY PROJECT ANALYSIS :,” *Water*, p. 10.
- [27] Huang, B. K., & Toksoy, M. (1983). Design and analysis of greenhouse solar systems in agricultural production. *Energy in agriculture*, 2, 115-136.
- [28] Aravindh, M. A., & Sreekumar, A. (2016). Efficiency enhancement in solar air heaters by modification of absorber plate-a review. *International journal of green energy*, 13(12), 1209-1223.
- [29] H. O. T. Wire, A. With, R. Time, and D. (1996). Logger, “HOT WIRE ANEMOMETER WITH *Experts, Toolpp*. 1–3.
- [30] Nagaie, A. (1980). *U.S. Patent No. 4,206,649*. Washington, DC: U.S. Patent and Trademark Office.
- [31] PCE Instruments, (2010) “*Manual: Digital Thermometer PCE-T 390*,” vol. 44, pp. 1–15.
- [32] King, D. L., Boyson, W. E., & Hansen, B. R. (1997). *Improved accuracy for low-cost solar irradiance sensors* (No. SAND-97-3175C; CONF-980735-). Sandia National Labs., Albuquerque, NM (United States).

- [33] The Eppley Laboratory, (1917) “*Standard Precision Pyranometer, Model SPP,*” p. 2840.
- [34] Maheshwari, B. K., Karwa, R., & Gharai, S. K. (2011). Performance study of solar air heater having absorber plate with half-perforated baffles. *ISRN Renewable Energy*.
- [35] Shawyer, M., & Medina Pizzali, A. F. (2003). The use of ice on small fishing vessels. In FAO. *Fisheries Technical Paper*. Retrieved from <http://www.fao.org/documents/card/en/c/94bc9f36072d5b6ea5a3795af528c71/>

APPENDICES

Appendix A: Assembly Drawings

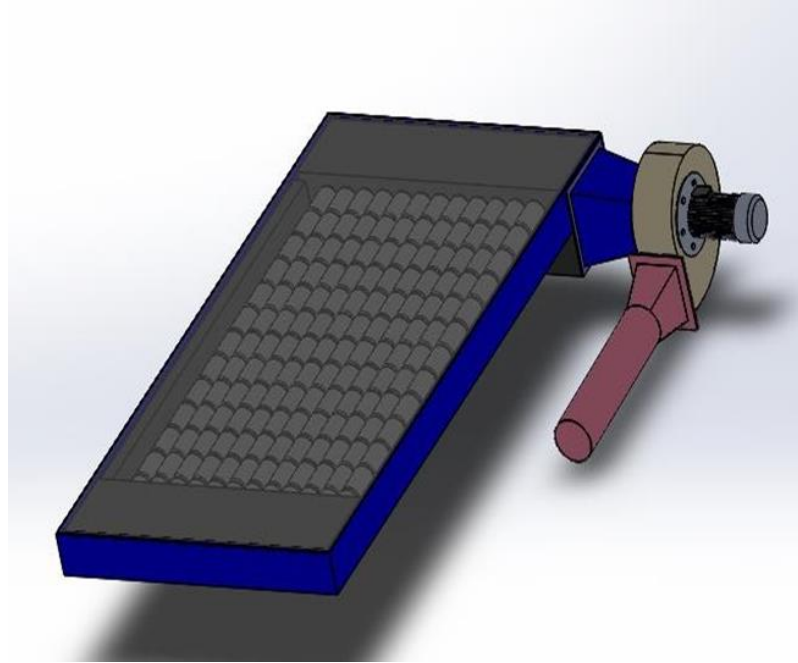


Figure 29: Aluminium Cola Can Type Collector

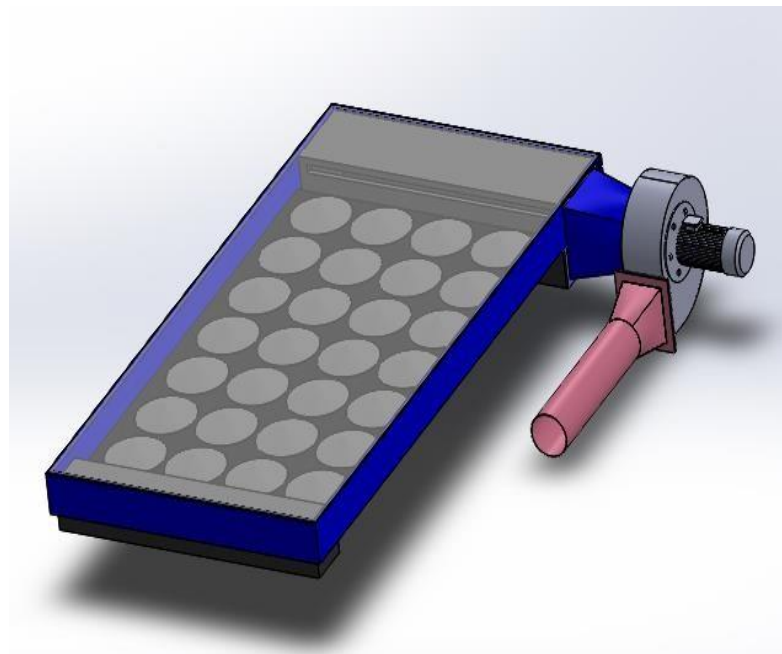


Figure 30: Conical Type Collector

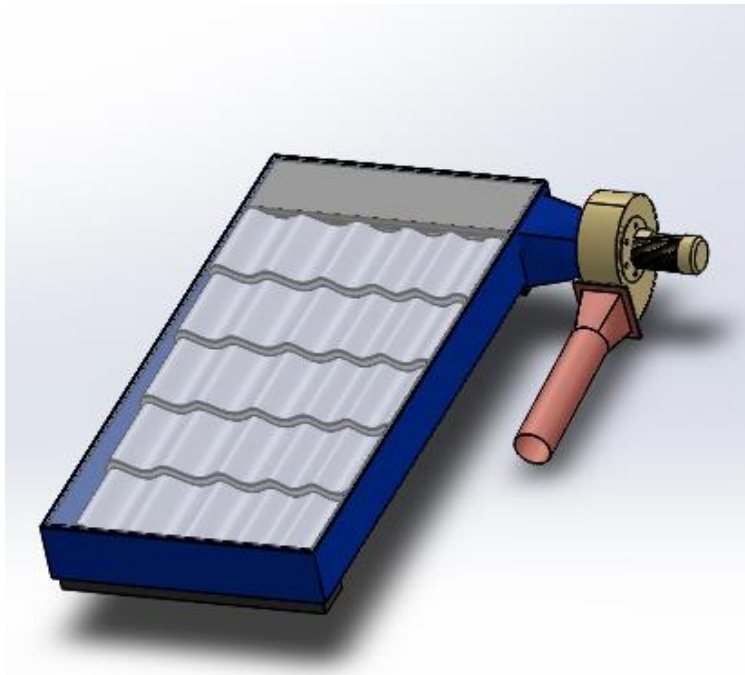


Figure 11: Polymer Panel Type Collector

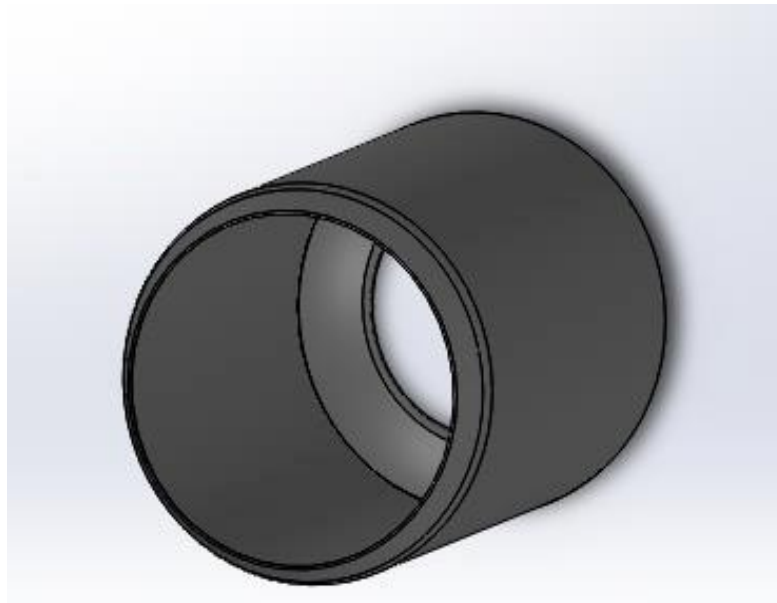


Figure 32: Aluminium Cola Can

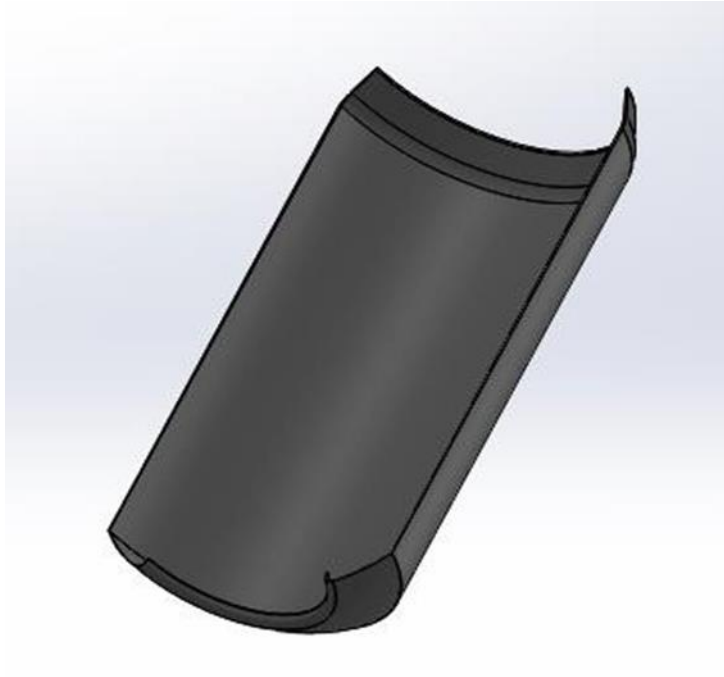


Figure 33: Aluminium Cola Can Break View

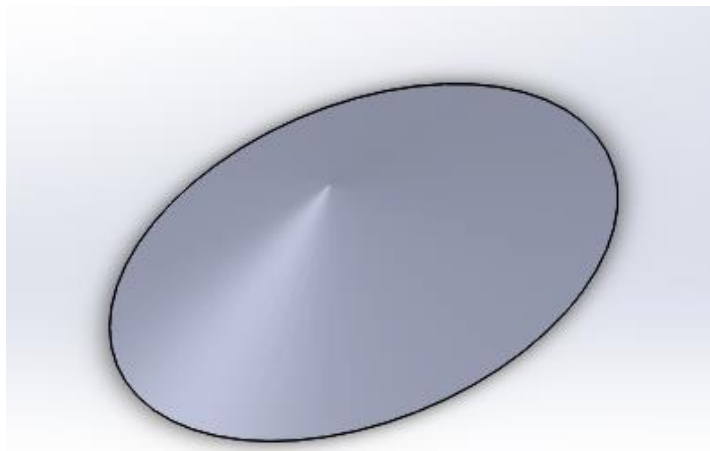


Figure 34: Aluminium Conic

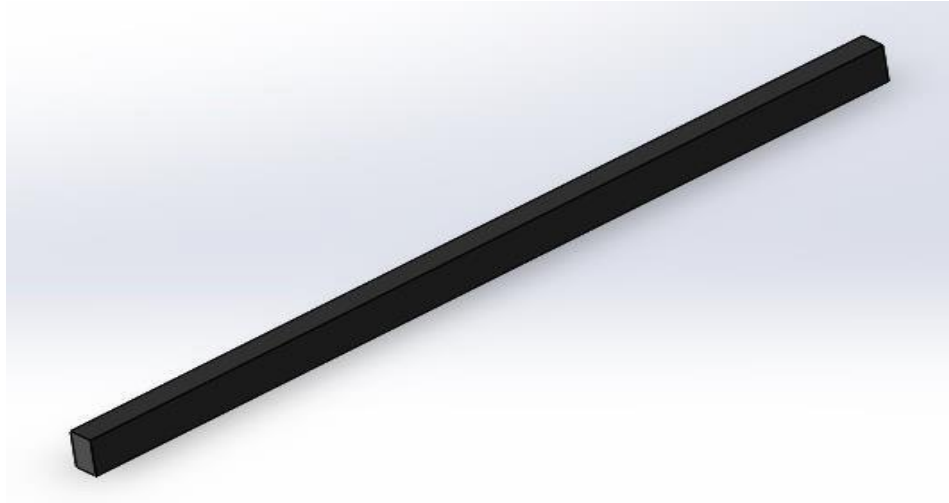


Figure 35: Heat-resistant Styrofoam

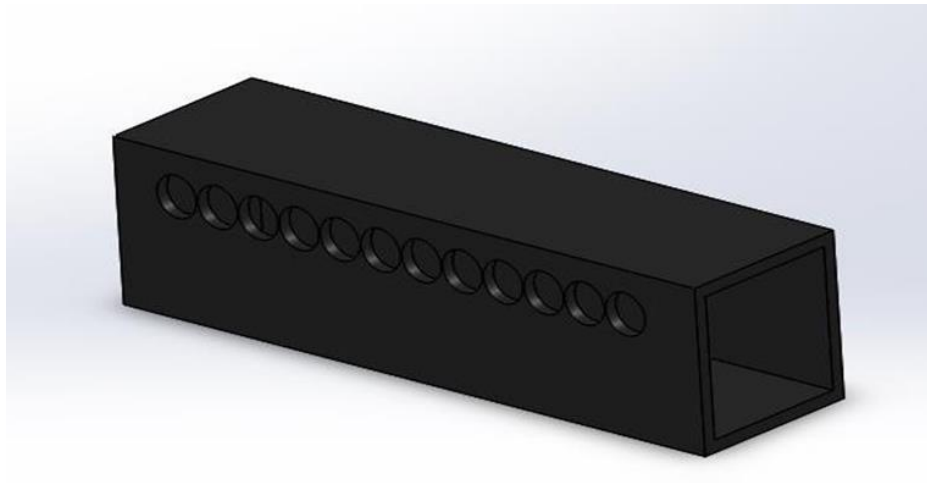


Figure 36: Wooden Cabinet Box (Can Cola Input)

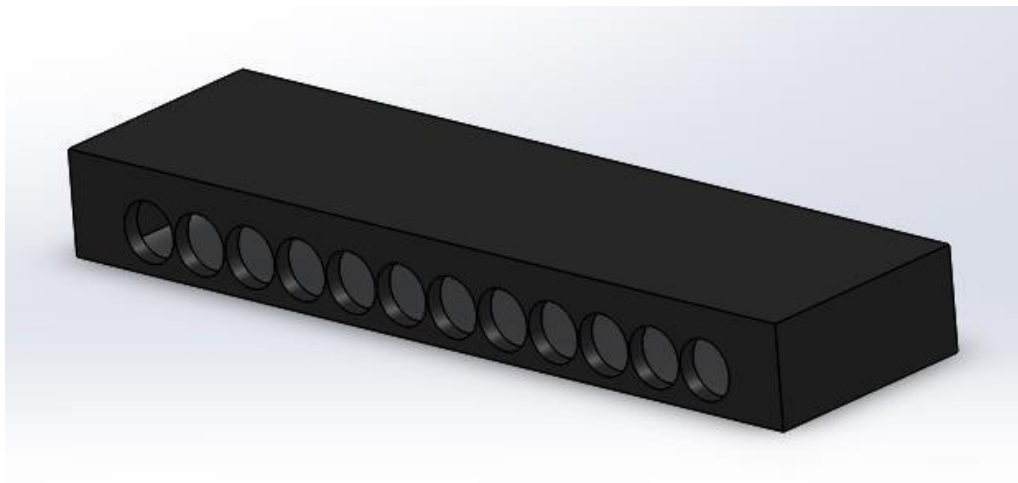


Figure 37: Wooden Cabinet Box (Can Cola Output)

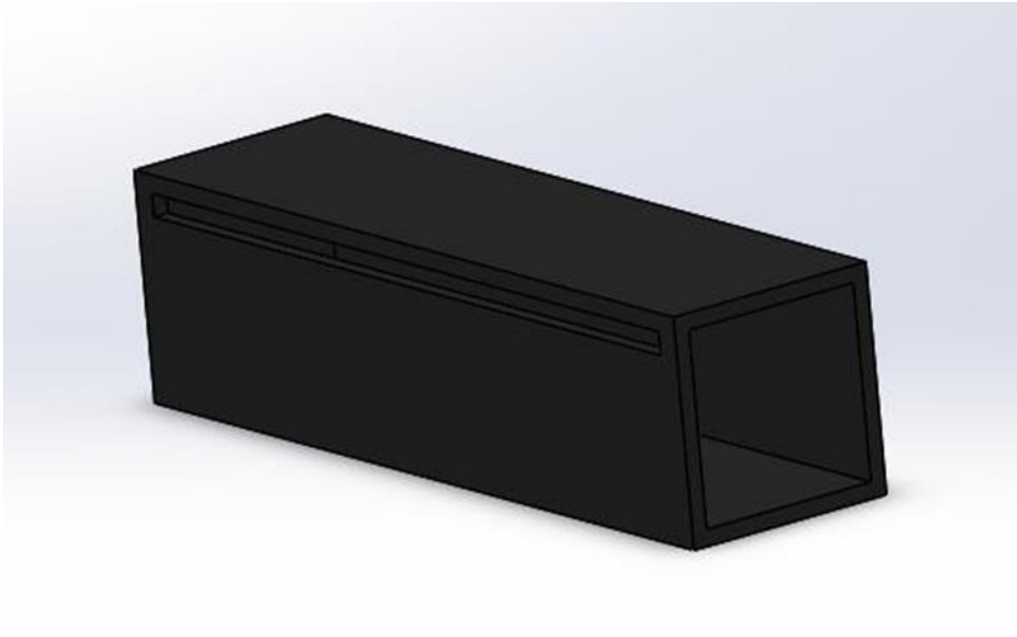


Figure 38: Conical Type Cabinet Box (Input)

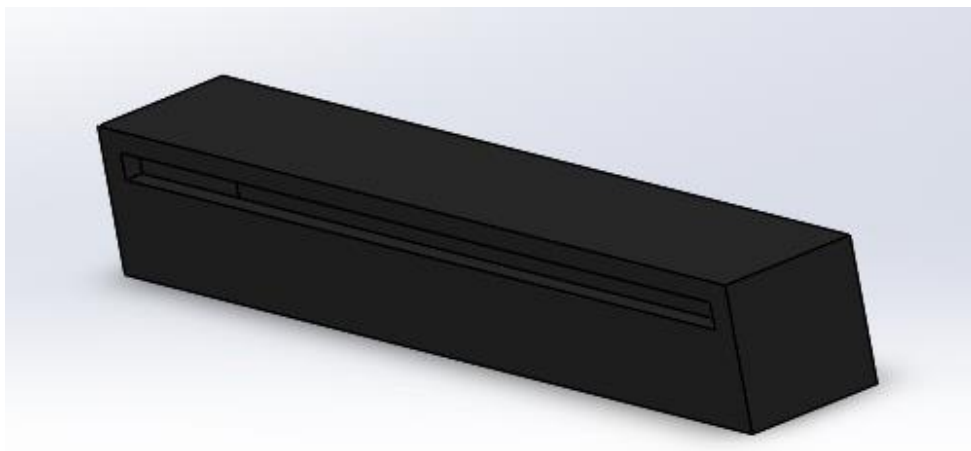


Figure 39: Conical Type Cabinet Box (Output)

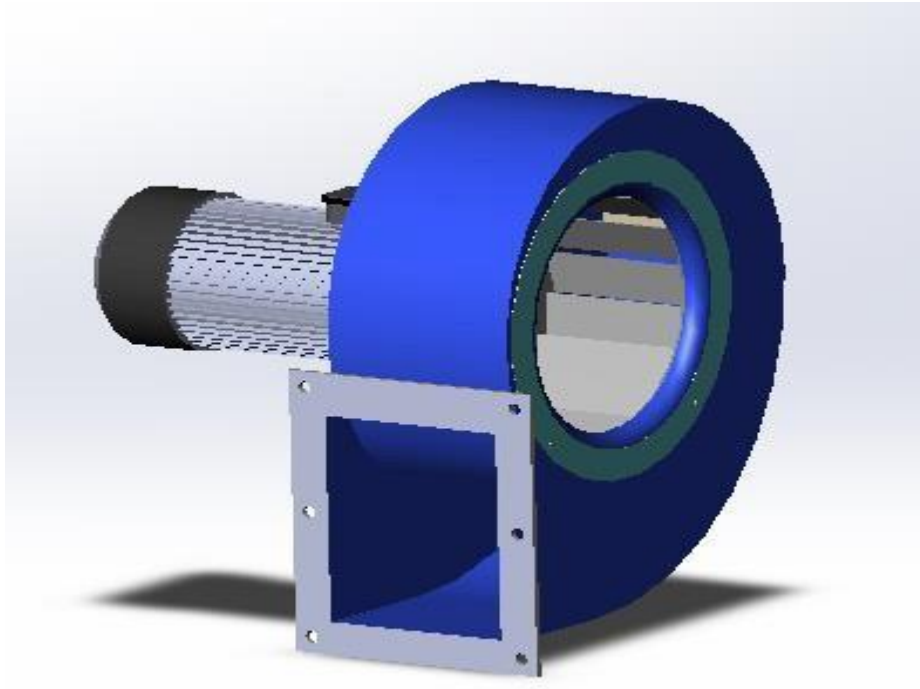


Figure 40: Fan Motor

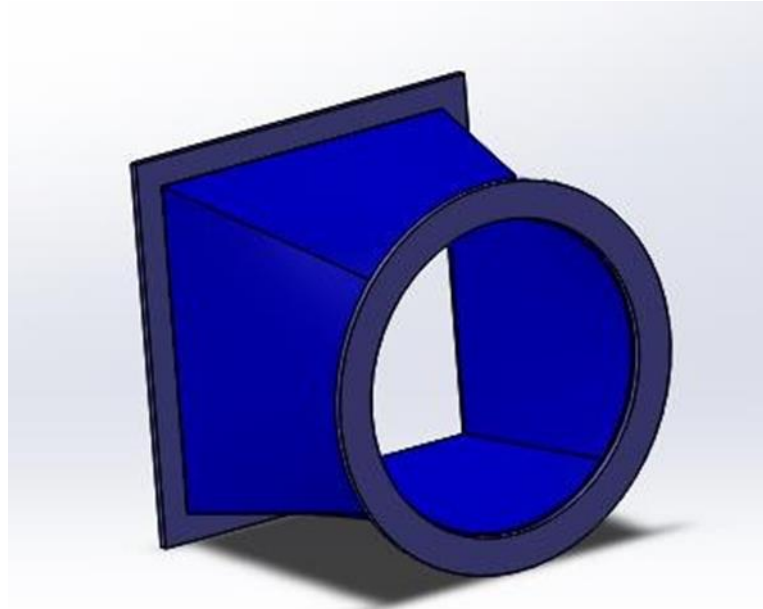


Figure 41: Connection element between cabinet and motor (Aluminium)

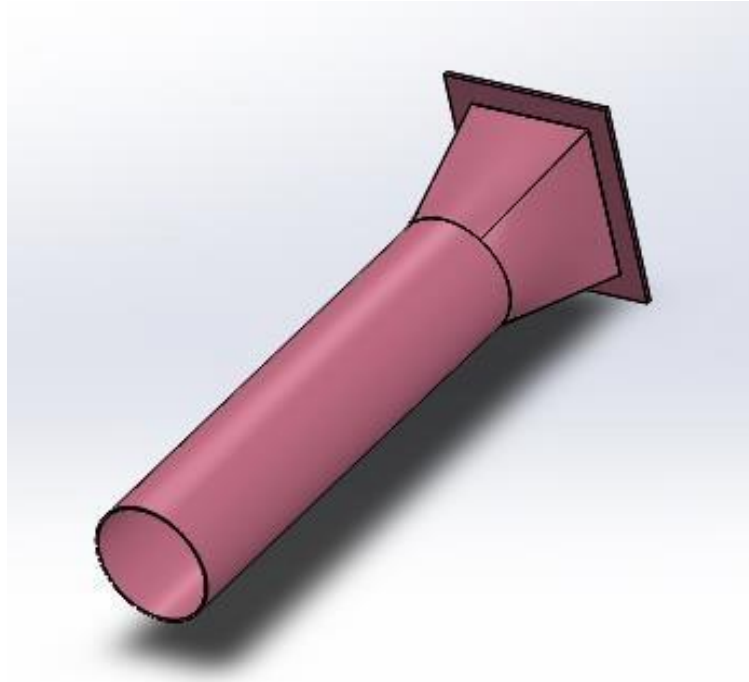


Figure 42: Plastic pipe

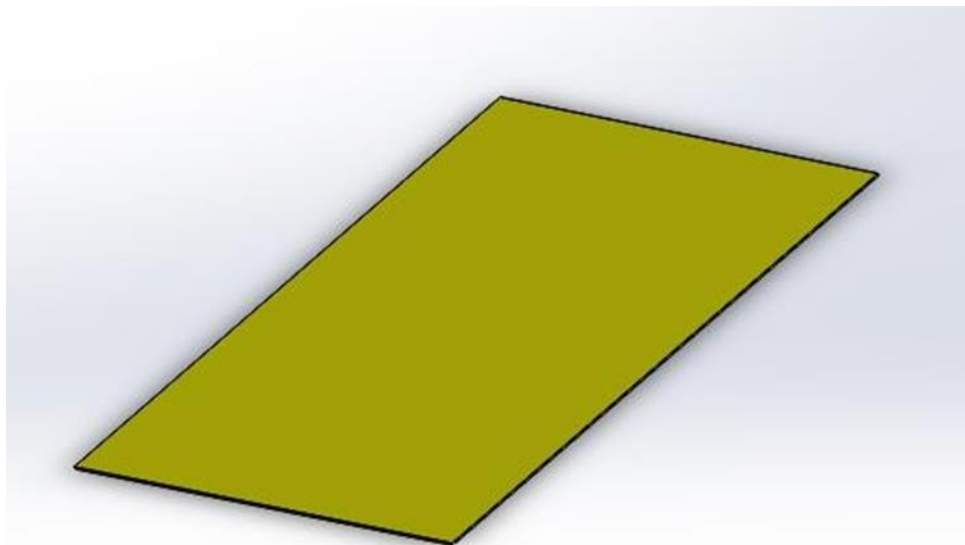


Figure 43: Glass wool

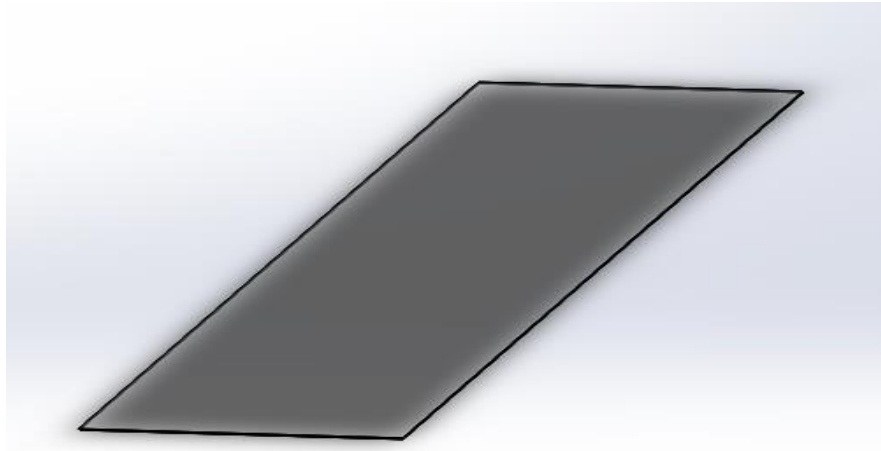


Figure 44: Glass



Figure 45: Osb-Board

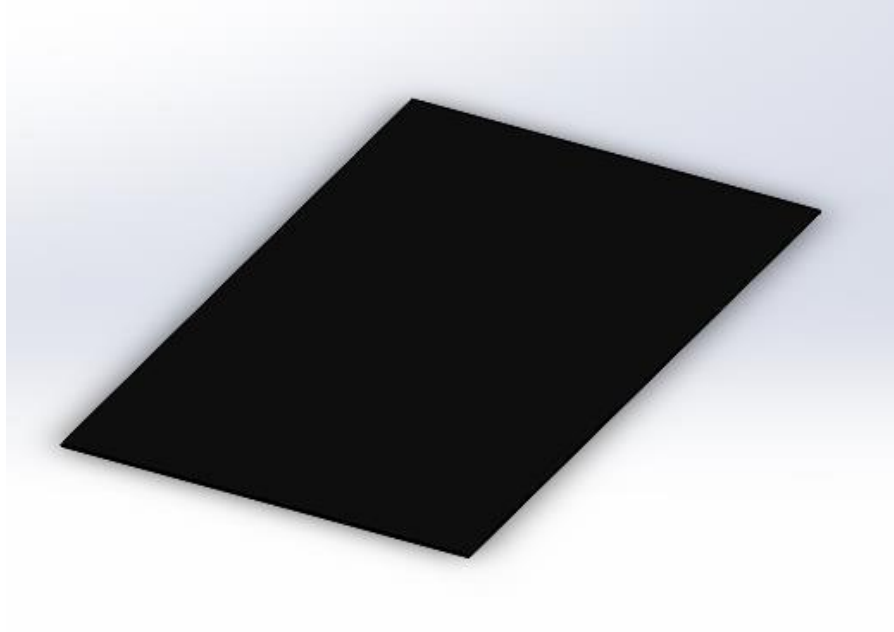
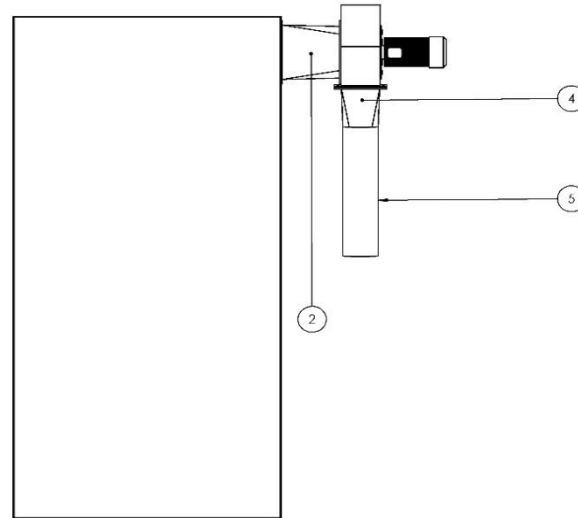
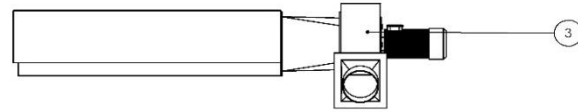
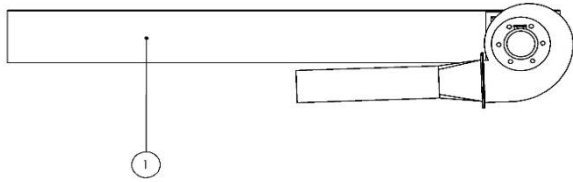
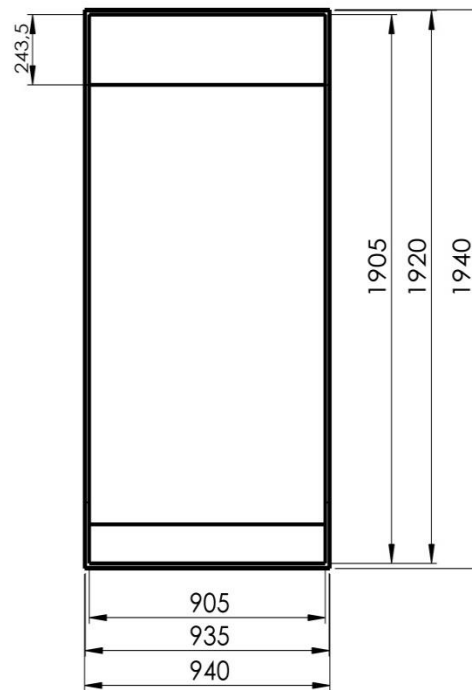
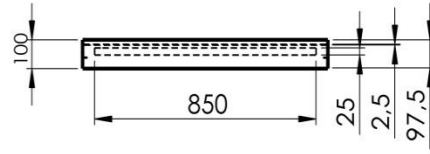


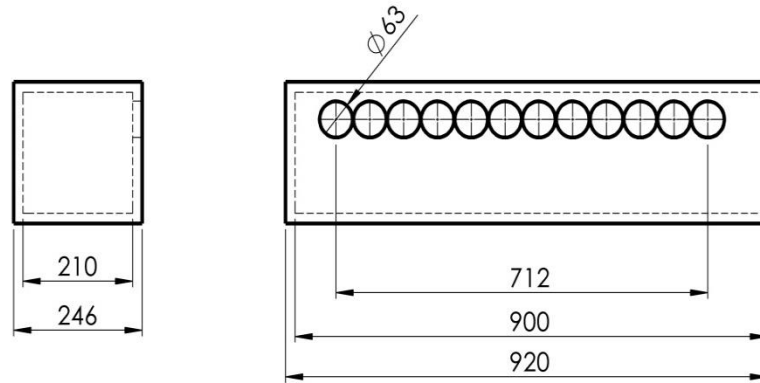
Figure 46: Absorber Aluminium Plate



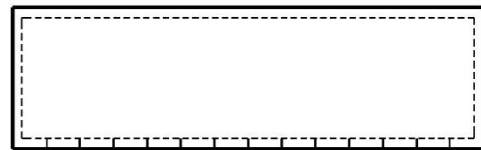
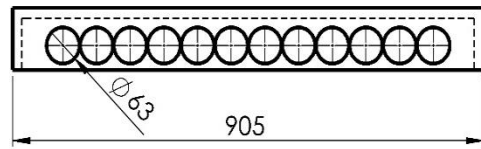
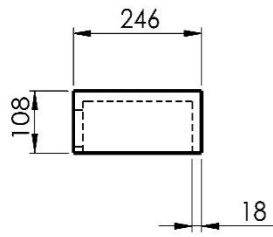
5	1	PIPE	Ø 122 PLASTIC PIPE
4	1	CONNECTION LUG-1	ALUMINUM
3	1	FAN MOTOR	POWER
2	1	CONNECTION LUG-2	ALUMINUM
1	1	COLLECTOR PANEL	ALUMINUM
PART NO	AMOUNT	NAME	DESCRIPTION
DRW. BY	M. KALAY	DATE	10/12/18
CHK. BY	H. HACISEVKI	DATE	10/12/18
SCALE	ASSEMBLY COLA CAN		DRAWING NO
1:10			1

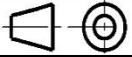


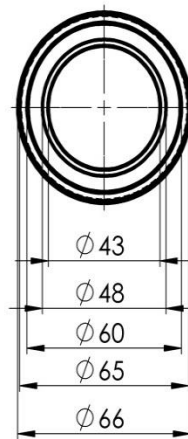
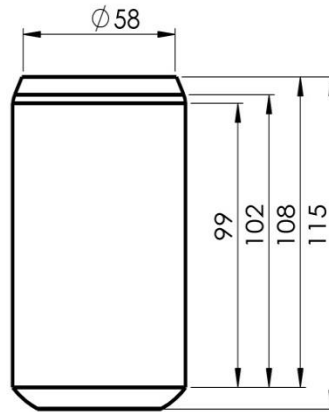
	NAME	DATE	SIGN	EMU
DRW. BY	SAH	12/18		
CHK. BY	H.H	12/18		
SCALE 1:20	COLLECTOR PANEL		DRW.NO 1-1	



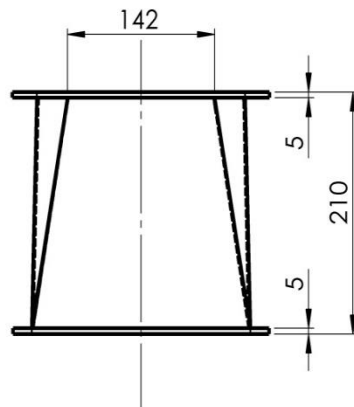
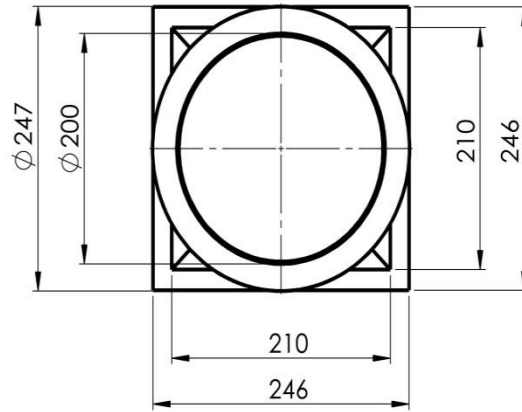
☐ ⊙	NAME	DATE	SIGN	EMU
DRW.BY	SAH	12/18		
CHK.BY	H.H	12/18		
SCALE 1:10	COLA CAN AIR (OUTPUT)		DRW.NO 1-1-1	



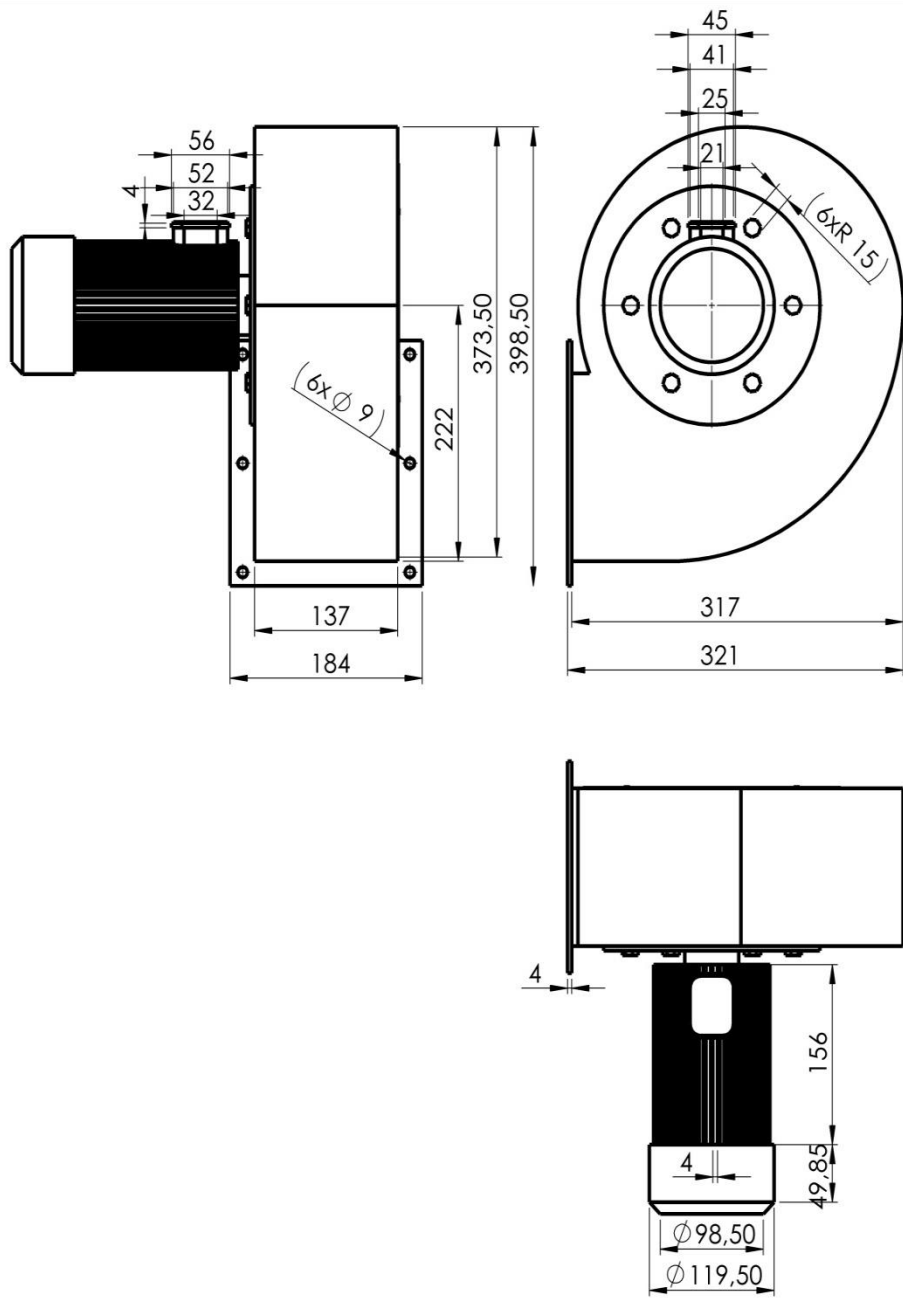
	NAME	DATE	SIGN	
DRW.BY	SAH	12/18		EMU
CHK.BY	H.H	12/18		
SCALE 1:10	COLA CAN AIR (INPUT)		DRW.NO 1-1-2	



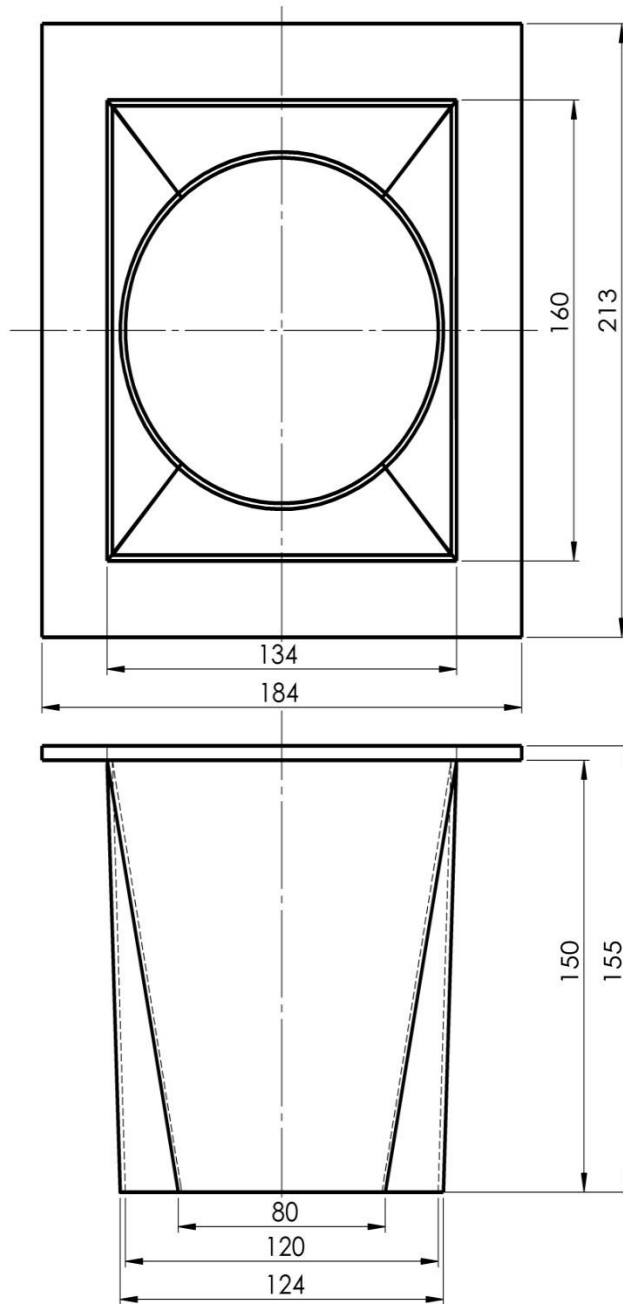
	NAME	DATE	SIGN	EMU
DRW.BY	SAH	12/18		
CHK.BY	H.H	12/18		
SCALE 1:2	COLA CAN		DRW.NO 1-1-3	



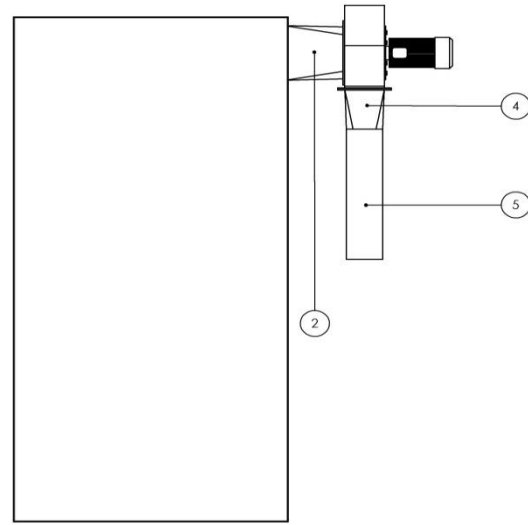
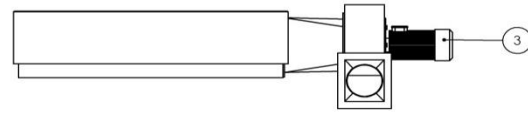
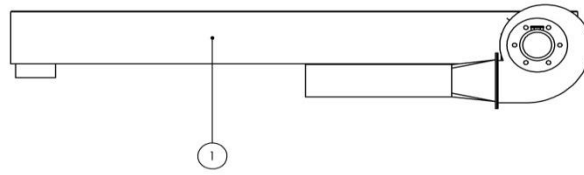
☐ ⊕	NAME	DATE	SIGN	EMU
DRW.BY	SAH	12/18		
CHK.BY	H.H	12/18		
SCALE 1:5	CONNECTION LUG (AL)		DRW.NO 1-2	



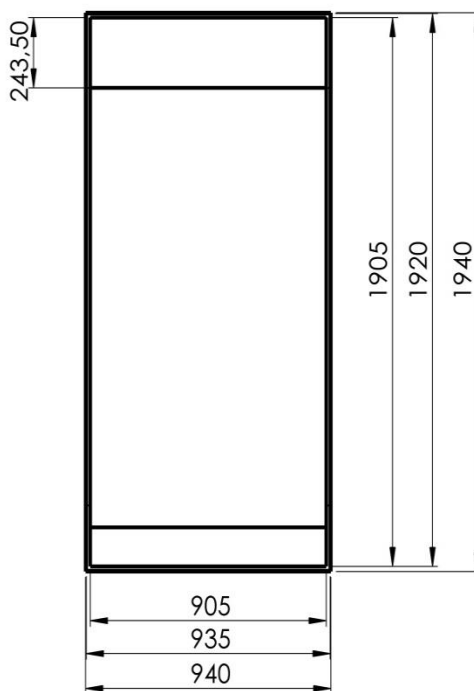
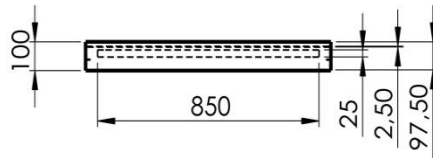
	NAME	DATE	SIGN	EMU
DRW. BY	SAH	12/18		
CHK. BY	H.H	12/18		
SCALE 1:5	FAN MOTOR		DRW.NO 1-3	



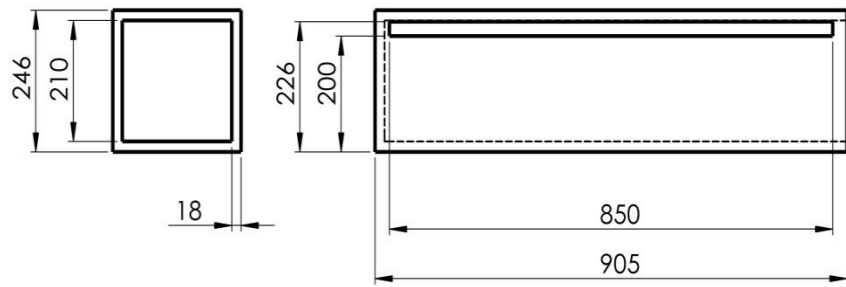
☐ ⊕	NAME	DATE	SIGN	
DRW.BY	SAH	12/18		EMU
CHK.BY	H.H	12/18		
SCALE 1:2	CONNECTION LUG (AL)		DRW.NO 1-4	




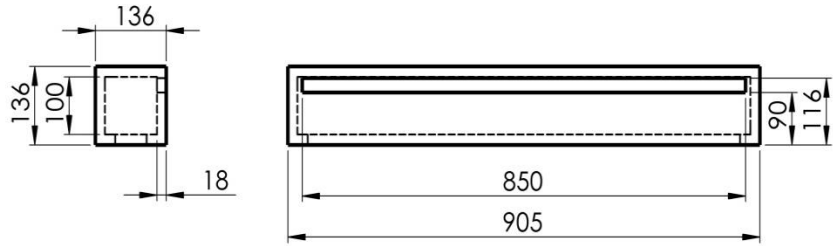
5	1	PIPE	Ø 122 PLACTIC PIPE
4	1	CONNECTION LUG-1	ALUMINUM
3	1	FAN MOTOR	POWER
2	1	CONNECTION LUG-2	ALUMINUM
1	1	COLLECTOR PANEL	ALUMINUM
PART NO	AMOUNT	NAME	DESCRIPTION
	NAME	DATE	SIGN
DRW. BY	M. KALAY	10/12/18	
CHK. BY	H. HACISEVKI	10/12/18	
SCALE 1:10	ASSEMBLY CONIC		DRAWING NO 2



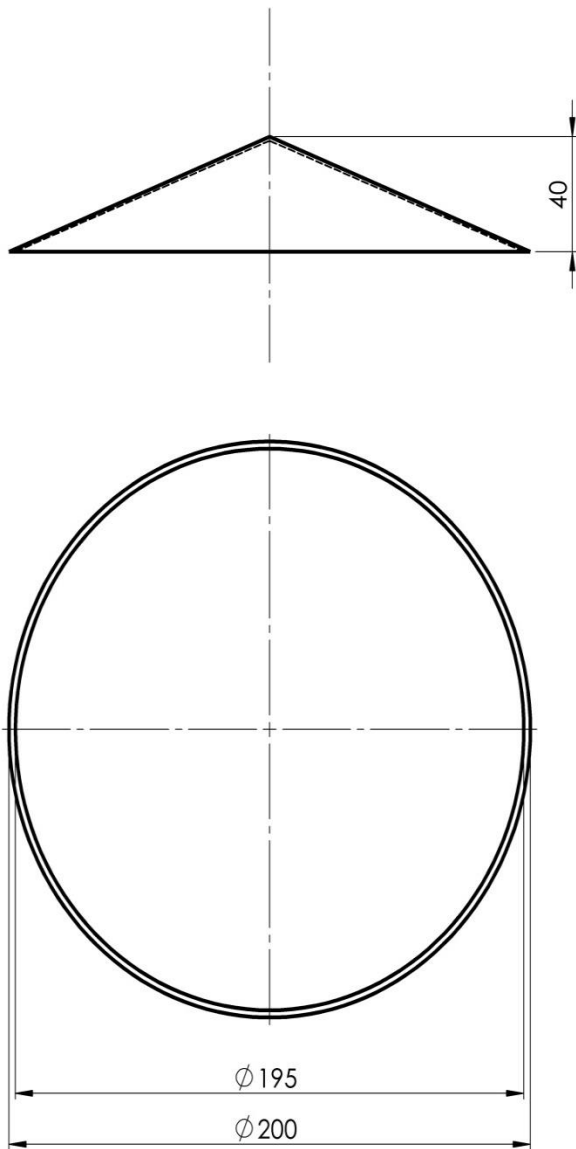
☐ ⊙	NAME	DATE	SIGN	EMU
DRW.BY	SAH	12/18		
CHK.BY	H.H	12/18		
SCALE 1:20	COLLECTOR PANEL		DRW.NO 2-1	




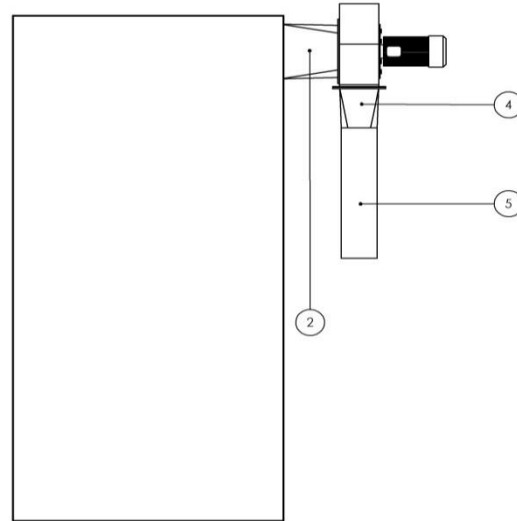
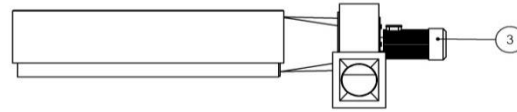
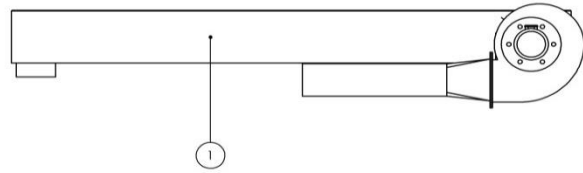
	NAME	DATE	SIGN	EMU
DRW.BY	SAH	12/18		
CHK.BY	H.H	12/18		
SCALE 1:10	CONIC BOX AIR(OUTPUT)		DRW.NO 2-1-1	



☐ ⊙	NAME	DATE	SIGN	
DRW.BY	SAH	12/18		EMU
CHK.BY	H.H	12/18		
SCALE 1:10	CONIC BOX AIR (INPUT)		DRW.NO 2-1-2	



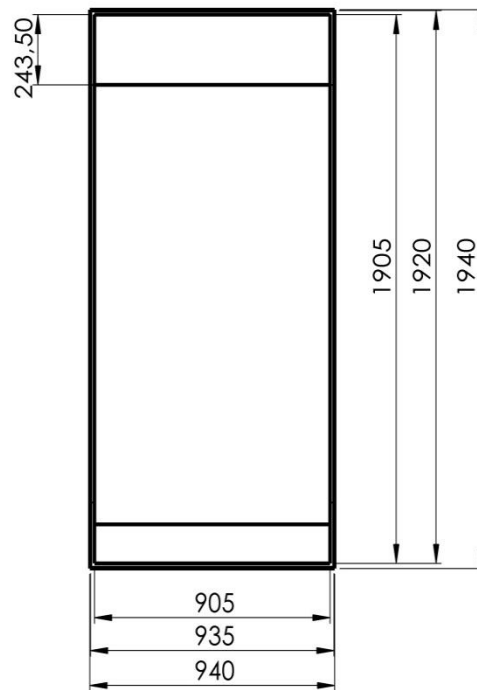
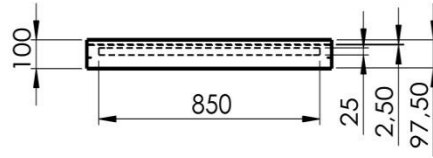
	NAME	DATE	SIGN	
DRW.BY	SAH	12/18		EMU
CHK.BY	H.H	12/18		
SCALE 1:2	CONIC PLATE		DRW.NO 2-1-3	



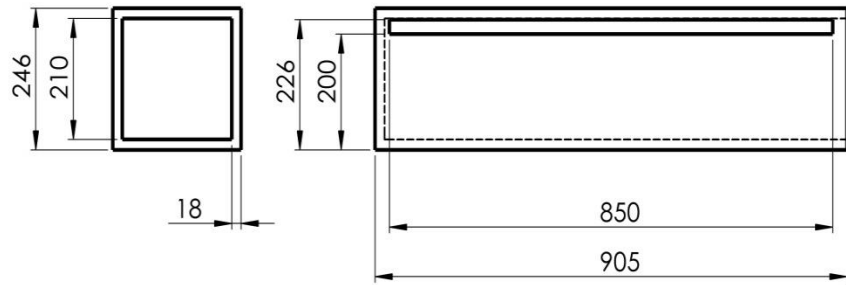
5	1	PIPE	Ø 122 PLACTIC PIPE
4	1	CONNECTION LUG-1	ALUMINUM
3	1	FAN MOTOR	POWER
2	1	CONNECTION LUG-2	ALUMINUM
1	1	COLLECTOR PANEL	ALUMINUM
PART NO	AMOUNT	NAME	DESCRIPTION
		NAME	DATE
DRW. BY	M. KALAY	10/12/18	SIGN
CHK. BY	H. HACISEVKI	10/12/18	
SCALE	ASSEMBLY POLYMER PANEL	DRAWING NO	
1:10		3	

EMU

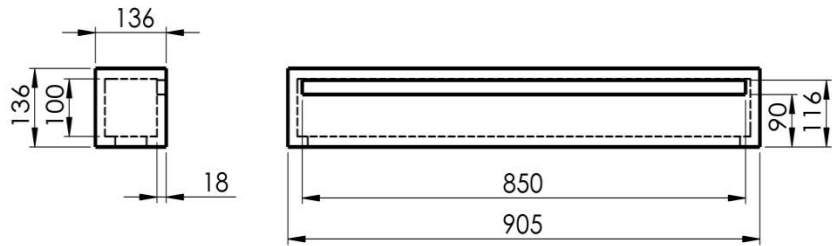
DRAWING NO
3



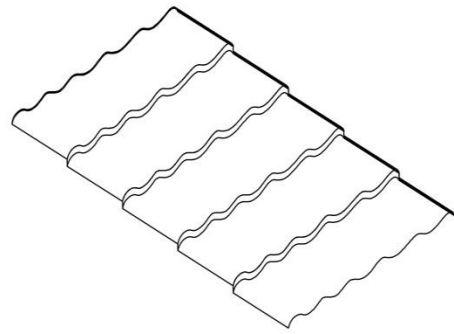
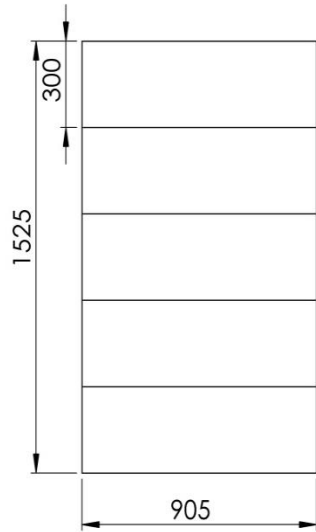
☐ ⊙	NAME	DATE	SIGN	EMU
DRW.BY	SAH	12/18		
CHK.BY	H.H	12/18		
SCALE 1:20	COLLECTOR PANEL		DRW.NO 3-1	



	NAME	DATE	SIGN	EMU
DRW.BY	SAH	12/18		
CHK.BY	H.H	12/18		
SCALE 1:10	POLYMER BOX AIR(OUTPUT)		DRW.NO 3-1-1	



☐ ⊙	NAME	DATE	SIGN	
DRW.BY	SAH	12/18		EMU
CHK.BY	H.H	12/18		
SCALE 1:10	POLYMER BOX AIR (INPUT)		DRW.NO 3-1-2	



☐ ⊕	NAME	DATE	SIGN	
DRW.BY	SAH	12/18		EMU
CHK.BY	H.H	12/18		
SCALE 1:2	POLYMER PLATE		DRW.NO 3-1-3	

Appendix B: Tables

Table 4: Obtained data at 0.02 kg/s air mass flow rate for cola can type (13.05.2019)

Overall Radiation [W/m ²]	Date	Time	T-in [°C]	T-glass [°C]	T-absorber [°C]	T-out [°C]	Area [m ²]	Q u [W]	Efficiency [η] [%]	ΔT [°C]	\dot{m} [kg/s]	Cp [J / kg.C]
835.8	13/05/2019	09:00	27.8	39.8	68.3	41.8	1.82	281.96	18.5359	14.0	0.02	1007
895.6	13/05/2019	09:30	26.4	40.8	66.5	42.1	1.82	316.20	19.3987	15.7	0.02	1007
933.1	13/05/2019	10:00	26.8	41.2	67.8	44.8	1.82	362.52	21.3468	18.0	0.02	1007
937.4	13/05/2019	10:30	27.6	40.9	69.0	46.6	1.82	382.66	22.4294	19.0	0.02	1007
1072.5	13/05/2019	11:00	29.7	43.9	68.5	48.2	1.82	372.59	19.0881	18.5	0.02	1007
1100.8	13/05/2019	11:30	30.5	44.5	69.7	52.6	1.82	445.09	22.2163	22.1	0.02	1007
1089.1	13/05/2019	12:00	32.6	45.8	68.4	52.8	1.82	406.83	20.5245	20.2	0.02	1007
1038.7	13/05/2019	12:30	31.8	44.6	70.3	54.9	1.82	465.23	24.6099	23.1	0.02	1007
1045.6	13/05/2019	13:00	30.9	47.8	70.7	53.5	1.82	455.16	23.9183	22.6	0.02	1007
1093.7	13/05/2019	13:30	31.5	48.1	69.1	56.7	1.82	507.53	25.4971	25.2	0.02	1007
1053.8	13/05/2019	14:00	30.6	45.1	70.6	55.7	1.82	505.51	26.3575	25.1	0.02	1007
1020.2	13/05/2019	14:30	29.8	41.1	68.7	53.4	1.82	475.30	25.5985	23.6	0.02	1007
999.7	13/05/2019	15:00	28.8	40.9	71.6	50.7	1.82	441.07	24.2417	21.9	0.02	1007
902.6	13/05/2019	15:30	29.4	42.3	70.5	47.6	1.82	366.55	22.3133	18.2	0.02	1007
898.5	13/05/2019	16:00	27.8	38.7	69.4	45.7	1.82	360.51	22.0457	17.9	0.02	1007

Table 5: Obtained data at 0.02 kg/s air mass flow rate for cola can type (16.07.2019)

Overall Radiation [W/m ²]	Date	Time	T-in [°C]	T-glass [°C]	T-absorber [°C]	T-out [°C]	Area [m ²]	Q u [W]	Efficiency [η] [%]	ΔT [°C]	\dot{m} [kg/s]	Cp [J / kg.C]
982.5	16/07/2019	09:00	30.7	47.1	70.1	49.1	1.82	370.58	20.7240	18.4	0.02	1007
982.1	16/07/2019	09:30	30.8	46.8	71.2	49.7	1.82	380.65	21.2958	18.9	0.02	1007
990.6	16/07/2019	10:00	31.5	51.2	72.3	52.2	1.82	416.90	23.1238	20.7	0.02	1007
1005.8	16/07/2019	10:30	32.1	51.8	73.2	55.9	1.82	479.33	26.1850	23.8	0.02	1007
1069.3	16/07/2019	11:00	32.8	53.9	70.9	56.1	1.82	469.26	24.1126	23.3	0.02	1007
1150.8	16/07/2019	11:30	33.2	54.3	72.6	57.2	1.82	483.36	23.0781	24.0	0.02	1007
1205.6	16/07/2019	12:00	34.8	55.2	75.4	61.2	1.82	531.70	24.2320	26.4	0.02	1007
1220.4	16/07/2019	12:30	35.9	57.6	78.9	61.8	1.82	521.63	23.4847	25.9	0.02	1007
1170.4	16/07/2019	13:00	34.1	56.1	76.8	63.0	1.82	582.05	27.3245	28.9	0.02	1007
1160.8	16/07/2019	13:30	33.9	53.9	75.3	62.9	1.82	584.06	27.6458	29.0	0.02	1007
1187.5	16/07/2019	14:00	30.6	48.9	72.1	61.8	1.82	628.37	29.0743	31.2	0.02	1007
1275.8	16/07/2019	14:30	32.1	51.6	74.6	62.8	1.82	618.30	26.6283	30.7	0.02	1007
1000.7	16/07/2019	15:00	31.7	50.9	73.8	56.9	1.82	507.53	27.8666	25.2	0.02	1007
1010.9	16/07/2019	15:30	30.5	47.9	71.9	54.9	1.82	491.42	26.7097	24.4	0.02	1007
1003.6	16/07/2019	16:00	29.7	46.9	70.8	52.7	1.82	463.22	25.3604	23.0	0.02	1007

Table 6: Obtained data at 0.02 kg/s air mass flow rate for conical type (13.05.2019)

Overall Radiation [W/m ²]	Date	Time	T-in [°C]	T-glass [°C]	T-absorber [°C]	T-out [°C]	Area [m ²]	Q u [W]	Efficiency [η] [%]	ΔT [°C]	\dot{m} [kg/s]	Cp [J / kg.C]
835.8	13/05/2019	09:00	27.5	39.5	68.5	38.1	1.67	213.48	15.2949	10.6	0.02	1007
895.6	13/05/2019	09:30	26.5	39.6	67.9	41.2	1.67	296.06	19.7946	14.7	0.02	1007
933.1	13/05/2019	10:00	26.7	40.1	68.0	42.2	1.67	312.17	20.0330	15.5	0.02	1007
937.4	13/05/2019	10:30	27.2	40.2	69.3	44.5	1.67	348.42	22.2569	17.3	0.02	1007
1072.5	13/05/2019	11:00	27.9	40.3	71.5	46.2	1.67	368.56	20.5777	18.3	0.02	1007
1100.8	13/05/2019	11:30	29.8	41.0	72.6	49.8	1.67	402.80	21.9111	20.0	0.02	1007
1089.1	13/05/2019	12:00	28.9	42.0	71.4	47.3	1.67	370.58	20.3748	18.4	0.02	1007
1038.7	13/05/2019	12:30	29.9	41.9	72.0	50.0	1.67	404.81	23.3372	20.1	0.02	1007
1045.6	13/05/2019	13:00	30.1	42.6	70.9	47.1	1.67	342.38	19.6077	17.0	0.02	1007
1093.7	13/05/2019	13:30	30.9	41.7	74.6	51.9	1.67	422.94	23.1560	21.0	0.02	1007
1053.8	13/05/2019	14:00	30.6	40.6	73.1	51.1	1.67	412.87	23.4606	20.5	0.02	1007
1020.2	13/05/2019	14:30	29.7	41.9	70.5	48.9	1.67	386.69	22.6965	19.2	0.02	1007
999.7	13/05/2019	15:00	28.7	41.2	67.8	42.9	1.67	285.99	17.1302	14.2	0.02	1007
1015.5	13/05/2019	15:30	29.1	42.4	68.5	43.5	1.67	290.02	17.1012	14.4	0.02	1007
1005.4	13/05/2019	16:00	28.9	42.5	64.7	40.8	1.67	259.81	15.4737	12.9	0.02	1007

Table 7: Obtained data at 0.02 kg/s air mass flow rate for conical type (16.07.2019)

Overall Radiation [W/m ²]	Date	Time	T-in [°C]	T-glass [°C]	T-absorber [°C]	T-out [°C]	Area [m ²]	Q u [W]	Efficiency [η] [%]	ΔT [°C]	\dot{m} [kg/s]	Cp [J / kg.C]
982.5	16/07/2019	09:00	30.8	43.8	69.7	46.7	1.67	320.23	19.5168	15.9	0.02	1007
982.1	16/07/2019	09:30	30.4	45.6	70.1	47.5	1.67	344.39	20.9983	17.1	0.02	1007
990.6	16/07/2019	10:00	31.2	46.7	71.3	49.9	1.67	376.62	22.7660	18.7	0.02	1007
1005.8	16/07/2019	10:30	32.4	49.8	72.3	53.1	1.67	416.90	24.8200	20.7	0.02	1007
1069.3	16/07/2019	11:00	32.5	50.3	71.9	54.7	1.67	447.11	25.0378	22.2	0.02	1007
1150.8	16/07/2019	11:30	32.9	51.9	73.2	56.9	1.67	483.36	25.1509	24.0	0.02	1007
1205.6	16/07/2019	12:00	34.2	54.7	74.6	57.6	1.67	471.28	23.4075	23.4	0.02	1007
1220.4	16/07/2019	12:30	34.6	53.9	75.0	57.1	1.67	453.15	22.2343	22.5	0.02	1007
1170.4	16/07/2019	13:00	33.1	52.5	73.8	61.9	1.67	580.03	29.6757	28.8	0.02	1007
1160.8	16/07/2019	13:30	34.1	55.6	74.0	58.7	1.67	495.44	25.5576	24.6	0.02	1007
1187.5	16/07/2019	14:00	31.2	53.1	71.9	57.8	1.67	535.72	27.0141	26.6	0.02	1007
999.8	16/07/2019	14:30	31.9	52.4	71.5	57.1	1.67	507.53	30.3970	25.2	0.02	1007
1000.7	16/07/2019	15:00	32.1	51.8	72.7	54.2	1.67	445.09	26.6337	22.1	0.02	1007
1010.9	16/07/2019	15:30	29.5	49.9	70.8	51.8	1.67	449.12	26.6036	22.3	0.02	1007
1003.6	16/07/2019	16:00	29.7	42.0	71.0	48.6	1.67	259.81	15.5014	12.9	0.02	1007

Table 8: Obtained data at 0.02 kg/s air mass flow rate for polymer panel type (13.05.2019)

Overall Radiation [W/m ²]	Date	Time	T-in [°C]	T-glass [°C]	T-absorber [°C]	T-out [°C]	Area [m ²]	Q u [W]	Efficiency [η] [%]	ΔT [°C]	\dot{m} [kg/s]	Cp [J / kg.C]
835.8	13/05/2019	09:00	27.9	40.2	67.8	37.6	1.75	195.36	13.3564	9.7	0.02	1007
895.6	13/05/2019	09:30	26.5	39.8	66.5	38.7	1.75	245.71	15.6772	12.2	0.02	1007
933.1	13/05/2019	10:00	26.4	39.5	65.9	38.9	1.75	251.75	15.4171	12.5	0.02	1007
937.4	13/05/2019	10:30	27.0	40.7	68.1	42.9	1.75	320.23	19.5206	15.9	0.02	1007
1072.5	13/05/2019	11:00	28.7	40.9	72.5	46.9	1.75	366.55	19.5297	18.2	0.02	1007
1100.8	13/05/2019	11:30	29.3	41.2	73.3	48.5	1.75	386.69	20.0731	19.2	0.02	1007
1089.1	13/05/2019	12:00	29.1	40.8	70.1	45.6	1.75	332.31	17.4356	16.5	0.02	1007
1038.7	13/05/2019	12:30	30.1	42.5	75.1	49.7	1.75	394.74	21.7164	19.6	0.02	1007
1045.6	13/05/2019	13:00	32.0	42.8	69.8	46.0	1.75	281.96	15.4093	14.0	0.02	1007
1093.7	13/05/2019	13:30	31.8	41.9	74.2	49.8	1.75	362.52	18.9407	18.0	0.02	1007
1053.8	13/05/2019	14:00	30.3	40.8	73.5	47.6	1.75	348.42	18.8934	17.3	0.02	1007
1020.2	13/05/2019	14:30	29.2	41.5	70.4	43.9	1.75	296.06	16.5826	14.7	0.02	1007
999.7	13/05/2019	15:00	29.4	41.8	69.8	42.7	1.75	267.86	15.3110	13.3	0.02	1007
1015.5	13/05/2019	15:30	28.9	40.8	65.7	42.1	1.75	265.85	14.9594	13.2	0.02	1007
1005.4	13/05/2019	16:00	28.2	42.0	63.9	38.9	1.75	215.50	12.2480	10.7	0.02	1007

Table 9: Obtained data at 0.02 kg/s air mass flow rate for polymer panel type (16.07.2019)

Overall Radiation [W/m ²]	Date	Time	T-in [°C]	T-glass [°C]	T-absorber [°C]	T-out [°C]	Area [m ²]	Q u [W]	Efficiency [η] [%]	ΔT [°C]	\dot{m} [kg/s]	Cp [J / kg.C]
982.5	16/07/2019	09:00	30.5	45.9	72.3	43.8	1.75	267.86	15.5790	13.3	0.02	1007
982.1	16/07/2019	09:30	29.9	44.8	69.5	43.4	1.75	271.89	15.8197	13.5	0.02	1007
990.6	16/07/2019	10:00	31.5	47.5	73.9	47.5	1.75	322.24	18.5884	16.0	0.02	1007
1005.8	16/07/2019	10:30	32.7	49.3	75.0	53.1	1.75	410.86	23.3421	20.4	0.02	1007
1069.3	16/07/2019	11:00	32.4	49.1	74.8	53.7	1.75	428.98	22.9246	21.3	0.02	1007
1150.8	16/07/2019	11:30	33.1	51.2	78.4	54.9	1.75	439.05	21.8011	21.8	0.02	1007
1205.6	16/07/2019	12:00	34.6	54.7	80.1	57.6	1.75	463.22	21.9556	23.0	0.02	1007
1220.4	16/07/2019	12:30	34.1	55.1	77.6	56.1	1.75	443.08	20.7464	22.0	0.02	1007
1170.4	16/07/2019	13:00	33.4	55.6	78.2	58.6	1.75	507.53	24.7792	25.2	0.02	1007
1160.8	16/07/2019	13:30	33.9	56.5	76.8	55.9	1.75	443.08	21.8116	22.0	0.02	1007
1187.5	16/07/2019	14:00	31.4	52.1	72.5	55.7	1.75	489.40	23.5502	24.3	0.02	1007
999.8	16/07/2019	14:30	31.7	51.9	71.9	51.0	1.75	388.70	22.2160	19.3	0.02	1007
1000.7	16/07/2019	15:00	30.8	52.4	72.3	47.5	1.75	336.34	19.2059	16.7	0.02	1007
1010.9	16/07/2019	15:30	29.7	49.8	70.5	50.9	1.75	426.97	24.1351	21.2	0.02	1007
1003.6	16/07/2019	16:00	29.1	48.5	69.4	45.4	1.75	328.28	18.6917	16.3	0.02	1007

Table 10: Obtained data at 0.04 kg/s air mass flow rate for cola can type (14.05.2019)

Overall Radiation [W/m ²]	Date	Time	T-in [°C]	T-glass [°C]	T-absorber [°C]	T-out [°C]	Area [m ²]	Q u [W]	Efficiency [η] [%]	ΔT [°C]	\dot{m} [kg/s]	Cp [J / kg.C]
998.6	14/05/2019	09:00	29.8	45.5	75.1	36.9	1.82	285.99	15.7357	7.1	0.04	1007
1028.7	14/05/2019	09:30	30.1	46.9	70.4	38.7	1.82	346.41	18.5024	8.6	0.04	1007
1001.5	14/05/2019	10:00	29.4	45.1	69.7	40.5	1.82	447.11	24.5296	11.1	0.04	1007
1008.9	14/05/2019	10:30	29.7	48.7	70.9	41.8	1.82	487.39	26.5433	12.1	0.04	1007
1040.8	14/05/2019	11:00	30.2	43.8	74.8	42.9	1.82	511.56	27.0056	12.7	0.04	1007
1100.9	14/05/2019	11:30	31.3	46.2	78.1	45.8	1.82	584.06	29.1500	14.5	0.04	1007
1095.7	14/05/2019	12:00	33.3	40.7	71.5	47.5	1.82	571.98	28.6824	14.2	0.04	1007
997.6	14/05/2019	12:30	32.9	43.8	69.4	46.2	1.82	535.72	29.5062	13.3	0.04	1007
1039.7	14/05/2019	13:00	32.5	44.9	68.7	46.1	1.82	547.81	28.9500	13.6	0.04	1007
1020.7	14/05/2019	13:30	31.9	46.1	73.4	44.7	1.82	515.58	27.7543	12.8	0.04	1007
985.4	14/05/2019	14:00	29.8	44.7	70.8	42.7	1.82	519.61	28.9731	12.9	0.04	1007
1042.7	14/05/2019	14:30	30.7	45.9	80.5	42.6	1.82	479.33	25.2584	11.9	0.04	1007
972.5	14/05/2019	15:00	28.9	46.0	78.4	39.5	1.82	426.97	24.1232	10.6	0.04	1007
981.7	14/05/2019	15:30	28.4	42.8	75.4	39.9	1.82	463.22	25.9261	11.5	0.04	1007
996.4	14/05/2019	16:00	27.8	43.5	73.2	38.7	1.82	439.05	24.2109	10.9	0.04	1007

Table 11: Obtained data at 0.04 kg/s air mass flow rate for cola can type (17.07.2019)

Overall Radiation [W/m ²]	Date	Time	T-in [°C]	T-glass [°C]	T-absorber [°C]	T-out [°C]	Area [m ²]	Q u [W]	Efficiency [η] [%]	ΔT [°C]	\dot{m} [kg/s]	Cp [J / kg.C]
1018.6	17/07/2019	09:00	30.3	45.8	71.5	40.4	1.82	406.83	21.9450	10.1	0.04	1007
1015.7	17/07/2019	09:30	30.9	44.7	70.9	42	1.82	447.11	24.1866	11.1	0.04	1007
1058.1	17/07/2019	10:00	31.6	45.6	73.4	44.9	1.82	535.72	27.8191	13.3	0.04	1007
1065.3	17/07/2019	10:30	32.4	46.3	75.8	46.5	1.82	567.95	29.2931	14.1	0.04	1007
1101.8	17/07/2019	11:00	32.5	46.0	74.3	47.1	1.82	588.09	29.3270	14.6	0.04	1007
1258.7	17/07/2019	11:30	34.2	48.1	78.9	50.9	1.82	672.68	29.3638	16.7	0.04	1007
1302.5	17/07/2019	12:00	35.4	52.9	81.4	52.9	1.82	704.90	29.7357	17.5	0.04	1007
1279.5	17/07/2019	12:30	34.9	55.4	80.1	51.6	1.82	672.68	28.8865	16.7	0.04	1007
1272.1	17/07/2019	13:00	34.7	54.7	79.0	52.0	1.82	696.84	30.0984	17.3	0.04	1007
1255.6	17/07/2019	13:30	34.9	56.2	74.5	50.8	1.82	640.45	28.0262	15.9	0.04	1007
1230.7	17/07/2019	14:00	32.6	53.5	71.9	48.1	1.82	624.34	27.8739	15.5	0.04	1007
1220.9	17/07/2019	14:30	33.1	55.3	74.6	48.6	1.82	624.34	28.0976	15.5	0.04	1007
1105.6	17/07/2019	15:00	31.8	50.9	71.6	45.9	1.82	567.95	28.2253	14.1	0.04	1007
1051.9	17/07/2019	15:30	32.3	50.1	70.5	45.7	1.82	539.75	28.1935	13.4	0.04	1007
1022.5	17/07/2019	16:00	30.9	49.9	69.4	44.8	1.82	559.89	30.0864	13.9	0.04	1007

Table 12: Obtained data at 0.04 kg/s air mass flow rate for conical type (14.05.2019)

Overall Radiation [W/m ²]	Date	Time	T-in [°C]	T-glass [°C]	T-absorber [°C]	T-out [°C]	Area [m ²]	Q u [W]	Efficiency [η] [%]	ΔT [°C]	\dot{m} [kg/s]	Cp [J / kg.C]
998.6	14/05/2019	09:00	29.5	43.1	70.4	36.1	1.67	265.85	15.9414	6.6	0.04	1007
1028.7	14/05/2019	09:30	29.8	44.8	72.3	36.9	1.67	285.99	16.6473	7.1	0.04	1007
1001.5	14/05/2019	10:00	30.1	45.0	76.4	39.8	1.67	390.72	23.3611	9.7	0.04	1007
1008.9	14/05/2019	10:30	29.6	44.9	78.0	42.8	1.67	531.70	31.5572	13.2	0.04	1007
1040.8	14/05/2019	11:00	30.1	46.0	78.2	41.5	1.67	459.19	26.4186	11.4	0.04	1007
1100.9	14/05/2019	11:30	31.8	47.6	75.1	43.9	1.67	487.39	26.5100	12.1	0.04	1007
1095.7	14/05/2019	12:00	32.5	44.7	52.6	46.9	1.67	580.03	31.6989	14.4	0.04	1007
997.6	14/05/2019	12:30	32.1	43.9	69.7	44.8	1.67	511.56	30.7058	12.7	0.04	1007
1039.7	14/05/2019	13:00	31.9	47.2	55.9	45.6	1.67	551.84	31.7823	13.7	0.04	1007
1020.7	14/05/2019	13:30	31.6	48.9	68.7	43.9	1.67	495.44	29.0656	12.3	0.04	1007
985.4	14/05/2019	14:00	28.6	43.5	77.9	39.0	1.67	418.91	25.4562	10.4	0.04	1007
1042.7	14/05/2019	14:30	30.5	45.9	65.8	41.8	1.67	455.16	26.1392	11.3	0.04	1007
972.5	14/05/2019	15:00	28.1	46.7	68.2	39.8	1.67	471.28	29.0181	11.7	0.04	1007
981.7	14/05/2019	15:30	28.2	43.9	76.4	38.1	1.67	398.77	24.3237	9.9	0.04	1007
996.4	14/05/2019	16:00	29.1	45.4	70.1	35.9	1.67	273.90	16.4607	6.8	0.04	1007

Table 13: Obtained data at 0.04 kg/s air mass flow rate for conical type (17.07.2019)

Overall Radiation [W/m ²]	Date	Time	T-in [°C]	T-glass [°C]	T-absorber [°C]	T-out [°C]	Area [m ²]	Q u [W]	Efficiency [η] [%]	ΔT [°C]	\dot{m} [kg/s]	Cp [J / kg.C]
1018.6	17/07/2019	09:00	30.1	44.7	69.7	39.7	1.67	386.69	22.7322	9.6	0.04	1007
1015.7	17/07/2019	09:30	30.7	43.9	70.1	41.4	1.67	431.00	25.4092	10.7	0.04	1007
1058.1	17/07/2019	10:00	31.7	42.8	71.8	42.6	1.67	439.05	24.8469	10.9	0.04	1007
1065.3	17/07/2019	10:30	31.5	45.1	74.5	43.9	1.67	499.47	28.0752	12.4	0.04	1007
1101.8	17/07/2019	11:00	31.9	45.4	73.6	45.6	1.67	551.84	29.9910	13.7	0.04	1007
1258.7	17/07/2019	11:30	33.9	47.9	80.5	48.9	1.67	604.20	28.7437	15	0.04	1007
1302.5	17/07/2019	12:00	35.2	53.6	82.7	50.7	1.67	624.34	28.7030	15.5	0.04	1007
1279.5	17/07/2019	12:30	34.7	56.7	83.1	49.8	1.67	608.23	28.4649	15.1	0.04	1007
1272.1	17/07/2019	13:00	34.5	54.9	81.9	52.1	1.67	708.93	33.3706	17.6	0.04	1007
1255.6	17/07/2019	13:30	34.8	55.1	80.4	52.9	1.67	729.07	34.7696	18.1	0.04	1007
1230.7	17/07/2019	14:00	32.9	52.4	75.7	49.7	1.67	676.70	32.9253	16.8	0.04	1007
1220.9	17/07/2019	14:30	32.8	54.8	76.8	49.0	1.67	652.54	32.0043	16.2	0.04	1007
1105.6	17/07/2019	15:00	32.2	48.9	71.6	47.6	1.67	620.31	33.5966	15.4	0.04	1007
1051.9	17/07/2019	15:30	31.6	49.5	69.8	46.9	1.67	616.28	35.0825	15.3	0.04	1007
1022.5	17/07/2019	16:00	30.5	48.7	72.3	45.2	1.67	592.12	34.6758	14.7	0.04	1007

Table 14: Obtained data at 0.04 kg/s air mass flow rate for polymer panel type (14.05.2019)

Overall Radiation [W/m ²]	Date	Time	T-in [°C]	T-glass [°C]	T-absorber [°C]	T-out [°C]	Area [m ²]	Q u [W]	Efficiency [η] [%]	ΔT [°C]	\dot{m} [kg/s]	Cp [J / kg.C]
998.6	14/05/2019	09:00	29.6	45.6	65.7	35.8	1.75	249.74	14.2906	6.2	0.04	1007
1028.7	14/05/2019	09:30	29.4	44.8	69.8	36.9	1.75	302.10	16.7812	7.5	0.04	1007
1001.5	14/05/2019	10:00	29.9	45.9	71.3	39.8	1.75	398.77	22.7528	9.9	0.04	1007
1008.9	14/05/2019	10:30	30.1	47.2	72.6	41.1	1.75	443.08	25.0955	11.0	0.04	1007
1040.8	14/05/2019	11:00	29.8	49.6	70.4	37.5	1.75	310.16	17.0284	7.7	0.04	1007
1100.9	14/05/2019	11:30	30.5	50.8	70.9	39.9	1.75	378.63	19.6531	9.4	0.04	1007
1095.7	14/05/2019	12:00	30.2	55.8	73.4	42.8	1.75	507.53	26.4686	12.6	0.04	1007
997.6	14/05/2019	12:30	29.8	52.4	73.5	41.8	1.75	483.36	27.6870	12.0	0.04	1007
1039.7	14/05/2019	13:00	30.6	49.6	60.8	43.8	1.75	531.70	29.2225	13.2	0.04	1007
1020.7	14/05/2019	13:30	29.5	48.2	65.4	39.4	1.75	398.77	22.3248	9.9	0.04	1007
985.4	14/05/2019	14:00	29.2	47.6	76.9	38.7	1.75	382.66	22.1903	9.5	0.04	1007
1042.7	14/05/2019	14:30	29.8	49.2	71.5	40.9	1.75	447.11	24.5028	11.1	0.04	1007
972.5	14/05/2019	15:00	28.5	48.1	75.2	37.4	1.75	358.49	21.0645	8.9	0.04	1007
981.7	14/05/2019	15:30	28.9	46.3	70.1	34.9	1.75	241.68	14.0677	6.0	0.04	1007
996.4	14/05/2019	16:00	29.7	48.7	72.6	34.7	1.75	201.40	11.5502	5.0	0.04	1007

Table 15: Obtained data at 0.04 kg/s air mass flow rate for polymer panel type (17.07.2019)

Overall Radiation [W/m ²]	Date	Time	T-in [°C]	T-glass [°C]	T-absorber [°C]	T-out [°C]	Area [m ²]	Q u [W]	Efficiency [η] [%]	ΔT [°C]	\dot{m} [kg/s]	Cp [J / kg.C]
1018.6	17/07/2019	09:00	29.8	45.1	65.0	38.4	1.75	346.41	19.4333	8.6	0.04	1007
1015.7	17/07/2019	09:30	30.3	46.0	68.4	39.8	1.75	382.66	21.5283	9.5	0.04	1007
1058.1	17/07/2019	10:00	31.2	46.2	74.3	42.1	1.75	439.05	23.7111	10.9	0.04	1007
1065.3	17/07/2019	10:30	31.5	46.1	75.2	41.9	1.75	418.91	22.4705	10.4	0.04	1007
1101.8	17/07/2019	11:00	32.1	47.5	77.9	43.2	1.75	447.11	23.1884	11.1	0.04	1007
1258.7	17/07/2019	11:30	33.7	50.8	81.5	46.8	1.75	527.67	23.9552	13.1	0.04	1007
1302.5	17/07/2019	12:00	35.4	54.7	84.9	51.2	1.75	636.42	27.9210	15.8	0.04	1007
1279.5	17/07/2019	12:30	34.5	55.4	82.1	50.6	1.75	648.51	28.9626	16.1	0.04	1007
1272.1	17/07/2019	13:00	34.2	53.7	83.7	52.0	1.75	716.98	32.2070	17.8	0.04	1007
1255.6	17/07/2019	13:30	34.8	54.1	79.4	51.1	1.75	656.56	29.8805	16.3	0.04	1007
1230.7	17/07/2019	14:00	33.1	56.7	75.8	47.0	1.75	559.89	25.9964	13.9	0.04	1007
1220.9	17/07/2019	14:30	32.7	53.2	77.1	45.8	1.75	527.67	24.6969	13.1	0.04	1007
1105.6	17/07/2019	15:00	32.6	53.8	72.6	45.0	1.75	499.47	25.8152	12.4	0.04	1007
1051.9	17/07/2019	15:30	31.3	51.6	68.7	44.3	1.75	523.64	28.4459	13.0	0.04	1007
1022.5	17/07/2019	16:00	30.6	51.0	68.1	43.6	1.75	523.64	29.2638	13.0	0.04	1007

Table 16: Obtained data at 0.06 kg/s air mass flow rate for cola can type (15.05.2019)

Overall Radiation [W/m ²]	Date	Time	T-in [°C]	T-glass [°C]	T-absorber [°C]	T-out [°C]	Area [m ²]	Q u [W]	Efficiency [η] [%]	ΔT [°C]	\dot{m} [kg/s]	Cp [J / kg°C]
981.6	15/05/2019	09:00	28.8	46.7	65.8	32.7	1.82	235.64	13.1898	3.9	0.06	1007
1010.5	15/05/2019	09:30	29.5	44.5	67.4	33.5	1.82	241.68	13.1411	4.0	0.06	1007
999.4	15/05/2019	10:00	30.2	47.2	74.6	34.7	1.82	271.89	14.9480	4.5	0.06	1007
975.5	15/05/2019	10:30	28.6	46.4	68.2	34.9	1.82	380.65	21.4399	6.3	0.06	1007
1030.8	15/05/2019	11:00	29.7	45.1	76.1	35.8	1.82	368.56	19.6456	6.1	0.06	1007
1055.6	15/05/2019	11:30	31.8	42.9	72.5	38.9	1.82	428.98	22.3289	7.1	0.06	1007
1084.9	15/05/2019	12:00	32.0	41.5	70.6	40.2	1.82	495.44	25.0919	8.2	0.06	1007
1045.3	15/05/2019	12:30	32.1	47.8	70.9	40.5	1.82	507.53	26.6777	8.4	0.06	1007
1005.7	15/05/2019	13:00	32.8	41.9	73.2	41.2	1.82	507.53	27.7281	8.4	0.06	1007
1028.1	15/05/2019	13:30	30.4	44.5	69.4	39.7	1.82	561.91	30.0301	9.3	0.06	1007
996.3	15/05/2019	14:00	29.1	46.3	67.1	37.4	1.82	501.49	27.6565	8.3	0.06	1007
1007.3	15/05/2019	14:30	30.2	46.7	64.8	35.7	1.82	332.31	18.1265	5.5	0.06	1007
983.4	15/05/2019	15:00	28.2	45.2	61.0	34.9	1.82	404.81	22.6180	6.7	0.06	1007
985.6	15/05/2019	15:30	28.6	43.9	62.7	33.4	1.82	290.02	16.1678	4.8	0.06	1007
997.2	15/05/2019	16:00	29.5	45.8	64.5	33.1	1.82	217.51	11.9848	3.6	0.06	1007

Table 17: Obtained data at 0.06 kg/s air mass flow rate for cola can type (18.07.2019)

Overall Radiation [W/m ²]	Date	Time	T-in [°C]	T-glass [°C]	T-absorber [°C]	T-out [°C]	Area [m ²]	Q u [W]	Efficiency [η] [%]	ΔT [°C]	\dot{m} [kg/s]	Cp [J / kg°C]
995.8	18/07/2019	09:00	29.5	42.6	67.4	34.7	1.82	314.18	17.3357	5.2	0.06	1007
1035.9	18/07/2019	09:30	30.2	43.0	68.2	34.9	1.82	283.97	15.0622	4.7	0.06	1007
1052.6	18/07/2019	10:00	30.9	43.4	69.3	35.8	1.82	296.06	15.4540	4.9	0.06	1007
1102.5	18/07/2019	10:30	31.2	43.2	72.1	37.8	1.82	398.77	19.8735	6.6	0.06	1007
1136.9	18/07/2019	11:00	32.3	44.3	73.8	40.9	1.82	519.61	25.1122	8.6	0.06	1007
1089.1	18/07/2019	11:30	31.9	41.8	71.9	39.5	1.82	459.19	23.1662	7.6	0.06	1007
1125.9	18/07/2019	12:00	31.7	42.5	71.5	41.1	1.82	567.95	27.7164	9.4	0.06	1007
1209.8	18/07/2019	12:30	32.6	43.5	74.6	43.6	1.82	664.62	30.1848	11.0	0.06	1007
1285.6	18/07/2019	13:00	32.9	44.9	75.3	44.5	1.82	700.87	29.9545	11.6	0.06	1007
1272.9	18/07/2019	13:30	31.1	42.6	69.8	41.9	1.82	652.54	28.1669	10.8	0.06	1007
1185.6	18/07/2019	14:00	30.7	41.9	68.7	40.8	1.82	610.24	28.2809	10.1	0.06	1007
1039.5	18/07/2019	14:30	28.6	41.0	66.1	37.9	1.82	561.91	29.7008	9.3	0.06	1007
1045.6	18/07/2019	15:00	29.3	42.5	65.9	37	1.82	465.23	24.4475	7.7	0.06	1007
1058.2	18/07/2019	15:30	29.4	43.1	65.4	36.6	1.82	435.02	22.5878	7.2	0.06	1007
978.2	18/07/2019	16:00	28.6	42.8	64.8	32.9	1.82	259.81	14.5932	4.3	0.06	1007

Table 18: Obtained data at 0.06 kg/s air mass flow rate for conical type (15.05.2019)

Overall Radiation [W/m ²]	Date	Time	T-in [°C]	T-glass [°C]	T-absorber [°C]	T-out [°C]	Area [m ²]	Q u [W]	Efficiency [η] [%]	ΔT [°C]	\dot{m} [kg/s]	Cp [J / kg·C]
981.6	15/05/2019	09:00	28.0	45.0	75.0	31.9	1.67	235.64	14.3746	3.9	0.06	1007
1010.5	15/05/2019	09:30	29.2	44.9	74.5	32.8	1.67	217.51	12.8893	3.6	0.06	1007
999.4	15/05/2019	10:00	29.9	46.8	76.1	34.3	1.67	265.85	15.9286	4.4	0.06	1007
975.5	15/05/2019	10:30	27.5	48.9	71.6	31.9	1.67	265.85	16.3189	4.4	0.06	1007
1030.8	15/05/2019	11:00	30.6	49.0	70.6	34.5	1.67	235.64	13.6885	3.9	0.06	1007
1055.6	15/05/2019	11:30	30.3	44.6	79.2	36.1	1.67	350.44	19.8789	5.8	0.06	1007
1084.9	15/05/2019	12:00	30.5	42.8	78.3	38.9	1.67	507.53	28.0126	8.4	0.06	1007
1045.3	15/05/2019	12:30	29.8	46.9	75.1	38.9	1.67	549.82	31.4967	9.1	0.06	1007
1005.7	15/05/2019	13:00	30.2	43.5	72.4	38.1	1.67	477.32	28.4199	7.9	0.06	1007
1028.1	15/05/2019	13:30	30.1	46.2	77.5	35.1	1.67	302.10	17.5954	5.0	0.06	1007
996.3	15/05/2019	14:00	29.5	47.1	72.9	35.6	1.67	368.56	22.1515	6.1	0.06	1007
1007.3	15/05/2019	14:30	30.0	49.7	72.0	33.4	1.67	205.43	12.2119	3.4	0.06	1007
983.4	15/05/2019	15:00	28.6	45.4	68.7	33.8	1.67	314.18	19.1310	5.2	0.06	1007
985.6	15/05/2019	15:30	28.9	40.9	69.2	33.1	1.67	253.76	15.4175	4.2	0.06	1007
997.2	15/05/2019	16:00	30.1	43.8	65.3	32.3	1.67	132.92	7.9819	2.2	0.06	1007

Table 19: Obtained data at 0.06 kg/s air mass flow rate for conical type (18.07.2019)

Overall Radiation [W/m ²]	Date	Time	T-in [°C]	T-glass [°C]	T-absorber [°C]	T-out [°C]	Area [m ²]	Q u [W]	Efficiency [η] [%]	ΔT [°C]	\dot{m} [kg/s]	Cp [J / kg·C]
995.8	18/07/2019	09:00	29.4	43.9	68.5	33.7	1.67	259.81	15.6229	4.3	0.06	1007
1035.9	18/07/2019	09:30	30	43.0	67.9	34	1.67	241.68	13.9703	4.0	0.06	1007
1052.6	18/07/2019	10:00	30.6	44.7	70.3	34.8	1.67	253.76	14.4361	4.2	0.06	1007
1102.5	18/07/2019	10:30	31.3	45.2	72.6	37.7	1.67	386.69	21.0022	6.4	0.06	1007
1136.9	18/07/2019	11:00	32.6	45.1	74.1	39.9	1.67	441.07	23.2308	7.3	0.06	1007
1089.1	18/07/2019	11:30	32.2	45.3	73.9	38.6	1.67	386.69	21.2606	6.4	0.06	1007
1125.9	18/07/2019	12:00	31.9	46.7	70.5	39.3	1.67	447.11	23.7791	7.4	0.06	1007
1209.8	18/07/2019	12:30	32.5	45.4	75.4	42.2	1.67	586.07	29.0083	9.7	0.06	1007
1285.6	18/07/2019	13:00	32.9	45.6	73.8	43.3	1.67	628.37	29.2679	10.4	0.06	1007
1272.9	18/07/2019	13:30	30.3	44.0	69.9	41.8	1.67	694.83	32.6865	11.5	0.06	1007
1185.6	18/07/2019	14:00	29.7	41.2	68.2	38.6	1.67	537.74	27.1591	8.9	0.06	1007
1039.5	18/07/2019	14:30	28.9	39.7	67.1	35.9	1.67	422.94	24.3634	7.0	0.06	1007
1045.6	18/07/2019	15:00	29.4	40.9	66.7	35.9	1.67	392.73	22.4912	6.5	0.06	1007
1058.2	18/07/2019	15:30	29.7	41.5	65.9	35.3	1.67	338.35	19.1463	5.6	0.06	1007
978.2	18/07/2019	16:00	28.5	40.7	63.2	31.8	1.67	199.39	12.2054	3.3	0.06	1007

Table 20: Obtained data at 0.06 kg/s air mass flow rate for polymer panel type (15.05.2019).

Overall Radiation [W/m ²]	Date	Time	T-in [°C]	T-glass [°C]	T-absorber [°C]	T-out [°C]	Area [m ²]	Q u [W]	Efficiency [η] [%]	ΔT [°C]	\dot{m} [kg/s]	Cp [J / kg·C]
981.6	15/05/2019	09:00	28.7	45.5	62.9	31.6	1.75	175.22	10.2001	2.9	0.06	1007
1010.5	15/05/2019	09:30	28.1	42.7	67.4	31.9	1.75	229.60	12.9834	3.8	0.06	1007
999.4	15/05/2019	10:00	29.7	46.1	71.1	33.9	1.75	253.76	14.5095	4.2	0.06	1007
975.5	15/05/2019	10:30	26.9	45.6	70.8	32.8	1.75	356.48	20.8818	5.9	0.06	1007
1030.8	15/05/2019	11:00	30.2	43.9	72.5	35.1	1.75	296.06	16.4121	4.9	0.06	1007
1055.6	15/05/2019	11:30	30.0	46.3	74.3	35.8	1.75	350.44	18.9702	5.8	0.06	1007
1084.9	15/05/2019	12:00	30.4	47.0	75.0	37.8	1.75	447.11	23.5497	7.4	0.06	1007
1045.3	15/05/2019	12:30	29.5	46.5	76.8	38.1	1.75	519.61	28.4054	8.6	0.06	1007
1005.7	15/05/2019	13:00	29.7	44.5	71.9	34.9	1.75	314.18	17.8516	5.2	0.06	1007
1028.1	15/05/2019	13:30	29.9	43.9	70.0	35.4	1.75	332.31	18.4701	5.5	0.06	1007
996.3	15/05/2019	14:00	30.0	41.2	69.5	35.4	1.75	326.27	18.7131	5.4	0.06	1007
1007.3	15/05/2019	14:30	30.5	44.5	68.7	34.9	1.75	265.85	15.0812	4.4	0.06	1007
983.4	15/05/2019	15:00	29.1	44.2	65.2	33.8	1.75	283.97	16.5010	4.7	0.06	1007
985.6	15/05/2019	15:30	29.3	43.9	65.1	33.4	1.75	247.72	14.3624	4.1	0.06	1007
997.2	15/05/2019	16:00	30.2	41.5	70.4	33.1	1.75	175.22	10.0406	2.9	0.06	1007

Table 21: Obtained data at 0.06 kg/s air mass flow rate for polymer panel type (18.07.2019)

Overall Radiation [W/m ²]	Date	Time	T-in [°C]	T-glass [°C]	T-absorber [°C]	T-out [°C]	Area [m ²]	Q u [W]	Efficiency [η] [%]	ΔT [°C]	\dot{m} [kg/s]	Cp [J / kg·C]
995.8	18/07/2019	09:00	29.1	42.0	67.0	32.9	1.75	229.60	13.1751	3.8	0.06	1007
1035.9	18/07/2019	09:30	29.9	43.5	68.1	34.1	1.75	253.76	13.9983	4.2	0.06	1007
1052.6	18/07/2019	10:00	30.2	43.9	70.3	34.2	1.75	241.68	13.1202	4	0.06	1007
1102.5	18/07/2019	10:30	31.1	44.1	71.9	36	1.75	296.06	15.3448	4.9	0.06	1007
1136.9	18/07/2019	11:00	32.4	46.7	73.8	39.2	1.75	410.86	20.6504	6.8	0.06	1007
1089.1	18/07/2019	11:30	32.4	44.5	73.9	38.6	1.75	374.60	19.6547	6.2	0.06	1007
1125.9	18/07/2019	12:00	32.3	47.6	68.4	38.5	1.75	374.60	19.0123	6.2	0.06	1007
1209.8	18/07/2019	12:30	32.8	49.0	65.8	40.5	1.75	465.23	21.9745	7.7	0.06	1007
1285.6	18/07/2019	13:00	33.1	50.6	70.3	43.3	1.75	616.28	27.3928	10.2	0.06	1007
1272.9	18/07/2019	13:30	29.9	44.2	69.7	40.3	1.75	628.37	28.2086	10.4	0.06	1007
1185.6	18/07/2019	14:00	29.7	43.8	65.6	36.9	1.75	435.02	20.9670	7.2	0.06	1007
1039.5	18/07/2019	14:30	29.1	44.1	64.8	34.5	1.75	326.27	17.9354	5.4	0.06	1007
1045.6	18/07/2019	15:00	30	45.0	66.9	35.6	1.75	338.35	18.4912	5.6	0.06	1007
1058.2	18/07/2019	15:30	29.5	44.7	64.5	34.2	1.75	283.97	15.3346	4.7	0.06	1007
978.2	18/07/2019	16:00	28.7	41.9	63.0	31.8	1.75	187.30	10.9415	3.1	0.06	1007

Table 22: Obtained data at 0.08 kg/s air mass flow rate for cola can type (16.05.2019)

Overall Radiation [W/m ²]	Date	Time	T-in [°C]	T-glass [°C]	T-absorber [°C]	T-out [°C]	Area [m ²]	Q u [W]	Efficiency [η] [%]	ΔT [°C]	\dot{m} [kg/s]	Cp [J / kg°C]
880.5	16/05/2019	09:00	27.4	45.5	61.8	29.8	1.82	193.34	12.0651	2.4	0.08	1007
890.7	16/05/2019	09:30	26.5	42.5	60.5	30.8	1.82	346.41	21.3690	4.3	0.08	1007
945.9	16/05/2019	10:00	27.9	45.1	63.1	32.8	1.82	394.74	22.9297	4.9	0.08	1007
995.6	16/05/2019	10:30	29.3	45.6	66.0	33.2	1.82	314.18	17.3391	3.9	0.08	1007
975.1	16/05/2019	11:00	29.7	44.9	60.9	34.7	1.82	402.80	22.6970	5.0	0.08	1007
1112.6	16/05/2019	11:30	30.9	46.3	64.5	36.3	1.82	435.02	21.4834	5.4	0.08	1007
1170.3	16/05/2019	12:00	33.2	48.0	61.7	38.2	1.82	402.80	18.9113	5.0	0.08	1007
1052.8	16/05/2019	12:30	30.0	46.0	59.7	36.2	1.82	499.47	26.0672	6.2	0.08	1007
987.2	16/05/2019	13:00	29.6	45.5	58.4	35.9	1.82	507.53	28.2477	6.3	0.08	1007
956.7	16/05/2019	13:30	28.9	43.9	59.6	34.1	1.82	418.91	24.0589	5.2	0.08	1007
978.3	16/05/2019	14:00	29.1	41.2	63.3	33.8	1.82	378.63	21.2654	4.7	0.08	1007
1071.6	16/05/2019	14:30	30.5	44.5	62.9	33.7	1.82	257.79	13.2180	3.2	0.08	1007
1093.8	16/05/2019	15:00	30.6	44.2	60.7	32.8	1.82	177.23	8.9029	2.2	0.08	1007
976.5	16/05/2019	15:30	28.7	43.9	58.4	30.9	1.82	177.23	9.9724	2.2	0.08	1007
928.3	16/05/2019	16:00	29.5	45.8	59.2	31.9	1.82	193.34	11.4438	2.4	0.08	1007

Table 23: Obtained data at 0.08 kg/s air mass flow rate for cola can type (19.07.2019)

Overall Radiation [W/m ²]	Date	Time	T-in [°C]	T-glass [°C]	T-absorber [°C]	T-out [°C]	Area [m ²]	Q u [W]	Efficiency [η] [%]	ΔT [°C]	\dot{m} [kg/s]	Cp [J / kg°C]
1153.2	19/07/2019	09:00	32.1	46.7	73.1	37.3	1.82	418.91	19.9594	5.2	0.08	1007
1125.6	19/07/2019	09:30	31.9	45.1	71.8	36.5	1.82	370.58	18.0893	4.6	0.08	1007
1159.5	19/07/2019	10:00	32.6	47.8	74.5	38.2	1.82	451.14	21.3779	5.6	0.08	1007
1145.1	19/07/2019	10:30	32.4	49.3	73.9	38.4	1.82	483.36	23.1929	6.0	0.08	1007
1165.3	19/07/2019	11:00	32.8	52.4	74.2	39.8	1.82	563.92	26.5894	7.0	0.08	1007
1287.9	19/07/2019	11:30	33.9	55.9	76.8	41.2	1.82	588.09	25.0893	7.3	0.08	1007
1290.5	19/07/2019	12:00	34.7	58.1	82.5	43.4	1.82	700.87	29.8407	8.7	0.08	1007
1320.9	19/07/2019	12:30	35	57.4	83.7	43.9	1.82	716.98	29.8242	8.9	0.08	1007
1338.7	19/07/2019	13:00	35.8	59.6	85.1	44.6	1.82	708.93	29.0970	8.8	0.08	1007
1284.2	19/07/2019	13:30	34.3	57.3	82.6	42.3	1.82	644.48	27.5744	8.0	0.08	1007
1237.1	19/07/2019	14:00	33.6	55.1	80.9	41.9	1.82	668.65	29.6976	8.3	0.08	1007
1177.3	19/07/2019	14:30	32.5	52.9	79.8	39.8	1.82	588.09	27.4463	7.3	0.08	1007
1110.1	19/07/2019	15:00	32.0	53.5	78.4	38.0	1.82	483.36	23.9242	6.0	0.08	1007
1130.8	19/07/2019	15:30	32.3	51.7	80.7	38.2	1.82	475.30	23.0948	5.9	0.08	1007
1087.3	19/07/2019	16:00	31.8	50.8	79.5	37.9	1.82	491.42	24.8330	6.1	0.08	1007

Table 24: Obtained data at 0.08 kg/s air mass flow rate for conical type (16.05.2019)

Overall Radiation [W/m ²]	Date	Time	T-in [°C]	T-glass [°C]	T-absorber [°C]	T-out [°C]	Area [m ²]	Q u [W]	Efficiency [η] [%]	ΔT [°C]	\dot{m} [kg/s]	Cp [J / kg·°C]
880.5	16/05/2019	09:00	26.9	48.0	58.9	30.5	1.67	290.02	19.7231	3.6	0.08	1007
890.7	16/05/2019	09:30	27.2	47.3	60.9	31.6	1.67	354.46	23.8300	4.4	0.08	1007
945.9	16/05/2019	10:00	29.8	44.3	62.3	33.1	1.67	265.85	16.8295	3.3	0.08	1007
995.6	16/05/2019	10:30	28.9	45.6	64.2	32.9	1.67	322.24	19.3811	4.0	0.08	1007
975.1	16/05/2019	11:00	29.9	46.5	66.5	34.6	1.67	378.63	23.2515	4.7	0.08	1007
1112.6	16/05/2019	11:30	30.6	48.2	68.1	35.4	1.67	386.69	20.8116	4.8	0.08	1007
1170.3	16/05/2019	12:00	32.9	48.0	69.0	38.5	1.67	451.14	23.0831	5.6	0.08	1007
1052.8	16/05/2019	12:30	30.3	46.3	72.5	36.8	1.67	523.64	29.7831	6.5	0.08	1007
987.2	16/05/2019	13:00	29.6	44.1	73.8	34.8	1.67	418.91	25.4098	5.2	0.08	1007
956.7	16/05/2019	13:30	28.8	41.9	71.9	34.2	1.67	435.02	27.2283	5.4	0.08	1007
978.3	16/05/2019	14:00	29.0	44.5	66.5	33.7	1.67	378.63	23.1755	4.7	0.08	1007
1071.6	16/05/2019	14:30	30.4	43.8	64.7	32.8	1.67	193.34	10.8039	2.4	0.08	1007
1093.8	16/05/2019	15:00	30.9	42.9	63.1	32.6	1.67	136.95	7.4975	1.7	0.08	1007
976.5	16/05/2019	15:30	28.9	41.5	60.5	30.9	1.67	161.12	9.8801	2.0	0.08	1007
928.3	16/05/2019	16:00	29.6	43.6	59.9	30.8	1.67	96.67	6.2359	1.2	0.08	1007

Table 25: Obtained data at 0.08 kg/s air mass flow rate for conical type (19.07.2019)

Overall Radiation [W/m ²]	Date	Time	T-in [°C]	T-glass [°C]	T-absorber [°C]	T-out [°C]	Area [m ²]	Q u [W]	Efficiency [η] [%]	ΔT [°C]	\dot{m} [kg/s]	Cp [J / kg·°C]
1153.2	19/07/2019	09:00	32	45.0	71.6	36.9	1.67	394.74	20.4972	4.9	0.08	1007
1125.6	19/07/2019	09:30	31.7	46.1	70.9	35.5	1.67	306.13	16.2856	3.8	0.08	1007
1159.5	19/07/2019	10:00	32.6	47.9	74.1	37.6	1.67	402.80	20.8019	5.0	0.08	1007
1145.1	19/07/2019	10:30	32.6	48.3	75.8	38.1	1.67	443.08	23.1698	5.5	0.08	1007
1165.3	19/07/2019	11:00	32.3	47.5	73.7	38.4	1.67	491.42	25.2520	6.1	0.08	1007
1287.9	19/07/2019	11:30	33.7	49.7	74.5	40.1	1.67	515.58	23.9718	6.4	0.08	1007
1290.5	19/07/2019	12:00	34.7	51.8	76.3	42.9	1.67	660.59	30.6520	8.2	0.08	1007
1320.9	19/07/2019	12:30	35.1	55.1	79.8	43.1	1.67	644.48	29.2162	8.0	0.08	1007
1338.7	19/07/2019	13:00	35.4	58.2	81.9	43.1	1.67	620.31	27.7466	7.7	0.08	1007
1284.2	19/07/2019	13:30	33.9	56.4	78.4	42.2	1.67	668.65	31.1780	8.3	0.08	1007
1237.1	19/07/2019	14:00	34.0	53.9	80.5	41.5	1.67	604.20	29.2455	7.5	0.08	1007
1177.3	19/07/2019	14:30	32.7	54.4	79.1	38.7	1.67	483.36	24.5848	6.0	0.08	1007
1110.1	19/07/2019	15:00	31.8	52.5	76.9	36.4	1.67	370.58	19.9894	4.6	0.08	1007
1130.8	19/07/2019	15:30	32.1	54.6	81.0	36.8	1.67	378.63	20.0500	4.7	0.08	1007
1087.3	19/07/2019	16:00	31.3	53.7	75.9	35.9	1.67	370.58	20.4085	4.6	0.08	1007

Table 26: Obtained data at 0.08 kg/s air mass flow rate for polymer panel type (16.05.2019)

Overall Radiation [W/m ²]	Date	Time	T-in [°C]	T-glass [°C]	T-absorber [°C]	T-out [°C]	Area [m ²]	Q u [W]	Efficiency [η] [%]	ΔT [°C]	\dot{m} [kg/s]	Cp [J / kg°C]
880.5	16/05/2019	09:00	27.0	45.0	56.0	29.1	1.75	169.18	10.9792	2.1	0.08	1007
890.7	16/05/2019	09:30	26.9	46.7	61.2	30.5	1.75	290.02	18.6060	3.6	0.08	1007
945.9	16/05/2019	10:00	28.1	43.9	63.5	30.6	1.75	201.40	12.1668	2.5	0.08	1007
995.6	16/05/2019	10:30	29.1	45.1	65.1	32.6	1.75	281.96	16.1832	3.5	0.08	1007
975.1	16/05/2019	11:00	29.8	46.0	68.4	34.5	1.75	378.63	22.1886	4.7	0.08	1007
1112.6	16/05/2019	11:30	30.4	47.9	65.0	34.9	1.75	362.52	18.6189	4.5	0.08	1007
1170.3	16/05/2019	12:00	32.9	47.0	66.6	37.8	1.75	394.74	19.2744	4.9	0.08	1007
1052.8	16/05/2019	12:30	30.1	46.5	63.9	35.9	1.75	467.25	25.3608	5.8	0.08	1007
987.2	16/05/2019	13:00	28.9	43.2	62.7	34.1	1.75	418.91	24.2482	5.2	0.08	1007
956.7	16/05/2019	13:30	29.1	39.8	69.4	34.6	1.75	443.08	26.4648	5.5	0.08	1007
978.3	16/05/2019	14:00	29.2	43.9	68.1	34.1	1.75	394.74	23.0571	4.9	0.08	1007
1071.6	16/05/2019	14:30	30.3	44.0	65.3	33.9	1.75	290.02	15.4650	3.6	0.08	1007
1093.8	16/05/2019	15:00	31.0	42.7	62.8	32.8	1.75	145.01	7.5756	1.8	0.08	1007
976.5	16/05/2019	15:30	29.0	41.1	59.7	30.8	1.75	145.01	8.4856	1.8	0.08	1007
928.3	16/05/2019	16:00	27.8	44.2	55.1	28.9	1.75	88.62	5.4549	1.1	0.08	1007

Table 27: Obtained data at 0.08 kg/s air mass flow rate for polymer panel type (19.07.2019)

Overall Radiation [W/m ²]	Date	Time	T-in [°C]	T-glass [°C]	T-absorber [°C]	T-out [°C]	Area [m ²]	Q u [W]	Efficiency [η] [%]	ΔT [°C]	\dot{m} [kg/s]	Cp [J / kg°C]
1153.2	19/07/2019	09:00	31.8	44.9	71.8	35.3	1.75	281.96	13.9716	3.5	0.08	1007
1125.6	19/07/2019	09:30	31.5	47.2	70.5	34.7	1.75	257.79	13.0872	3.2	0.08	1007
1159.5	19/07/2019	10:00	32.7	46.8	72.6	36.2	1.75	281.96	13.8956	3.5	0.08	1007
1145.1	19/07/2019	10:30	32.6	47.1	73.1	37.4	1.75	386.69	19.2965	4.8	0.08	1007
1165.3	19/07/2019	11:00	32.5	48.9	75.4	37.1	1.75	370.58	18.1719	4.6	0.08	1007
1287.9	19/07/2019	11:30	33.4	52.4	76.8	38.9	1.75	443.08	19.6590	5.5	0.08	1007
1290.5	19/07/2019	12:00	34.3	55.4	78.9	40.7	1.75	515.58	22.8299	6.4	0.08	1007
1320.9	19/07/2019	12:30	34.8	56.7	81.3	41.8	1.75	563.92	24.3955	7.0	0.08	1007
1338.7	19/07/2019	13:00	34.9	57.6	83.4	42.6	1.75	620.31	26.4782	7.7	0.08	1007
1284.2	19/07/2019	13:30	33.5	55.8	80.8	41.0	1.75	604.20	26.8850	7.5	0.08	1007
1237.1	19/07/2019	14:00	34.0	54.1	82.6	40.9	1.75	555.86	25.6759	6.9	0.08	1007
1177.3	19/07/2019	14:30	31.9	53.7	78.4	37.1	1.75	418.91	20.3328	5.2	0.08	1007
1110.1	19/07/2019	15:00	31.5	51.5	77.1	35.2	1.75	298.07	15.3434	3.7	0.08	1007
1130.8	19/07/2019	15:30	32.3	54.3	79.0	36.7	1.75	354.46	17.9122	4.4	0.08	1007
1087.3	19/07/2019	16:00	31.1	52.2	75.5	35.1	1.75	322.24	16.9353	4.0	0.08	1007

Table 28: Obtained data at 0.02 kg/s air mass flow rate heat loss for cola can type (13.05.2019)

Date	Time	U-overall [W/m ² .K]	Area [m ²]	ΔT [°C]	Q-loss [W/m ² .K]
13/05/2019	09:00	3.7700	1.82	14	96.0596
13/05/2019	09:30	3.7700	1.82	15.7	107.7240
13/05/2019	10:00	3.7700	1.82	18	123.5052
13/05/2019	10:30	3.7700	1.82	19	130.3666
13/05/2019	11:00	3.7700	1.82	19.8	135.8557
13/05/2019	11:30	3.7700	1.82	23.1	158.4983
13/05/2019	12:00	3.7700	1.82	22.6	155.0676
13/05/2019	12:30	3.7700	1.82	24.6	168.7904
13/05/2019	13:00	3.7700	1.82	22.6	155.0676
13/05/2019	13:30	3.7700	1.82	25.2	172.9073
13/05/2019	14:00	3.7700	1.82	25.1	172.2211
13/05/2019	14:30	3.7700	1.82	23.6	161.9290
13/05/2019	15:00	3.7700	1.82	21.9	150.2647
13/05/2019	15:30	3.7700	1.82	18.2	124.8775
13/05/2019	16:00	3.7700	1.82	16.9	115.9577

Table 29: Obtained data at 0.02 kg/s air mass flow rate heat loss for cola can type (16.07.2019)

Date	Time	U-overall [W/m ² .K]	Area [m ²]	ΔT [°C]	Q-loss [W/m ² .K]
16/07/2019	09:00	3.7700	1.82	18.4	126.2498
16/07/2019	09:30	3.7700	1.82	18.9	129.6805
16/07/2019	10:00	3.7700	1.82	20.7	142.0310
16/07/2019	10:30	3.7700	1.82	23.8	163.3013
16/07/2019	11:00	3.7700	1.82	23.3	159.8706
16/07/2019	11:30	3.7700	1.82	24	164.6736
16/07/2019	12:00	3.7700	1.82	26.4	181.1410
16/07/2019	12:30	3.7700	1.82	25.9	177.7103
16/07/2019	13:00	3.7700	1.82	28.9	198.2945
16/07/2019	13:30	3.7700	1.82	29	198.9806
16/07/2019	14:00	3.7700	1.82	31.2	214.0757
16/07/2019	14:30	3.7700	1.82	30.7	210.6450
16/07/2019	15:00	3.7700	1.82	25.2	172.9073
16/07/2019	15:30	3.7700	1.82	24.4	167.4182
16/07/2019	16:00	3.7700	1.82	23	157.8122

Table 30: Obtained data at 0.02 kg/s air mass flow rate heat loss for conical type (13.05.2019)

Date	Time	U-overall [W/m ² .K]	Area [m ²]	ΔT [°C]	Q-loss [W/m ² .K]
13/05/2019	09:00	3.7700	1.67	10.6	66.7365
13/05/2019	09:30	3.7700	1.67	14.7	92.5497
13/05/2019	10:00	3.7700	1.67	15.5	97.5865
13/05/2019	10:30	3.7700	1.67	17.3	108.9191
13/05/2019	11:00	3.7700	1.67	18.3	115.2150
13/05/2019	11:30	3.7700	1.67	20	125.9180
13/05/2019	12:00	3.7700	1.67	18.4	115.8446
13/05/2019	12:30	3.7700	1.67	20.1	126.5476
13/05/2019	13:00	3.7700	1.67	17	107.0303
13/05/2019	13:30	3.7700	1.67	21	132.2139
13/05/2019	14:00	3.7700	1.67	20.5	129.0660
13/05/2019	14:30	3.7700	1.67	19.2	120.8813
13/05/2019	15:00	3.7700	1.67	14.2	89.4018
13/05/2019	15:30	3.7700	1.67	14.4	90.6610
13/05/2019	16:00	3.7700	1.67	11.9	74.9212

Table 31: Obtained data at 0.02 kg/s air mass flow rate heat loss for conical type (16.07.2019)

Date	Time	U-overall [W/m ² .K]	Area [m ²]	ΔT [°C]	Q-loss [W/m ² .K]
16/07/2019	09:00	3.7700	1.67	15.9	100.1048
16/07/2019	09:30	3.7700	1.67	17.1	107.6599
16/07/2019	10:00	3.7700	1.67	18.7	117.7333
16/07/2019	10:30	3.7700	1.67	20.7	130.3251
16/07/2019	11:00	3.7700	1.67	22.2	139.7690
16/07/2019	11:30	3.7700	1.67	24	151.1016
16/07/2019	12:00	3.7700	1.67	23.4	147.3241
16/07/2019	12:30	3.7700	1.67	22.5	141.6578
16/07/2019	13:00	3.7700	1.67	28.8	181.3219
16/07/2019	13:30	3.7700	1.67	24.6	154.8791
16/07/2019	14:00	3.7700	1.67	26.6	167.4709
16/07/2019	14:30	3.7700	1.67	25.2	158.6567
16/07/2019	15:00	3.7700	1.67	22.1	139.1394
16/07/2019	15:30	3.7700	1.67	22.3	140.3986
16/07/2019	16:00	3.7700	1.67	12.9	81.2171

Table 32: Obtained data at 0.02 kg/s air mass flow rate heat loss for polymer panel type (13.05.2019)

Date	Time	U-overall [W/m ² .K]	Area [m ²]	ΔT [°C]	Q-loss [W/m ² .K]
13/05/2019	09:00	3.7700	1.75	9.7	63.9958
13/05/2019	09:30	3.7700	1.75	12.2	80.4895
13/05/2019	10:00	3.7700	1.75	12.5	82.4688
13/05/2019	10:30	3.7700	1.75	15.9	104.9003
13/05/2019	11:00	3.7700	1.75	18.2	120.0745
13/05/2019	11:30	3.7700	1.75	19.2	126.6720
13/05/2019	12:00	3.7700	1.75	16.5	108.8588
13/05/2019	12:30	3.7700	1.75	19.6	129.3110
13/05/2019	13:00	3.7700	1.75	14	92.3650
13/05/2019	13:30	3.7700	1.75	18	118.7550
13/05/2019	14:00	3.7700	1.75	17.3	114.1368
13/05/2019	14:30	3.7700	1.75	14.7	96.9833
13/05/2019	15:00	3.7700	1.75	13.3	87.7468
13/05/2019	15:30	3.7700	1.75	13.2	87.0870
13/05/2019	16:00	3.7700	1.75	10.7	70.5933

Table 33: Obtained data at 0.02 kg/s air mass flow rate heat loss for polymer panel type (16.07.2019)

Date	Time	U-overall [W/m ² .K]	Area [m ²]	ΔT [°C]	Q-loss [W/m ² .K]
16/07/2019	09:00	3.7700	1.75	13.3	87.7468
16/07/2019	09:30	3.7700	1.75	13.5	89.0663
16/07/2019	10:00	3.7700	1.75	16	105.5600
16/07/2019	10:30	3.7700	1.75	20.4	134.5890
16/07/2019	11:00	3.7700	1.75	21.3	140.5268
16/07/2019	11:30	3.7700	1.75	21.8	143.8255
16/07/2019	12:00	3.7700	1.75	23	151.7425
16/07/2019	12:30	3.7700	1.75	22	145.1450
16/07/2019	13:00	3.7700	1.75	25.2	166.2570
16/07/2019	13:30	3.7700	1.75	22	145.1450
16/07/2019	14:00	3.7700	1.75	24.3	160.3193
16/07/2019	14:30	3.7700	1.75	19.3	127.3318
16/07/2019	15:00	3.7700	1.75	16.7	110.1783
16/07/2019	15:30	3.7700	1.75	21.2	139.8670
16/07/2019	16:00	3.7700	1.75	16.3	107.5393

Table 34: Obtained data at 0.04 kg/s air mass flow rate heat loss for cola can type (14.05.2019)

Date	Time	U-overall [W/m ² .K]	Area [m ²]	ΔT [°C]	Q-loss [W/m ² .K]
14/05/2019	09:00	3.7700	1.82	7.1	48.7159
14/05/2019	09:30	3.7700	1.82	8.6	59.0080
14/05/2019	10:00	3.7700	1.82	11.1	76.1615
14/05/2019	10:30	3.7700	1.82	12.1	83.0229
14/05/2019	11:00	3.7700	1.82	12.7	87.1398
14/05/2019	11:30	3.7700	1.82	14.5	99.4903
14/05/2019	12:00	3.7700	1.82	14.2	97.4319
14/05/2019	12:30	3.7700	1.82	13.3	91.2566
14/05/2019	13:00	3.7700	1.82	13.6	93.3150
14/05/2019	13:30	3.7700	1.82	12.8	87.8259
14/05/2019	14:00	3.7700	1.82	12.9	88.5121
14/05/2019	14:30	3.7700	1.82	11.9	81.6507
14/05/2019	15:00	3.7700	1.82	10.6	72.7308
14/05/2019	15:30	3.7700	1.82	11.5	78.9061
14/05/2019	16:00	3.7700	1.82	10.9	74.7893

Table 35: Obtained data at 0.04 kg/s air mass flow rate heat loss for cola can type (17.07.2019)

Date	Time	U-overall [W/m ² .K]	Area [m ²]	ΔT [°C]	Q-loss [W/m ² .K]
17/07/2019	09:00	3.7700	1.82	10.1	69.3001
17/07/2019	09:30	3.7700	1.82	11.1	76.1615
17/07/2019	10:00	3.7700	1.82	13.3	91.2566
17/07/2019	10:30	3.7700	1.82	14.1	96.7457
17/07/2019	11:00	3.7700	1.82	14.6	100.1764
17/07/2019	11:30	3.7700	1.82	16.7	114.5854
17/07/2019	12:00	3.7700	1.82	17.5	120.0745
17/07/2019	12:30	3.7700	1.82	16.7	114.5854
17/07/2019	13:00	3.7700	1.82	17.3	118.7022
17/07/2019	13:30	3.7700	1.82	15.9	109.0963
17/07/2019	14:00	3.7700	1.82	15.5	106.3517
17/07/2019	14:30	3.7700	1.82	15.5	106.3517
17/07/2019	15:00	3.7700	1.82	14.1	96.7457
17/07/2019	15:30	3.7700	1.82	13.4	91.9428
17/07/2019	16:00	3.7700	1.82	13.9	95.3735

Table 36: Obtained data at 0.04 kg/s air mass flow rate heat loss for conical type (14.05.2019)

Date	Time	U-overall [W/m ² .K]	Area [m ²]	ΔT [°C]	Q-loss [W/m ² .K]
14/05/2019	09:00	3.7700	1.67	6.6	41.5529
14/05/2019	09:30	3.7700	1.67	7.1	44.7009
14/05/2019	10:00	3.7700	1.67	9.7	61.0702
14/05/2019	10:30	3.7700	1.67	13.2	83.1059
14/05/2019	11:00	3.7700	1.67	11.4	71.7733
14/05/2019	11:30	3.7700	1.67	12.1	76.1804
14/05/2019	12:00	3.7700	1.67	14.4	90.6610
14/05/2019	12:30	3.7700	1.67	12.7	79.9579
14/05/2019	13:00	3.7700	1.67	13.7	86.2538
14/05/2019	13:30	3.7700	1.67	12.3	77.4396
14/05/2019	14:00	3.7700	1.67	10.4	65.4774
14/05/2019	14:30	3.7700	1.67	11.3	71.1437
14/05/2019	15:00	3.7700	1.67	11.7	73.6620
14/05/2019	15:30	3.7700	1.67	9.9	62.3294
14/05/2019	16:00	3.7700	1.67	6.8	42.8121

Table 37: Obtained data at 0.04 kg/s air mass flow rate heat loss for conical type (17.07.2019)

Date	Time	U-overall [W/m ² .K]	Area [m ²]	ΔT [°C]	Q-loss [W/m ² .K]
17/07/2019	09:00	3.7700	1.67	9.6	60.4406
17/07/2019	09:30	3.7700	1.67	10.7	67.3661
17/07/2019	10:00	3.7700	1.67	10.9	68.6253
17/07/2019	10:30	3.7700	1.67	12.4	78.0692
17/07/2019	11:00	3.7700	1.67	13.7	86.2538
17/07/2019	11:30	3.7700	1.67	15	94.4385
17/07/2019	12:00	3.7700	1.67	15.5	97.5865
17/07/2019	12:30	3.7700	1.67	15.1	95.0681
17/07/2019	13:00	3.7700	1.67	17.6	110.8078
17/07/2019	13:30	3.7700	1.67	18.1	113.9558
17/07/2019	14:00	3.7700	1.67	16.8	105.7711
17/07/2019	14:30	3.7700	1.67	16.2	101.9936
17/07/2019	15:00	3.7700	1.67	15.4	96.9569
17/07/2019	15:30	3.7700	1.67	15.3	96.3273
17/07/2019	16:00	3.7700	1.67	14.7	92.5497

Table 38: Obtained data at 0.04 kg/s air mass flow rate heat loss for polymer panel type (14.05.2019)

Date	Time	U-overall [W/m ² .K]	Area [m ²]	ΔT [°C]	Q-loss [W/m ² .K]
14/05/2019	09:00	3.7700	1.75	6.2	40.9045
14/05/2019	09:30	3.7700	1.75	7.5	49.4813
14/05/2019	10:00	3.7700	1.75	9.9	65.3153
14/05/2019	10:30	3.7700	1.75	11	72.5725
14/05/2019	11:00	3.7700	1.75	7.7	50.8008
14/05/2019	11:30	3.7700	1.75	9.4	62.0165
14/05/2019	12:00	3.7700	1.75	12.6	83.1285
14/05/2019	12:30	3.7700	1.75	12	79.1700
14/05/2019	13:00	3.7700	1.75	13.2	87.0870
14/05/2019	13:30	3.7700	1.75	9.9	65.3153
14/05/2019	14:00	3.7700	1.75	9.5	62.6763
14/05/2019	14:30	3.7700	1.75	11.1	73.2323
14/05/2019	15:00	3.7700	1.75	8.9	58.7178
14/05/2019	15:30	3.7700	1.75	6	39.5850
14/05/2019	16:00	3.7700	1.75	5	32.9875

Table 39: Obtained data at 0.04 kg/s air mass flow rate heat loss for polymer panel type (17.07.2019)

Date	Time	U-overall [W/m ² .K]	Area [m ²]	ΔT [°C]	Q-loss [W/m ² .K]
17/07/2019	09:00	3.7700	1.75	8.6	56.7385
17/07/2019	09:30	3.7700	1.75	9.5	62.6763
17/07/2019	10:00	3.7700	1.75	10.9	71.9128
17/07/2019	10:30	3.7700	1.75	10.4	68.6140
17/07/2019	11:00	3.7700	1.75	11.1	73.2323
17/07/2019	11:30	3.7700	1.75	13.1	86.4273
17/07/2019	12:00	3.7700	1.75	15.8	104.2405
17/07/2019	12:30	3.7700	1.75	16.1	106.2198
17/07/2019	13:00	3.7700	1.75	17.8	117.4355
17/07/2019	13:30	3.7700	1.75	16.3	107.5393
17/07/2019	14:00	3.7700	1.75	13.9	91.7053
17/07/2019	14:30	3.7700	1.75	13.1	86.4273
17/07/2019	15:00	3.7700	1.75	12.4	81.8090
17/07/2019	15:30	3.7700	1.75	13	85.7675
17/07/2019	16:00	3.7700	1.75	13	85.7675

Table 40: Obtained data at 0.06 kg/s air mass flow rate heat loss for cola can type (15.05.2019)

Date	Time	U-overall [W/m ² .K]	Area [m ²]	ΔT [°C]	Q-loss [W/m ² .K]
15/05/2019	09:00	3.7700	1.82	3.9	26.7595
15/05/2019	09:30	3.7700	1.82	4	27.4456
15/05/2019	10:00	3.7700	1.82	4.5	30.8763
15/05/2019	10:30	3.7700	1.82	6.3	43.2268
15/05/2019	11:00	3.7700	1.82	6.1	41.8545
15/05/2019	11:30	3.7700	1.82	7.1	48.7159
15/05/2019	12:00	3.7700	1.82	8.2	56.2635
15/05/2019	12:30	3.7700	1.82	8.4	57.6358
15/05/2019	13:00	3.7700	1.82	8.4	57.6358
15/05/2019	13:30	3.7700	1.82	9.3	63.8110
15/05/2019	14:00	3.7700	1.82	8.3	56.9496
15/05/2019	14:30	3.7700	1.82	5.5	37.7377
15/05/2019	15:00	3.7700	1.82	6.7	45.9714
15/05/2019	15:30	3.7700	1.82	4.8	32.9347
15/05/2019	16:00	3.7700	1.82	3.6	24.7010

Table 41: Obtained data at 0.06 kg/s air mass flow rate heat loss for cola can type (18.07.2019)

Date	Time	U-overall [W/m ² .K]	Area [m ²]	ΔT [°C]	Q-loss [W/m ² .K]
18/07/2019	09:00	3.7700	1.82	5.2	35.6793
18/07/2019	09:30	3.7700	1.82	4.7	32.2486
18/07/2019	10:00	3.7700	1.82	4.9	33.6209
18/07/2019	10:30	3.7700	1.82	6.6	45.2852
18/07/2019	11:00	3.7700	1.82	8.6	59.0080
18/07/2019	11:30	3.7700	1.82	7.6	52.1466
18/07/2019	12:00	3.7700	1.82	9.4	64.4972
18/07/2019	12:30	3.7700	1.82	11	75.4754
18/07/2019	13:00	3.7700	1.82	11.6	79.5922
18/07/2019	13:30	3.7700	1.82	10.8	74.1031
18/07/2019	14:00	3.7700	1.82	10.1	69.3001
18/07/2019	14:30	3.7700	1.82	9.3	63.8110
18/07/2019	15:00	3.7700	1.82	7.7	52.8328
18/07/2019	15:30	3.7700	1.82	7.2	49.4021
18/07/2019	16:00	3.7700	1.82	4.3	29.5040

Table 42: Obtained data at 0.06 kg/s air mass flow rate heat loss for conical type (15.05.2019)

Date	Time	U-overall [W/m ² .K]	Area [m ²]	ΔT [°C]	Q-loss [W/m ² .K]
15/05/2019	09:00	3.7700	1.67	3.9	24.5540
15/05/2019	09:30	3.7700	1.67	3.6	22.6652
15/05/2019	10:00	3.7700	1.67	4.4	27.7020
15/05/2019	10:30	3.7700	1.67	4.4	27.7020
15/05/2019	11:00	3.7700	1.67	3.9	24.5540
15/05/2019	11:30	3.7700	1.67	5.8	36.5162
15/05/2019	12:00	3.7700	1.67	8.4	52.8856
15/05/2019	12:30	3.7700	1.67	9.1	57.2927
15/05/2019	13:00	3.7700	1.67	7.9	49.7376
15/05/2019	13:30	3.7700	1.67	5	31.4795
15/05/2019	14:00	3.7700	1.67	6.1	38.4050
15/05/2019	14:30	3.7700	1.67	3.4	21.4061
15/05/2019	15:00	3.7700	1.67	5.2	32.7387
15/05/2019	15:30	3.7700	1.67	4.2	26.4428
15/05/2019	16:00	3.7700	1.67	2.2	13.8510

Table 43: Obtained data at 0.06 kg/s air mass flow rate heat loss for conical type (18.07.2019)

Date	Time	U-overall [W/m ² .K]	Area [m ²]	ΔT [°C]	Q-loss [W/m ² .K]
18/07/2019	09:00	3.7700	1.67	4.3	27.0724
18/07/2019	09:30	3.7700	1.67	4	25.1836
18/07/2019	10:00	3.7700	1.67	4.2	26.4428
18/07/2019	10:30	3.7700	1.67	6.4	40.2938
18/07/2019	11:00	3.7700	1.67	7.3	45.9601
18/07/2019	11:30	3.7700	1.67	6.4	40.2938
18/07/2019	12:00	3.7700	1.67	7.4	46.5897
18/07/2019	12:30	3.7700	1.67	9.7	61.0702
18/07/2019	13:00	3.7700	1.67	10.4	65.4774
18/07/2019	13:30	3.7700	1.67	11.5	72.4029
18/07/2019	14:00	3.7700	1.67	8.9	56.0335
18/07/2019	14:30	3.7700	1.67	7	44.0713
18/07/2019	15:00	3.7700	1.67	6.5	40.9234
18/07/2019	15:30	3.7700	1.67	5.6	35.2570
18/07/2019	16:00	3.7700	1.67	3.3	20.7765

Table 44: Obtained data at 0.06 kg/s air mass flow rate heat loss for polymer panel type (15.05.2019)

Date	Time	U-overall [W/m ² .K]	Area [m ²]	ΔT [°C]	Q-loss [W/m ² .K]
15/05/2019	09:00	3.7700	1.75	2.9	19.1328
15/05/2019	09:30	3.7700	1.75	3.8	25.0705
15/05/2019	10:00	3.7700	1.75	4.2	27.7095
15/05/2019	10:30	3.7700	1.75	5.9	38.9253
15/05/2019	11:00	3.7700	1.75	4.9	32.3278
15/05/2019	11:30	3.7700	1.75	5.8	38.2655
15/05/2019	12:00	3.7700	1.75	7.4	48.8215
15/05/2019	12:30	3.7700	1.75	8.6	56.7385
15/05/2019	13:00	3.7700	1.75	5.2	34.3070
15/05/2019	13:30	3.7700	1.75	5.5	36.2863
15/05/2019	14:00	3.7700	1.75	5.4	35.6265
15/05/2019	14:30	3.7700	1.75	4.4	29.0290
15/05/2019	15:00	3.7700	1.75	4.7	31.0083
15/05/2019	15:30	3.7700	1.75	4.1	27.0498
15/05/2019	16:00	3.7700	1.75	2.9	19.1328

Table 45: Obtained data at 0.06 kg/s air mass flow rate heat loss for polymer panel type (18.07.2019)

Date	Time	U-overall [W/m ² .K]	Area [m ²]	ΔT [°C]	Q-loss [W/m ² .K]
18/07/2019	09:00	3.7700	1.75	3.8	25.0705
18/07/2019	09:30	3.7700	1.75	4.2	27.7095
18/07/2019	10:00	3.7700	1.75	4	26.3900
18/07/2019	10:30	3.7700	1.75	4.9	32.3278
18/07/2019	11:00	3.7700	1.75	6.8	44.8630
18/07/2019	11:30	3.7700	1.75	6.2	40.9045
18/07/2019	12:00	3.7700	1.75	6.2	40.9045
18/07/2019	12:30	3.7700	1.75	7.7	50.8008
18/07/2019	13:00	3.7700	1.75	10.2	67.2945
18/07/2019	13:30	3.7700	1.75	10.4	68.6140
18/07/2019	14:00	3.7700	1.75	7.2	47.5020
18/07/2019	14:30	3.7700	1.75	5.4	35.6265
18/07/2019	15:00	3.7700	1.75	5.6	36.9460
18/07/2019	15:30	3.7700	1.75	4.7	31.0083
18/07/2019	16:00	3.7700	1.75	3.1	20.4523

Table 46: Obtained data at 0.08 kg/s air mass flow rate heat loss for cola can type (16.05.2019)

Date	Time	U-overall [W/m ² .K]	Area [m ²]	ΔT [°C]	Q-loss [W/m ² .K]
16/05/2019	09:00	3.7700	1.82	2.4	16.4674
16/05/2019	09:30	3.7700	1.82	4.3	29.5040
16/05/2019	10:00	3.7700	1.82	4.9	33.6209
16/05/2019	10:30	3.7700	1.82	3.9	26.7595
16/05/2019	11:00	3.7700	1.82	5	34.3070
16/05/2019	11:30	3.7700	1.82	5.4	37.0516
16/05/2019	12:00	3.7700	1.82	5	34.3070
16/05/2019	12:30	3.7700	1.82	6.2	42.5407
16/05/2019	13:00	3.7700	1.82	6.3	43.2268
16/05/2019	13:30	3.7700	1.82	5.2	35.6793
16/05/2019	14:00	3.7700	1.82	4.7	32.2486
16/05/2019	14:30	3.7700	1.82	3.2	21.9565
16/05/2019	15:00	3.7700	1.82	2.2	15.0951
16/05/2019	15:30	3.7700	1.82	2.2	15.0951
16/05/2019	16:00	3.7700	1.82	2.4	16.4674

Table 47: Obtained data at 0.08 kg/s air mass flow rate heat loss for cola can type (19.07.2019)

Date	Time	U-overall [W/m ² .K]	Area [m ²]	ΔT [°C]	Q-loss [W/m ² .K]
19/07/2019	09:00	3.7700	1.82	5.2	35.6793
19/07/2019	09:30	3.7700	1.82	4.6	31.5624
19/07/2019	10:00	3.7700	1.82	5.6	38.4238
19/07/2019	10:30	3.7700	1.82	6	41.1684
19/07/2019	11:00	3.7700	1.82	7	48.0298
19/07/2019	11:30	3.7700	1.82	7.3	50.0882
19/07/2019	12:00	3.7700	1.82	8.7	59.6942
19/07/2019	12:30	3.7700	1.82	8.9	61.0665
19/07/2019	13:00	3.7700	1.82	8.8	60.3803
19/07/2019	13:30	3.7700	1.82	8	54.8912
19/07/2019	14:00	3.7700	1.82	8.3	56.9496
19/07/2019	14:30	3.7700	1.82	7.3	50.0882
19/07/2019	15:00	3.7700	1.82	6	41.1684
19/07/2019	15:30	3.7700	1.82	5.9	40.4823
19/07/2019	16:00	3.7700	1.82	6.1	41.8545

Table 48: Obtained data at 0.08 kg/s air mass flow rate heat loss for conical type (16.05.2019)

Date	Time	U-overall [W/m ² .K]	Area [m ²]	ΔT [°C]	Q-loss [W/m ² .K]
16/05/2019	09:00	3.7700	1.67	3.6	22.6652
16/05/2019	09:30	3.7700	1.67	4.4	27.7020
16/05/2019	10:00	3.7700	1.67	3.3	20.7765
16/05/2019	10:30	3.7700	1.67	4	25.1836
16/05/2019	11:00	3.7700	1.67	4.7	29.5907
16/05/2019	11:30	3.7700	1.67	4.8	30.2203
16/05/2019	12:00	3.7700	1.67	5.6	35.2570
16/05/2019	12:30	3.7700	1.67	6.5	40.9234
16/05/2019	13:00	3.7700	1.67	5.2	32.7387
16/05/2019	13:30	3.7700	1.67	5.4	33.9979
16/05/2019	14:00	3.7700	1.67	4.7	29.5907
16/05/2019	14:30	3.7700	1.67	2.4	15.1102
16/05/2019	15:00	3.7700	1.67	1.7	10.7030
16/05/2019	15:30	3.7700	1.67	2	12.5918
16/05/2019	16:00	3.7700	1.67	1.2	7.5551

Table 49: Obtained data at 0.08 kg/s air mass flow rate heat loss for conical type (19.07.2019)

Date	Time	U-overall [W/m ² .K]	Area [m ²]	ΔT [°C]	Q-loss [W/m ² .K]
19/07/2019	09:00	3.7700	1.67	4.9	30.8499
19/07/2019	09:30	3.7700	1.67	3.8	23.9244
19/07/2019	10:00	3.7700	1.67	5	31.4795
19/07/2019	10:30	3.7700	1.67	5.5	34.6275
19/07/2019	11:00	3.7700	1.67	6.1	38.4050
19/07/2019	11:30	3.7700	1.67	6.4	40.2938
19/07/2019	12:00	3.7700	1.67	8.2	51.6264
19/07/2019	12:30	3.7700	1.67	8	50.3672
19/07/2019	13:00	3.7700	1.67	7.7	48.4784
19/07/2019	13:30	3.7700	1.67	8.3	52.2560
19/07/2019	14:00	3.7700	1.67	7.5	47.2193
19/07/2019	14:30	3.7700	1.67	6	37.7754
19/07/2019	15:00	3.7700	1.67	4.6	28.9611
19/07/2019	15:30	3.7700	1.67	4.7	29.5907
19/07/2019	16:00	3.7700	1.67	4.6	28.9611

Table 50: Obtained data at 0.08 kg/s air mass flow rate heat loss for polymer panel type (16.05.2019)

Date	Time	U-overall [W/m ² .K]	Area [m ²]	ΔT [°C]	Q-loss [W/m ² .K]
16/05/2019	09:00	3.7700	1.75	2.1	13.8548
16/05/2019	09:30	3.7700	1.75	3.6	23.7510
16/05/2019	10:00	3.7700	1.75	2.5	16.4938
16/05/2019	10:30	3.7700	1.75	3.5	23.0913
16/05/2019	11:00	3.7700	1.75	4.7	31.0083
16/05/2019	11:30	3.7700	1.75	4.5	29.6888
16/05/2019	12:00	3.7700	1.75	4.9	32.3278
16/05/2019	12:30	3.7700	1.75	5.8	38.2655
16/05/2019	13:00	3.7700	1.75	5.2	34.3070
16/05/2019	13:30	3.7700	1.75	5.5	36.2863
16/05/2019	14:00	3.7700	1.75	4.9	32.3278
16/05/2019	14:30	3.7700	1.75	3.6	23.7510
16/05/2019	15:00	3.7700	1.75	1.8	11.8755
16/05/2019	15:30	3.7700	1.75	1.8	11.8755
16/05/2019	16:00	3.7700	1.75	1.1	7.2572

Table 51: Obtained data at 0.08 kg/s air mass flow rate heat loss for polymer panel type (19.07.2019)

Date	Time	U-overall [W/m ² .K]	Area [m ²]	ΔT [°C]	Q-loss [W/m ² .K]
19/07/2019	09:00	3.7700	1.75	3.5	23.0913
19/07/2019	09:30	3.7700	1.75	3.2	21.1120
19/07/2019	10:00	3.7700	1.75	3.5	23.0913
19/07/2019	10:30	3.7700	1.75	4.8	31.6680
19/07/2019	11:00	3.7700	1.75	4.6	30.3485
19/07/2019	11:30	3.7700	1.75	5.5	36.2863
19/07/2019	12:00	3.7700	1.75	6.4	42.2240
19/07/2019	12:30	3.7700	1.75	7	46.1825
19/07/2019	13:00	3.7700	1.75	7.7	50.8008
19/07/2019	13:30	3.7700	1.75	7.5	49.4813
19/07/2019	14:00	3.7700	1.75	6.9	45.5228
19/07/2019	14:30	3.7700	1.75	5.2	34.3070
19/07/2019	15:00	3.7700	1.75	3.7	24.4108
19/07/2019	15:30	3.7700	1.75	4.4	29.0290
19/07/2019	16:00	3.7700	1.75	4	26.3900

Table 52: Calculation of U-overall of collector types

Insulation Material	k	Units	Length				Length	Unit	r1	r2	A	Count				U Overall [W/m ² .K]
			L	Units	L	Units						Conic	polymer	Can Cola		
Ri	0.123	W/ m °C			0	m					m ²	1	1	1	U Overall [W/m ² .K] Top 0.5595	
Soft wooden fan box	0.140	W/ m °C	18	mm	0.018	m					m ²	1	1	1	U Overall [W/m ² .K] Edge 1.6253	
Aluminum Conics	213	W/ m °C	0.4	mm	0.0004	m				0.0338	m ²	28	0	0	U Overall [W/m ² .K] Bottom 1.5769	
Soft Wooden collector box	0.140	W/ m °C	15	mm	0.015	m					m ²	1	1	1		
Cola Can	213	W/ m °C	0.5	mm	0.0005	m	1.44	m	0.0327	0.033	0.0250	m ²	0		159	
Aluminum Polymer panel	213	W/ m °C	2.5	mm	0.0025	m					1.7500	m ²		1		
Glass at the mid point	1.090	W/ m °C	4	mm	0.004	m					1.8200	m ²	1	1	1	
OSB	0.160	W/ m °C	10	mm	0.01	m					1.3800	m ²	1	1	1	
Glass wool	0.080	W/ m °C	10	mm	0.01	m					1.3800	m ²	1	1	1	
Outside glass	1.090	W/ m °C	4	mm	0.004	m					1.8200	m ²	1	1	1	
Aluminum Collector panel	213	W/ m °C	1	mm	0.001	m					1.6700	m ²	1	1	1	
Polyurethane foam	0.023	W/ m °C	35	mm	0.035	m					0.0570	m ²	2	2	2	
Rgap_conic	0.180	W/ m °C											4		12	
Rgap_polymer	0.180	W/ m °C												1		
Rgap_can cola	0.180	W/ m °C											0		12	
Cellular Glass	0.058	W/ m °C	10	mm	0.01	m					1.3800	m ²	1	1	1	
Ro	0.055	W/ m °C			0	m						m ²	1	1	1	

Conical Type				Polymer Panel Type				Cola Can Type			
Single R Values	Unit	Total R values	Unit	Single R Values	Unit	Total R values	Unit	Single R Values	Unit	Total R values	Unit
0.1230	m ² °C/W	0.1230	m ² °C/W	0.1230	m ² °C/W	0.1230	m ² °C/W	0.1230	m ² °C/W	0.1230	m ² °C/W
	m ² °C/W		m ² °C/W		m ² °C/W		m ² °C/W		m ² °C/W		m ² °C/W
0.0001	m ² °C/W	0.0000	m ² °C/W		m ² °C/W		m ² °C/W		m ² °C/W		m ² °C/W
	m ² °C/W		m ² °C/W		m ² °C/W		m ² °C/W		m ² °C/W		m ² °C/W
	m ² °C/W		m ² °C/W		m ² °C/W		m ² °C/W	0.0002	m ² °C/W	0.0002	m ² °C/W
	m ² °C/W		m ² °C/W	0.0002	m ² °C/W	0.0002	m ² °C/W		m ² °C/W		m ² °C/W
0.0020	m ² °C/W	0.0020	m ² °C/W	0.0020	m ² °C/W	0.0020	m ² °C/W	0.0020	m ² °C/W	0.0020	m ² °C/W
0.0453	m ² °C/W	0.0453	m ² °C/W	0.0453	m ² °C/W	0.0453	m ² °C/W	0.0453	m ² °C/W	0.0453	m ² °C/W
0.0906	m ² °C/W	0.0906	m ² °C/W	0.0906	m ² °C/W	0.0906	m ² °C/W	0.0906	m ² °C/W	0.0906	m ² °C/W
0.0020	m ² °C/W	0.0020	m ² °C/W	0.0020	m ² °C/W	0.0020	m ² °C/W	0.0020	m ² °C/W	0.0020	m ² °C/W
0.0000	m ² °C/W	0.0000	m ² °C/W	0.0000	m ² °C/W	0.0000	m ² °C/W	0.0000	m ² °C/W	0.0000	m ² °C/W
26.6972	m ² °C/W		m ² °C/W	26.6972	m ² °C/W		m ² °C/W	26.6972	m ² °C/W	0.0000	m ² °C/W
0.1800	m ² °C/W	0.0450	m ² °C/W		m ² °C/W		m ² °C/W		m ² °C/W		m ² °C/W
	m ² °C/W		m ² °C/W	0.1800	m ² °C/W	0.1800	m ² °C/W		m ² °C/W		m ² °C/W
	m ² °C/W		m ² °C/W		m ² °C/W		m ² °C/W	0.1800	m ² °C/W	0.0150	m ² °C/W
0.1249	m ² °C/W	0.1249	m ² °C/W	0.1249	m ² °C/W		m ² °C/W	0.1249	m ² °C/W	0.1249	m ² °C/W
0.0550	m ² °C/W	0.0550	m ² °C/W	0.0550	m ² °C/W		m ² °C/W	0.0550	m ² °C/W	0.0550	m ² °C/W